Investigation of the Impact of Copper Homeostasis on Cellular Physiology

by

Xinyu Zhu

A dissertation submitted to the Graduate Faculty of
Auburn University
in partial fulfillment of the
requirements for the Degree of
Doctor of Philosophy

Auburn, Alabama
May 4, 2024

Keywords: copper, *Saccharomyces cerevisiae*, mitochondrial carrier family, mitochondria, cellular physiology, metabolite

Approved by

Paul A. Cobine, Chair, Professor of Biological Sciences
Aaron M. Rashotte, Professor of Biological Sciences
Alexey Petrov, Assistant Professor of Biological Sciences
Katherine M. Buckley, Assistant Professor of Biological Sciences

Abstract

The copper pool within the mitochondrial matrix is required for assembly and activity of cytochrome *c* oxidase and a portion of copper/zinc superoxide dismutase. The mitochondrial copper exists bound to an anionic, fluorescent molecule known as the copper ligand (CuL). The CuL is imported into mammalian mitochondria through mitochondrial carrier family (MCF) protein SLC25A3, while in *Saccharomyces cerevisiae* Pic2 mediates the translocation. SLC25A3 has promiscuity for phosphate and CuL, but yeast has dedicated MCFs to transport these two substrates, Pic2 transports copper and Mir1 transports phosphate. To better understand the mechanism for substrate selection, we adopted phylogenetic approach to identify the critical residues dictate the substrate specificity of MCF. We tested the identified candidates by site directed mutations and expression of the mutants in *Lactococcus lactis* for copper and silver uptake. In SLC25A3, we were able to demonstrate that transport specificity could be modulated by mutating leucine 175 to alanine. The mutant transporter retained copper transporting capacity but lost its ability to import phosphate. We speculated that mutating the leucine residue caused changes in protein structure which most likely resulted in movement of residues with positive charges used for substrate binding.

It is estimated that only 10%-20% of the mitochondrial copper is associated with mitochondria-localized cupro-enzymes. To identify novel targets of which the mitochondrial copper binds to, we performed synthetic genetic array in yeast and found a copper repressible lysine auxotroph phenotype. ACO2 is a paralog of ACO1 that is required in the de novo lysine synthesis pathway. We observed that the lysine auxotroph of an *aco2*Δ yeast can be rescued by copper if ACO1 is present and intermediate rescue can be achieved by modulating the

transcriptional level of ACO1. We hypothesized the copper binds to Aco1 at a remote allosteric site, changes the active site of the enzyme so that it can accommodate the larger substrate, homoaconitate, thus bypassing the requirement for Aco2. We demonstrated the copper bound to the mitochondrial aconitase and switched its substrate specificity.

Acknowledgments

My greatest gratitude goes to my major advisor, Dr. Paul Cobine. He has been the most inspirational, empowering and pateient throughout the course of my Ph.D. His mentorship guides me to grow as a scientist, while his life philosophy will continue to guide me to grow as a human being. I would also like to thank my committee members: Dr. Katherine Buckley, Dr. Alexey Petrov, and Dr. Aaron Rashotte for their unreserved support and brilliant advice. I appreciate Dr. Jeffery Coleman for his support during my Ph.D. and being the university reader. I am grateful to the previous and current members of the Cobine lab, whom I was lucky to have: Alex Matthews, Shelby Cole, Catrice Hixon, Laura Oldfather, Huachen Gan, and Devadatta Gosavi for their friendship and support. I would like to thank the undergraduate students who allowed me to learn more by teaching them. Finally, I am grateful to my parents, my wife Cai Chen and my friends for their continuous and unconditional supports through my graduate career.

Table of Contents

List of Figures

List of Abbreviations

IM	Inner mitochondrial membrane
OM	Outer mitochondrial membrane
IMS	Inter-membrane space
ETC	Electron transport chain
COX	Cytochrome c oxidase
BCS	Bathocuproine disulfonic acid

Chapter 1: Literature Review

From Vest, K.E., Zhu, X. and Cobine, P.A. (2019) "Copper disposition in yeast", in Clinical and Translational Perspectives on Wilson Disease, edited by Nanda Kerkar and Eve A. Roberts, Academic Press, pp.115-126.

Introduction

Many of the paradigms for intracellular trafficking of copper have been established in genetically tractable models. Yeasts have been a particularly attractive model organism. Yeasts are fungi that grow as single cells and reproduce through budding or binary fission. Growth as a single cell rather than in a hyphae form is a distinction between yeasts and fungi. However, it should be noted that some fungi can alternate between the yeast and hyphal forms depending on environmental conditions. Two well-studied unicellular models are the budding yeast, *Saccharomyces cerevisiae* and the fission yeast *Schizosaccharomyces pombe*[1–3]. In this chapter, *S. cerevisiae* is referred to budding yeast or yeast and any reference to *S. pombe* will be specified as fission yeast. As we learn more about the regulation of copper including new targets, transient binding to proteins to regulate activity and the role of small molecules in copper homeostasis in multicellular organisms, these yeasts remain viable and important models. Herein, the standard nomenclature will be used. For *S. cerevisiae* genes in all capitals with italics (*GENE*) and sentence case with no italics for proteins (Protein), while in *S. pombe*, genes will be lower case italics (*gene*). In all cases, the origin naming of the gene is included in parentheses. Since membranes form the major barrier to the distribution of copper in all biological systems, transporters play a key role in controlling the distribution of copper in the cell. Yeast has been used to discover and investigate several of the conserved copper transporters, including Ctr1/2/3 (copper transporter 1/2/3), Ccc2 (cross-complements calcium phenotype of csg1), and Pic2 [Phosphate (Pi) carrier 2] (Figure 1.1). The yeast plasma membrane has both high- and low-

affinity transport systems that bring copper into the cell [2]. Once inside the cell, copper must still make its way to targets without spurious interaction. This is facilitated by the copper chaperones that distribute it to target enzymes using metal-assisted protein-protein interactions [4]. These reactions proceed due to increasing affinity for copper in the target protein [5]. Copper must be distributed to the secretory pathway for insertion into enzymes required for high-affinity iron transport, to cytosolic targets for insertion into superoxide dismutase for protection against oxidative stress, and to mitochondria to be assembled into the terminal electron accepting complex in the energy-producing electron transport chain, cytochrome c oxidase complex. The requirement of a copper chaperone for superoxide dismutase (Ccs1) in yeast led to the calculation of cytoplasmic "free" copper as being equal to zero [6]. However, the reason for an absolute requirement for Ccs1 in yeast appears to be structural requirement for the chaperone to align copper-binding ligands in Sod1, which is the Cu/Zn superoxide dismutase important for cytoprotection [7]. Yet, this calculation has driven many of the research directions in copper homeostasis, with numerous investigations culminating in genetic and biochemical dissection of the delivery of copper to each of the three major copper enzymes.

The classic βαββαβ-folded copper chaperone Atx1 (antioxidant 1), which was first described in yeast, delivers copper to the secretory pathway for the multicopper ferroxidase (Fet3) (ferrous transport 3), while Ccs1 is involved in both copper delivery and activation of superoxide dismutase (Sod1) [8]. Cox17 (cytochrome c oxidase assembly 17), Sco1 (synthesis of cytochrome c oxidase 1), and Cox11 (cytochrome c oxidase assembly 11) collaborate to facilitate cytochrome c oxidase assembly in the intermembrane space of the mitochondrion. Rather than recruiting copper directly from the cytoplasm, the mitochondrial copper chaperones obtain copper from a bioavailable pool in the mitochondrial matrix. Accumulation of this matrix pool is

dependent on the mitochondrial carrier family (MCF) protein Pic2. However, the exact identity of the molecules responsible for the distribution of copper to mitochondria and of the transporter that redistributes copper from the matrix to the intermembrane space is unknown.

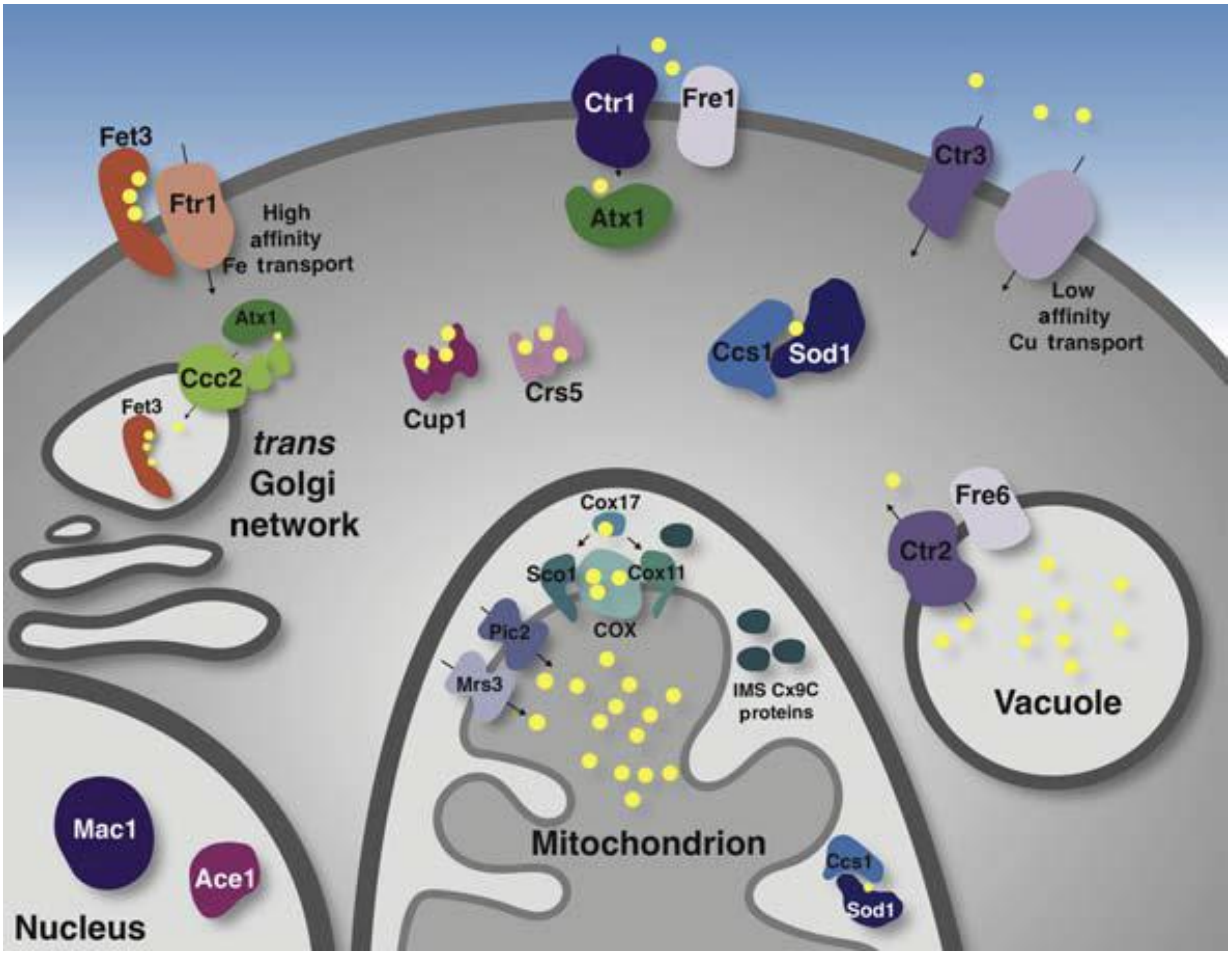

Figure 1.1: Copper homeostasis in *Saccharomyces cerevisiae*.

Copper is transported in cuprous (Cu(I)) form after reduction by metalloreductases (Fre1) by high- (Ctr1) and low- (Fet4) affinity systems. Once in the cytosol, copper is delivered to superoxide dismutase (Sod1) by the copper chaperone Ccs1; to the P-type ATPase Ccc2 by Atx1 for assembly of the multicopper oxidase Fet3; and to the mitochondrion by an unknown mechanism. After translocation to the mitochondria, copper is sequestered into the matrix pool by Pic2 and Mrs3, then it is made available in the intermembrane space for Cox17-, Cox11-, and Sco1-mediated assembly of cytochrome c oxidase. When copper reaches toxic levels, it is bound by the metallothioneins Cup1 and Crs5. Copper that is in the vacuole can be remobilized by the high affinity transporter Ctr2. Regulation of a number of these targets is via direct copper-binding to the transcription factors, Mac1 and Ace1.

Copper homeostasis in yeast diverges from mammalian copper homeostasis in two ways. First, the metallothionein and high-affinity cytoplasmic membrane transporters are regulated with unique transcription factors, Ace1 (activator of CUP1 expression 1) and Mac1 (metal binding activator 1). These transcription factors directly bind copper to regulate transcription, whereas in other eukaryotes expression of the metallothionein genes and cytoplasmic membrane transporter (CTR) is controlled by a zinc-regulated transcription factor (MTF1) (metal regulatory transcription factor 1)[9, 10]. Second, yeasts lack an export pathway. Instead of removing cytoplasmic copper via export, yeast uses the vacuole as a storage pool that can be depleted by cell division. Alternatively, the copper can be redistributed to the cytoplasm as needed by a vacuolar specific transport system (Table 1.1).

Table 1.1: Major Copper Homeostasis Proteins in Yeast and the Mammalian Equivalent

Yeast Gene Product	Function	Name Origin	Mammalian Equivalent
Ctr1	Plasma membrane transporter	Copper transport	SLC31A1
Ccc2	Trans-Golgi network transporter	Cross-complements calcium phenotype of csg1	ATP7A/ATP7B
Pic2	Mitochondrial inner membrane transporter	Phosphate carrier	SLC25A3
Fet3	Multicopper oxidase	Ferrous transporter	Ceruloplasmin
Fre1	Reduces ferric iron and cuprous copper for uptake	Ferric reductase	
COX	Converts oxygen to water as a terminal electron acceptor of electron transport chain		COX
Atx1	Delivery of copper to Ccc2 for Fet3	Antioxidant 1	ATOX1
Sco1	Assembly of COX	Synthesis of COX	SCO1/2
Cox17	Assembly of COX	COX assembly	COX17
Cox11	Assembly of COX	COX assembly	COX11
Mac1	Controlling expression of copper uptake genes	Metal binding activator	Fungal specific
Ace1	Controlling expression of copper detoxification machinery	Activator of CUP1 expression	Fungal specific

Major copper enzymes of yeast

Three major enzymes require copper in yeast. The multicopper oxidase Fet3 converts ferrous iron (Fe^{2+}) to ferric iron (Fe^{3+}) and is required for high-affinity iron transport in yeast (Figure 1.2) [11]. The copper ions in Fet3 mediate the oxidation of the substrate and the reduction of oxygen to water. For high-affinity iron transport to proceed, ferrous iron must be oxidized to a ferric ion. Therefore, in the absence of Fet3 yeast cells require supplemental iron to be added to the medium (Figure 1.3). Using this requirement, several other proteins have been identified that participate in the activation of Fet3 including a chloride channel (Gef1) (glycerol, ethanol, ferric requiring 1) and a potassium proton exchanger (Kha1) [potassium (K), proton (H) antiporter 1] that have roles in maintain the correct vesicular conditions where the pH and ion compositions are optimal for the correct folding of the oxidase [12–14]. The ferroxidase family can have multiple substrates, and in addition to oxidizing iron, Fet3 has been shown to oxidize cuprous copper at the plasma membrane [15]. This has been suggested to be responsible for copper stress phenotypes associated with overexpression of Fet3 [15]. A high level of Fet3 presumably induces of cycling of copper between Cu(I) and Cu(II) states leading to lipid damage and toxicity.

The Cu/Zn superoxide dismutase (Sod1) is a homodimeric free radical scavenging enzyme that breaks down superoxide radicals to molecular oxygen and hydrogen peroxide via a copper-mediated disproportionation reaction (Fig. 1.2). Sod1 is expressed predominantly in the cytoplasm of yeast but is also found in the mitochondrial intermembrane space [16]. The monomer structure consists of an eight-stranded beta-barrel that binds a copper ion and a zinc ion that play both catalytic and structural roles [17]. Different yeast mutants with Sod1

deficiencies have phenotypes such as amino-acid auxotroph and reduced growth rate under aerobic conditions (Fig. 1.3). Sod1 is very abundant in the cytoplasm and only a fraction of this total protein is sufficient to protect against oxidative stress. The other major role this enzyme plays is to form a conduit for the regulation of respiration in response to glucose and oxygen levels via interaction with the casein kinase pathway [18].

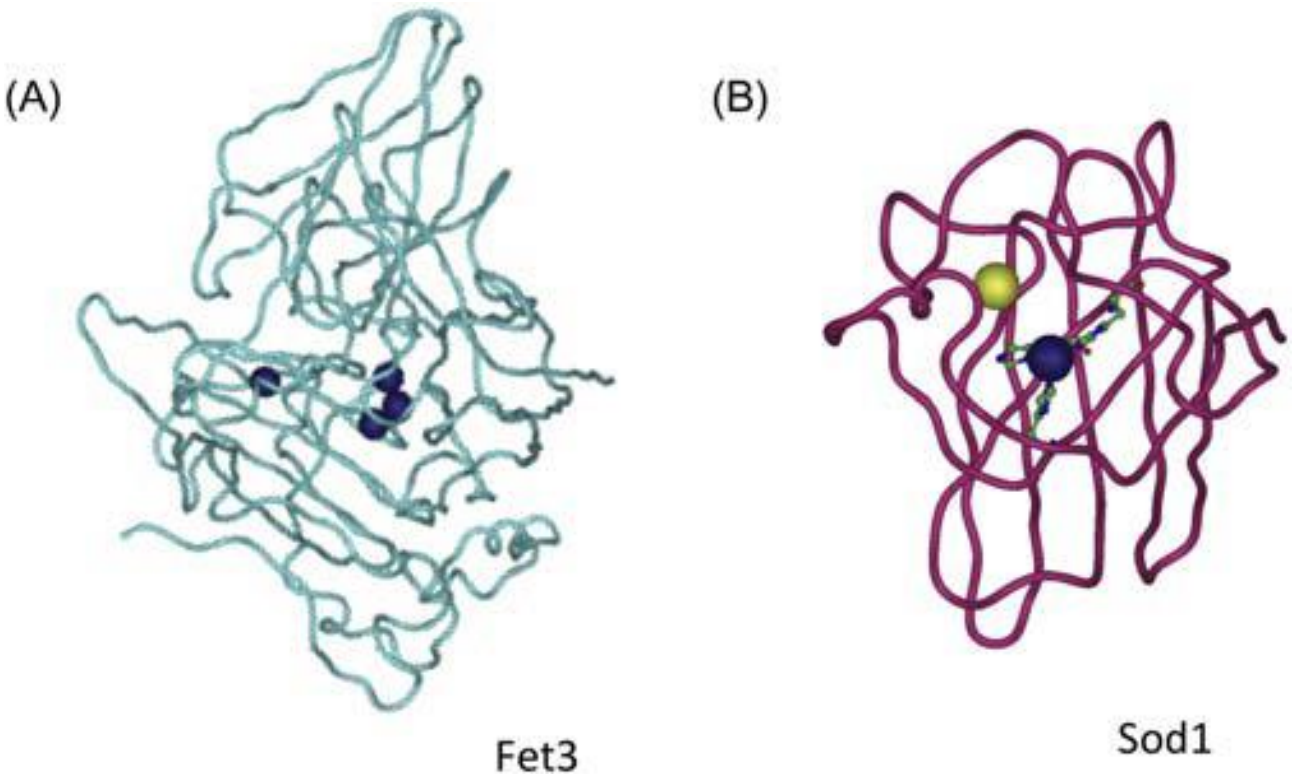

Figure 1.2: Structures of yeast version of major cuproenzymes.

(A) Fet3 is a multicopper oxidase that has three repeated plastocyanin-like domains that position the four copper ions (PDB: 1zpu). (B) Superoxide dismutase from yeast shown as a monomer with copper (blue) and zinc (yellow) cofactors. The histidine residues coordinating the copper are shown in ball and stick (PDB: 1b4l).

Cytochrome c oxidase (COX) is the final enzyme complex of the electron transport chain; it accepts electrons from the soluble electron carrier cytochrome c and donates them to oxygen, reducing it to water. The process occurs in the inner membrane of mitochondria and results in the translocation of protons that contribute to the formation of membrane potential [19]. COX contains multiple cofactors (copper, heme, magnesium, and zinc) that are required for its assembly and activity [20]. Cox1, Cox2, and Cox3 (cytochrome c oxidase 1/2/3) are the catalytic core of the enzyme and are encoded by the mitochondrial genome. Cox1 and Cox2 subunits bind two heme *a* moieties and three copper ions. The heme *a3* molecule is coordinated to a copper ion to form the Cu_B center in Cox1, while Cox2 binds a mixed valence, binuclear copper site (Cu_A). The Cu_B site is required for substrate binding, while Cu_A accepts electrons from cytochrome c that are transferred to the Cu_B site and then to oxygen [21]. The catalytic core of the COX is surrounded by nuclear-encoded structural subunits, which stabilize and may allow for allosteric regulation of the holoenzyme. The assembly process, including cofactor insertion, requires the action of at least 30 different accessory proteins [22]. Many of these assembly factors have been identified by the inability of yeast to grow on nonfermentable carbon sources when cytochrome c oxidase is absent (Figure 1.3).

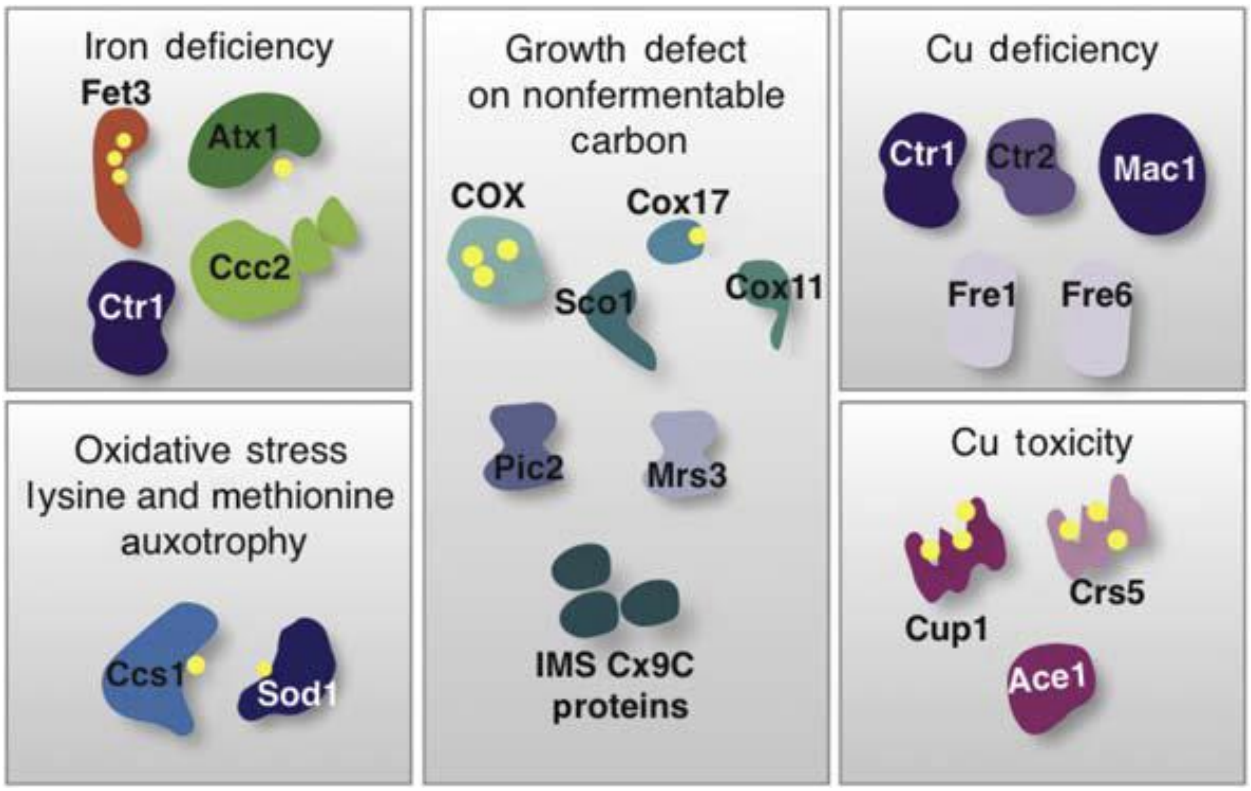

Figure 1.3: Copper phenotypes in *Saccharomyces cerevisiae*.

Cartoon representation of the phenotypes that result from mutation of the gene encoding the major cuproenzymes or their chaperones. Copper deficiency phenotypes can be revealed by deletion of the transporters or the metalloreductases or the transcription factor controlling them. Individual mutants result in phenotypes of (1) failure to support high affinity iron uptake, (2) inability to grow on nonfermentable carbon sources due to loss of electron transport chain activity, and (3) oxidative stress and methionine and lysine auxotrophy. Removal of the metallothioneins or the transcription factor controlling the expression of these metallothineins results in copper toxicity due to loss of iron sulfur enzymes, mismetallation, and oxidative damage.

Membrane transport of copper

Ctr1 (copper transporter 1) is a high-affinity copper transport protein in the plasma membrane that is active as a trimer [23]. Each monomer has three transmembrane domains, with methionine-rich MXM, MXXM, or MXXXM motifs (methionine motifs) in the extracellular amino-terminal domain [24]. Ctr1 transports copper in the cuprous form, so an extracellular metalloreductase (Fre1) is required to efficient copper transport [25, 26]. The Ctr1 homotrimer forms a pore lined by a methionine motif found in the second transmembrane domain [23, 27]. Copper first binds to the methionine motif on the extracellular domain and then is transferred to the pore. A conserved histidine residue close to the exit side mediates the rate-limiting step of transport, as evidence showed mutating this residue to an arginine significantly increase the K_m value for copper [28]. Once copper traverses the plasma membrane, it is bound to a carboxyterminal CXC domain of Ctr1 before being distributed to the cytosol. The CXC containing domain has been shown to interact with and deliver copper to the chaperone Atx1 that is required for transport to the trans-Golgi network [29].

Additional transport systems exist at the plasma membrane in yeast. CTR3 was discovered in a genetic screen to identify suppressors of defects in yeast lacking CTR1. Expression of CTR3 is naturally suppressed in some yeast strains due to the insertion of a transposable element in the promoter region, but when expressed Ctr3 (copper transporter 3) can carry out high-affinity copper transport. Ctr3 exists as a homotrimer but lacks the methionine motifs found in Ctr1[30]. Yeasts also use a series of low-affinity copper transporters, Fet4 (ferrous transport 4) and Smf1 (suppressor of mitochondria import function 1) [31, 32]. A feature that is conserved for both low and high-affinity transport is that Cu(I) is used specifically as a substrate. Thus, cells need cell surface reductases or an exogenous reductant to uptake necessary

copper [33].

CCC2 encodes a trans-Golgi P-type ATPase, that is the yeast homolog of the Wilson and Menkes ATPases (ATP7A/B) [34, 35]. Like the other P-type ATPases, it has multiple domains required for the translocation of copper. The channel is made up of eight transmembrane domains and a cytosol domain required for ATP hydrolysis to and phosphorylation of a conserved invariant aspartic acid residue to mediate the transfer of copper ion into the downstream target, vesicular multicopper oxidase Fet3. In addition, Ccc2 has two amino-terminal βαββαβ-folded CXXC metal-binding domains which serve to bind copper [36]. Though partially dispensable, these domains serve as targets for the delivery of copper from the similarly folded copper chaperone, Atx1. Electrostatic patches allow for specific interaction, and a shallow thermodynamic gradient between the chaperon, Atx1, and Ccc2 drives copper transfer via a ligand exchange mechanism to the ATPase and therefore into the secretory pathway [37, 38]. The sharing of ligands in the exposed copper-binding sites enhances the interaction between the proteins, and this allows for transient interaction via relatively small interface made up of charged and some hydrophobic residues [4].

Pic2 transports copper across the mitochondrial inner membrane into a matrix copper pool that is required for metalation of cytochrome c oxidase and superoxide dismutase [39–41]. Pic2 is a member of the MCF: this family of transporters is responsible for the transport of numerous metabolites into and out of the matrix [42]. Yeast strains with a deletion of PIC2 show copper-dependent growth defects, and mitochondria from these cells have lower total mitochondrial copper [41]. Importantly, Pic2 expressed in *Lactococcus lactis* was able to transport copper [41]. The mitochondrial iron-transporting protein Mrs3 (mitochondrial RNA splicing 3), also in the MCF, contributes to copper import into mitochondria [43]. However,

since deletion of both PIC2 and Mrs3 in yeast did not eliminate copper accumulation in the matrix, additional transport systems likely exist. Importantly, the insertion of the copper cofactors into cytochrome c oxidase and superoxide dismutase occurs in the intermembrane space; thus, inner membrane localized carriers are required to move copper both into and out of the mitochondrial matrix [39, 40]. Yet, no transporter has been identified for the export of copper from the matrix to the intermembrane space.

Yeast lacks an export pathway for copper; the only equivalent of export is import into the vacuole. Once copper is in the vacuole, it must exist as cuprous copper as a metalloreductase (Fre6) (ferric reductase 6) is required for mobilization of copper into the cytosol via Ctr2 [44, 45]. Ctr2 (copper transporter 2) is a homolog of Ctr1, and deletion of CTR2 causes hyperaccumulation of copper in the vacuole. The identification of Ctr2 as a copper transporter was confirmed by mutation analysis that showed it can function as a high-affinity copper transporter when localized to the plasma membrane [45].

Cytoplasmic copper chaperons

The requirement for copper chaperones in the cytoplasm to overcome spurious inappropriate interactions was first suggested by the discovery of Atx1[46]. Atx1 (antioxidant 1) is a non-catalytic copper-binding protein that interacts with the N-terminal domain of Ccc2. During the interaction, copper is exchanged from the chaperone to the target. As shown in Figure 1.4, Atx1 has a stable βαββαβ-folded protein with an exposed CXXC copper-binding unit [47]. After obtaining copper via an interaction with the Ctr1, or via scavenging in the cytosol, Atx1 binds copper in a linear 2-coordinated site using cysteine residues from CXXC site. After acquiring copper, it translocates to the trans-Golgi network and delivers copper to Ccc2, where

the copper transfer proceeds via a ligand exchange reaction [48]. Ccc2 accepts the copper in a homologous βαββαβ-folded amino-terminal domain that has the same CXXC binding site (Figure 1.5). A series of lysine residues in Atx1 provide an electrostatic surface to enhance the interaction[49]. During the transfer, copper moves to a planar 3-coordinate site sharing ligands from both proteins. The final step is complete transfer of the copper into a linear 2-coordinate site in Ccc2. Copper is then transported into the trans-Golgi vesicles to be assembled into the multicopper oxidase Fet3 [29, 46, 50].

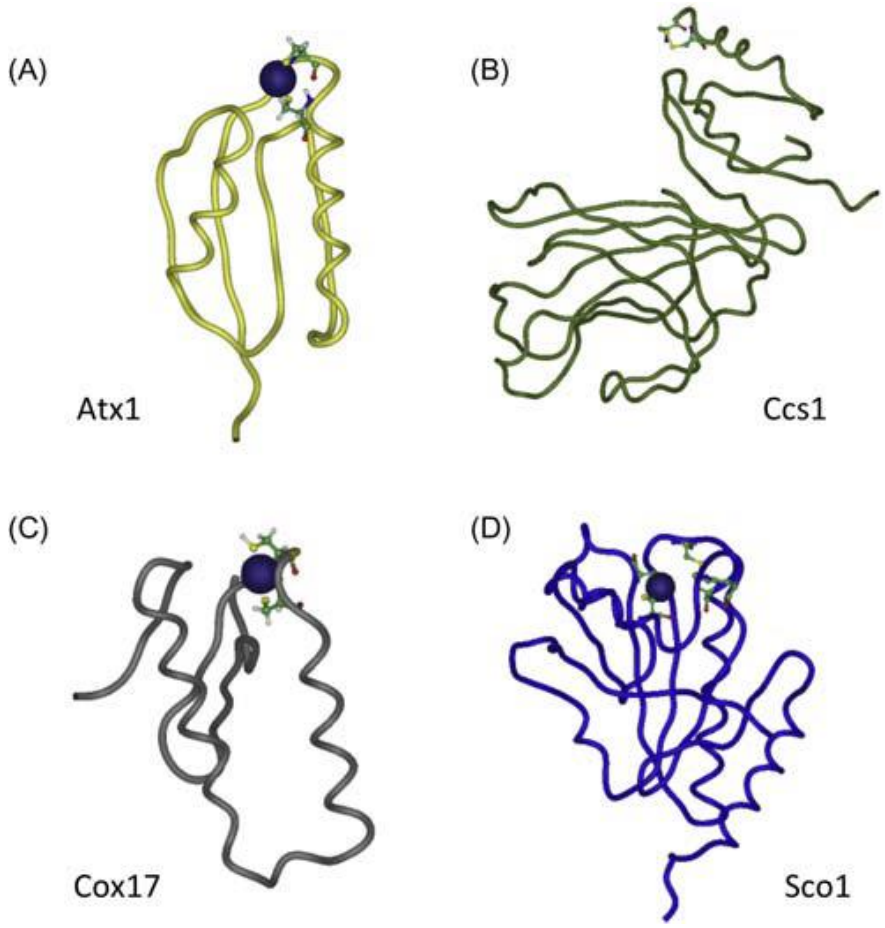

Figure 1.4: Structures of yeast version of copper chaperones.

(A) Atx1 structure is defined as a βαββαβ: this fold consists primarily of a beta sheet with the two helices lying this sheet presenting the copper-binding ligands in an exposed loop. The copper ion is shown in blue and is coordinated by cysteine residues (in ball and stick) of the CXXC motif (PDB: 1fd8). (B) Copper chaperone for Sod1 in the apo state: Ccs1 h
as multiple domains including a Sod1-like domain that is used for heterodimer formation and a βαββαβ Atx1-like domain with CXXC motif that is shown in ball and stick (PDB: 1qup). (C) Helical hairpin structure of Cox17 with copper bound to two cysteine residues (PDB: 1u96). (D) Intermembrane space domain of copper Sco1 with a disulfide bond in the CXXXC copper-binding residues and has copper bound by additional cysteines (PDB: 2b7j).

The copper chaperone for superoxide dismutase, Ccs1, activates Sod1 by inserting copper into the newly synthesized apoprotein in the cytoplasm and then catalyzing the formation of an essential disulfide bond within Sod1 [51]. The structure of Ccs1 contains three defined domains: a βαββαβ-folded Atx1-like domain, a central Sod1-like domain, and a carboxyterminal domain (Figure 1.4) [52, 53]. Ccs1 interacts with Sod1 as a heterodimer via the Sod-like domain that is also required for the activation (Figure 1.5) [54]. Ccs1 docks with the disulfide-reduced apo-Sod1and subsequently transfers the metal ion to this disulfide-reduced apo-Sod1[52, 55, 56]. Ccs1 interacts with a partially folded conformation of apo-reduced Sod1, facilitates the insertion of copper, and the formation of the disulfide bond in a reaction that is dependent on oxygen [51]. The peptide mapping analyses show that the disulfide within the domain III of Ccs1 can be transferred to Sod1 through a disulfide isomerization reaction. The change in structure decreases the affinity of the interaction as disordered loops adopt a more rigid structure in the copper-bound, disulfide bonded folded protein.

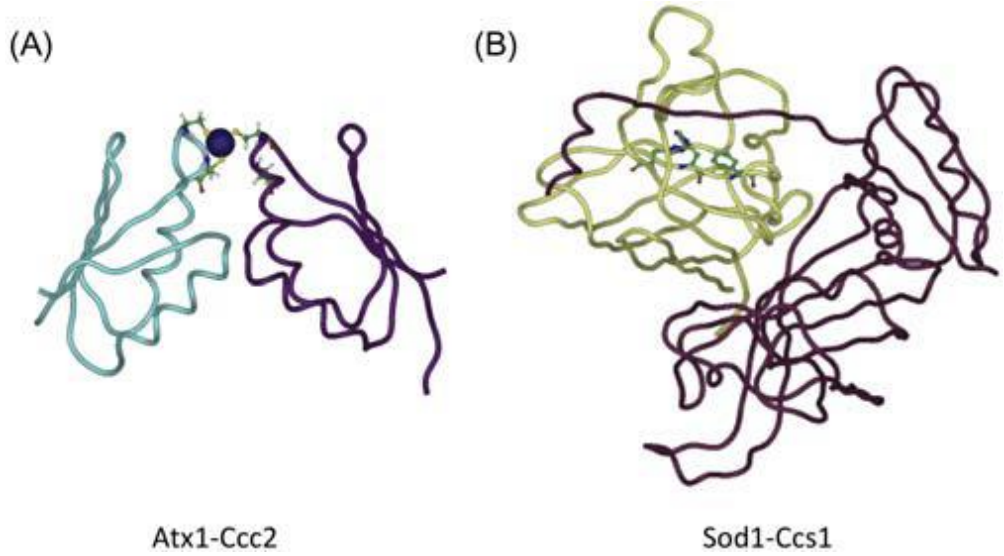

Figure 1.5: Structure of copper chaperones in complex with target.

(A) Solution structure of Atx1 and Ccc2 interacting with copper bound in the three-coordinate site sharing ligands between the two proteins (PDB: 2ggp). (B) Crystal structure of the complex of Sod1 and Ccs1 (PDB: 1jk9).

Mitochondrial copper

Estimates indicate that 20% to 40% of copper in mitochondria is associated with the electron accepting complex, cytochrome c oxidase [39, 57]. This enzyme is assembled in the intermembrane space via a series of copper chaperones called Cox17, Sco1, and Cox11 (cytochrome c oxidase assembly 11). The copper chaperone Cox17 is a cysteine-rich protein that is localized to the intermembrane space of the mitochondria and binds copper for the delivery to the other copper-binding assembly proteins [58, 59]. Cox17 adopts a conformation with two disulfide bonds that binds a single copper. Mutational analyses have shown that copper coordination and function are not dependent on the presence of two disulfide crosslinks; however, they do provide stability to the fold (Figure 1.4) [60]. Cox17 delivers copper to both Sco1 and Cox11 in yeast, donating copper to each molecule through transient interactions that are mediated by distinct structural interfaces [61, 62].

Sco1 is anchored in the inner membrane protein by a single transmembrane helix with the carboxy-terminal domain protruding into the intermembrane space (Figure 1.4)[63]. The peroxiredoxin-like fold of the globular carboxy-terminal domain exposes a single copper-binding site made up of two cysteine residues within a CXXXC motif and a conserved histidine residue [63]. Sco1 is required to deliver copper to binuclear Cu_A site in Cox2 of the COX, and mutation of either cysteine residues or the histidine residue in Sco1 abrogates copper binding and results in decreased COX activity[63–65]. In addition to binding Cu (I), Sco proteins bind Cu (II) [66]. It is not clear whether Sco1 transfers both Cu (I) and Cu (II) ions to build the mixed valence binuclear site in cytochrome c oxidase or if Cu (II) plays some other role in assembly. SCO1 is a genetic suppressor of a COX17 mutant: when supplied in multi-copy plasmid, it can reverse this mutant's failure to grow on non-fermentable carbon sources. The ability to bypass COX17 defect

with SCO1 suggests that these two proteins are in the same pathway. In the absence of Cox17, the high levels of Sco1 could be either holding Cox2 in a conformation that allows spontaneous formation of CuA or the increased Sco1 levels may help facilitate scavenging of limited amounts of copper in the intermembrane space for direct delivery to Cox2 [67]. It should be noted that no suppressor of a SCO1 deletion has been identified in yeast, reflecting its crucial role in the CuA site assembly. In addition to recombinant expressed protein, copper binding to Sco1 was confirmed by a study that purified full length Sco1 from yeast mitochondria [68].

Cox11 is also an inner membrane tethered protein with a single transmembrane helix and a carboxy-terminal domain that contains cysteine residues used for copper binding[69]. The copper in Cox11 is transferred to Cox1 to form the Cu_B site in the COX that is required for binding and reduction of dioxygen. In vitro experiments showed that yeast Cox11 could bind copper via cysteine residues in a CXC motif and that these ligands were required for cytochrome c oxidase assembly in vivo [69, 70]. Consistent with the coordinated insertion of heme *a3* and copper, Cox11 transiently interacts with Shy1 (SURF1 homolog in yeast) that is required for heme *a3* insertion into Cox1 [71]. The importance of this interaction was uncovered by a peroxide sensitivity that is induced by deletion of COX11 (or SCO1) by formation of a pro-oxidant intermediate of Cox1 that contains the heme a but not copper [72].

Yeasts also have a series of CX9C proteins [Coa6 (cytochrome c oxidase assembly 6), Cox19 (cytochrome c oxidase assembly 19), Cmc1, Cmc2 (Cx9C mitochondrial protein necessary for full assembly of cytochrome c oxidase 1/2), and Cox23 (cytochrome c oxidase assembly 23)] in the intermembrane space that can bind copper and are required for cytochrome c oxidase assembly [73]. Cox19 has been shown to interact with oxidized Cox11; this interaction allows for reduction of the disulfide bond in Cox11 and therefore provide reduced sulfurs for

copper binding [74]. Coa6 has been shown to have genetic and physical interactions with Sco proteins and weakly with Pic2, reinforcing the important role this protein has in mitochondrial copper distribution [75–77]. Further investigations are required to determine the exact functional significance of copper binding to all these Cx9C proteins.

Ccs1 also localizes to the intermembrane space of mitochondria where it activates the 1%-5% of the total cellular Sod1 that is found in this compartment [16]. The mitochondrial localization of Ccs1 is dependent on a redox-mediated import system (Mia40-Erv1) that uses a disulfide relay exchange system and a pair of cysteines present in the Atx1-like domain on Ccs1 that are not exposed CXXC motif [78]. Once both Ccs1 and apo-Sod1 are in the intermembrane space, Ccs1 acquires copper by an unknown mechanism and activates Sod1. In yeast cells genetically modified to express a copper-binding metallothionein in the matrix, steady state levels of Sod1 decrease due to the attenuated availability of copper to be translocated to the IMS in order to metalate and activate IMS-localized Sod1. This decrease in intermembrane space Sod1 is also present in yeast lacking CCS1, suggesting that the matrix pool is the source of copper for this enzyme. The activity of Sod1 in the intermembrane space has also been linked with the levels of the CX9C protein Cmc1. Yeast with CMC1 deleted have increased Sod1 activity in this compartment [79]. However, the exact role of Cmc1 in this pathway is yet to be fully elucidated.

Sequestration and regulation

The concentration of cytoplasmic free copper has been estimated to be near zero, necessitating specific chaperone-mediated metallation of targets [6]. This low cytoplasmic concentration indicates that yeast must efficiently sequester copper [80]. Sequestration can be

achieved by transport into organelles including trans-Golgi network, vacuole, or mitochondria. Alternatively, copper can bound in biologically inert complexes in the cytoplasm. These complexes can be proteins such as metallothioneins, or metabolites such as the redox-active tripeptide glutathione.

Two metallothioneins, Cup1 (cuprum 1) and Crs5 (copper resistant suppressor 5), are produced in *S. cerevisiae* [81, 82]. Metallothioneins are cysteine-rich proteins with essentially no secondary structure: they bind multiple copper atoms and prevent redox cycling or inappropriate binding interactions. Cup1 is a highly expressed, duplicated gene in yeast and is responsible for a significant proportion of the copper resistance in yeast [83]. Cup1 has unique cysteine spacing and is considered a copper-specific metallothionein. Crs5 has different cysteine spacing arrangement to Cup1 that is more similar to other eukaryotes metallothioneins, but it plays a much less significant role in protection against copper toxicity [83].

In *S. cerevisiae*, transcriptional regulation is the major mechanism used to balance the need for copper with its potential toxicity. Mac1 controls expression of transporters under copper-deficient growth conditions, upregulating transcription of the high-affinity copper transporter CTR1, as well as the metalloreductases involved in Cu(I) import, FRE1 and FRE7 (ferric reductase 1/7) [25, 26]. However, once copper reaches toxic levels, Ace1 induces the transcription of the metallothionein genes, CUP1 and CRS5 [84]. Both transcription factors bind copper via cysteine residues in copper-thiolate clusters [85]. The mechanism for copper translocation to the nucleus for binding to Mac1 and Ace1 remains unknown. In addition to transcriptional regulation, yeast can also use post-transcriptional internalization and degradation of Ctr1 at high copper concentrations to limit toxic influx of copper [86].

Copper deficiency and toxicity in yeast

Three major phenotypes of copper deficiency are observed in yeast strains lacking the gene CTR1, these phenotypes including growth defect on non-fermentable carbon sources, iron deficiency, and increased sensitivity to oxidative stress. These phenotypes can be mimicked, and exacerbated, by extracellular copper chelators (Figure 1.3). The decreased flow of copper to the trans-Golgi network via Atx1 impairs the metallation of Fet3 and therefore high-affinity iron transport [24, 87]. Under conditions of low iron, copper deficiency can be detected by a failure to grow on fermentable carbon sources (such as glucose) due to the requirement for iron to synthesize heme and iron sulfur that are essential in a number of pathways including ergosterol biosynthesis and assembly of the ribosome. The inability to metallate Sod1 due to copper deficiency results in increased oxidative stress; this phenotype manifests as a failure to grow under hyperoxic conditions and as a lysine and methionine auxotrophy [88]. These copper-related phenotypes were the basis for the identification of genes encoding the copper chaperones, ATX1 and CCS1. The final phenotype of copper deficiency is the loss of cytochrome c oxidase, which is observed as a failure to grow on non-fermentable carbon sources (such as glycerol) or as a decrease in oxygen consumption [58].

Yeasts are extremely tolerant to copper with some strains able to survive in 2.5 g/L of copper on rich complex medium [89]. The majority of this resistance is due to the high expression of Cup1. However, when uptake exceeds the buffering capacity of the cell, copper becomes toxic. It has been demonstrated that copper can displace iron sulfur cluster cofactors from the enzymes and inhibits biosynthesis of iron sulfur clusters by interacting with proteins involve in the iron sulfur cluster biosynthesis at elevated intracellular level. The toxicity of copper is caused by a combination of loss of iron sulfur containing enzymes, inactivation of

iron sulfur assembly proteins, oxidative stress including damage of lipids and proteins, and other inappropriate binding interactions including the displacement of other metal cofactors. Copper toxicity can be enhanced via addition of ionophores that dramatically increase the intracellular concentrations of copper [90, 91]. These ionophores demonstrate the critical role that membrane barriers play in suppressing copper toxicity and suggest that the controlled copper uptake also allows for the cell to manage copper stores appropriately. The demonstration of unexpected interaction of copper with numerous targets including kinases and regulatory proteins has opened the possibility for more copper-regulated pathways but also increases the possibilities for a spectrum of inappropriate binding reactions [92].

Unique insights from fission yeast

The fission yeast *Schizosaccharomyces pombe* has proven to be a valuable model organism for uncovering both the conserved pathways of copper homeostasis as well as some important nuances and some clear differences that can help us understand the complexity observed in multicellular organisms. Fission yeast has copper processes that include respiration, resistance to reactive oxygen species, iron transport, and xenobiotic amine metabolism because they have cytochrome c oxidase, superoxidase dismutase, multicopper ferroxidase, and a copper amine oxidase [93]. Many of the studies have focused on vegetative growth *S. pombe*; however, some very exciting and new work related to copper during sporulation and germination is opening many new directions in understanding the roles of copper and copper enzymes in this organism.

During vegetative growth, copper import is mediated by the CTR family proteins, Ctr4, Ctr5 [94]. Interestingly, in the fission yeast, these proteins function only in a complex. The

transit to the cell surface is dependent on the Met-X_3-Met motif of Ctr4. The complex is a heterotrimer consisting of two Ctr4 and one Ctr5 molecules. Copper transport by Ctr4/5 complex requires a Cys/Trp motif in extracellular N-terminal domain [95]. Similar to other CTR proteins, they contain methionine motifs MXM and MXXM that may serve as binding sites for copper. The primary structure of Ctr4 and Ctr5 comprises three transmembrane domains. In the second transmembrane domain, a MXXXM motif plays an important role in localization of Ctr4-Ctr5 complex at the plasma membrane. Structure function analysis revealed that MXXXM motif in Ctr5 is not required for Ctr4-Ctr5 complex to be functional, whereas the same motif in Ctr4 is necessary for proper localization of the complex. A similar motif with glycine,a GXXXG motif, within the third transmembrane domain is essential for trimeric assembly of the complex. It also has been shown that the carboxy-terminal region of Ctr5 regulates the exit of Ctr4-Ctr5 complex from the secretory pathway. In high-copper conditions, the trimeric complex undergoes internalization, whereas when copper becomes deficient, it will be recycled back to the cell surface.

As in budding yeast, the vacuole forms a storage pool of excess or recycled copper proteins, and an additional CTR protein, Ctr6, is embedded in the vacuolar membrane [93]. In contrast to the Ctr4/5 complex, Ctr6 functions as a homotrimer. The vacuolar location means that the amino-terminal region is located inside the vacuole, whereas its carboxy terminus is in the cytoplasm. A trimerization GXXXG motif is present in the third transmembrane domain of Ctr6.

To ensure sufficient cytoplasmic copper is available under copper stress ctr4, ctr5, and ctr6 are transcriptionally controlled by the Cuf1, a homolog of Mac1 in budding yeast [93]. Under copper limiting conditions, Cuf1 binds to copper-signaling element in promoters of the target genes and activates transcription. It has been shown that Cuf1 has copper dependent

nuclear localization. Under high-copper conditions, a cysteine-rich domain at carboxy-terminus and a leucine-rich nuclear export signal facilitate the exit of Cuf1 from the nucleus. The binding of copper to the cysteine residues in Cuf1 leads to a conformation that masks a nuclear localization sequence, leading to accumulation in the cytosol. This copper-bound state is not able to bind to the copper-signaling element suggesting this blocks transcription even if Cuf1 is in the nucleus.

In *S. pombe*, copper is required for meiosis and sporulation with ctr4, ctr5, or cuf1 mutants showing a germination arrest phenotype. After the initiation of meiosis, Ctr4 and Ctr5 are decreased, and the developing forespore acquires copper through the expression of a novel copper transporter from the major facilitator family called Mfc1 [96]. Mfc1 is not under the control of Cuf1; instead, it is controlled by a zinc-finger transcription factor called Mca1. Deletion of mfc1 or mca1 entails meiosis/sporulation defects; however, *mca1* mutants have a more severe defect, suggesting that it controls additional targets required for this program. When germination and outgrowth are initiated, the spore again activates the expression of Ctr4/5 system to acquire copper for growth. In these same studies, it was determined that labile copper within the germinating spore is retained in the spore body, and SOD1 activity is critical to correct development of the germ tube. Therefore, fission yeast is proving to be an excellent model to uncover previously unappreciated roles for copper. A limitation of all yeast models is that they cannot be used to examine some important aspect of copper homeostasis such as signaling of copper status between tissues [97].

Conclusion

Copper plays a critical role in normal physiology of eukaryotic cells. Yeast has been an effective and highly informative model for studying the mechanisms of copper delivery. Unexpected protein-protein interactions, changes to the copper proteome, and defining unique copper-binding sites continue to add levels of detail and richness to the roles of copper in the cell. Here we have focused on *S. cerevisiae* and briefly on *S. pombe*, but very important insights and advances have also come from a range of fungal organisms such as *Podospora anserina*, *Neurospora crassa, Cryptococcus neoformans*, and others. However, the yeast models cannot be used to examine some of the developing areas of copper homeostasis including signaling of copper status between tissues. Tissue-specific mutations in laboratory animals have been describing changes that induce changes in the importer and exporters of copper in other tissues. This is presumably to compensate and preserve copper homeostasis across the whole organism, single cell yeast models do not always exhibit the same "cooperative" responses. Biochemical techniques have improved to a point where previously undetectable copper-mediated cellular events are now being visualized. Synthesis of copper-specific fluorescent probes that can be used in imaging of live cells and the application of synchrotron X-ray technology has enabled the study of several molecular level events that are tied to exchangeable pools of copper. The creation of more soluble and sensitive probes and better resolution for data collection will allow for detailed investigations of copper-related cellular events in response to different biotic and abiotic stressors.

References

1. Rees EM, Thiele DJ (2004) From aging to virulence: forging connections through the study of copper homeostasis in eukaryotic microorganisms. Curr Opin Microbiol 7:175–184. https://doi.org/10.1016/j.mib.2004.02.004

2. Culotta VC, Lin SJ, Schmidt P, Klomp LW, Casareno RL, Gitlin J (1999) Intracellular pathways of copper trafficking in yeast and humans. Adv Exp Med Biol 448:247–254. https://doi.org/10.1007/978-1-4615-4859-1_22

3. Puig S, Thiele DJ (2002) Molecular mechanisms of copper uptake and distribution. Curr Opin Chem Biol 6:171–180. https://doi.org/10.1016/s1367-5931(02)00298-3

4. Banci L, Bertini I, Calderone V, Della-Malva N, Felli IC, Neri S, Pavelkova A, Rosato A (2009) Copper(I)-mediated protein-protein interactions result from suboptimal interaction surfaces. Biochem J 422:37–42. https://doi.org/10.1042/BJ20090422

5. Banci L, Bertini I, Ciofi-Baffoni S, Kozyreva T, Zovo K, Palumaa P (2010) Affinity gradients drive copper to cellular destinations. Nature 465:645–648. https://doi.org/10.1038/nature09018

6. Rae TD, Schmidt PJ, Pufahl RA, Culotta VC, O'Halloran TV (1999) Undetectable intracellular free copper: The requirement of a copper chaperone for superoxide dismutase. Science 284:805–808. https://doi.org/10.1126/science.284.5415.805

7. Carroll MC, Girouard JB, Ulloa JL, Subramaniam JR, Wong PC, Valentine JS, Culotta VC (2004) Mechanisms for activating Cu- and Zn-containing superoxide dismutase in the absence of the CCS Cu chaperone. Proceedings of the National Academy of Sciences of the United States of America 101:5964–5969. https://doi.org/10.1073/pnas.0308298101

8. Culotta VC, Yang M, O'Halloran TV (2006) Activation of superoxide dismutases: Putting the metal to the pedal. Biochimica et Biophysica Acta (BBA) - Molecular Cell Research 1763:747–758. https://doi.org/10.1016/j.bbamcr.2006.05.003

9. Westin G, Schaffner W (1988) A zinc-responsive factor interacts with a metal-regulated enhancer element (MRE) of the mouse metallothionein-I gene. The EMBO Journal 7:3763–3770. https://doi.org/10.1002/j.1460-2075.1988.tb03260.x

10. Heuchel R, Radtke F, Georgiev O, Stark G, Aguet M, Schaffner W (1994) The transcription factor MTF-1 is essential for basal and heavy metal-induced metallothionein gene expression. The EMBO Journal 13:2870–2875. https://doi.org/10.1002/j.1460-2075.1994.tb06581.x

11. Askwith C, Eide D, Van Ho A, Bernard PS, Li L, Davis-Kaplan S, Sipe DM, Kaplan J (1994) The *FET3* gene of S. cerevisiae encodes a multicopper oxidase required for ferrous iron uptake. Cell 76:403–410. https://doi.org/10.1016/0092-8674(94)90346-8

12. Davis-Kaplan SR, Askwith CC, Bengtzen AC, Radisky D, Kaplan J (1998) Chloride is an allosteric effector of copper assembly for the yeast multicopper oxidase Fet3p: An unexpected role for intracellular chloride channels. Proceedings of the National Academy of Sciences of the United States of America 95:13641–13645. https://doi.org/10.1073/pnas.95.23.13641

13. Gaxiola RA, Yuan DS, Klausner RD, Fink GR (1998) The yeast CLC chloride channel functions in cation homeostasis. Proceedings of the National Academy of Sciences of the United States of America 95:4046–4050. https://doi.org/10.1073/pnas.95.7.4046

14. Wu X, Kim H, Seravalli J, Barycki JJ, Hart PJ, Gohara DW, Di Cera E, Jung WH, Kosman DJ, Lee J (2016) Potassium and the K+/H+ Exchanger Kha1p Promote Binding of Copper to ApoFet3p Multi-copper Ferroxidase*. Journal of Biological Chemistry 291:9796–9806. https://doi.org/10.1074/jbc.M115.700500

15. Shi X, Stoj C, Romeo A, Kosman DJ, Zhu Z (2003) Fre1p Cu2+ Reduction and Fet3p Cu1+ Oxidation Modulate Copper Toxicity in *Saccharomyces cerevisiae**. Journal of Biological Chemistry 278:50309–50315. https://doi.org/10.1074/jbc.M307019200

16. Sturtz LA, Diekert K, Jensen LT, Lill R, Culotta VC (2001) A Fraction of Yeast Cu,Zn-Superoxide Dismutase and Its Metallochaperone, CCS, Localize to the Intermembrane Space of Mitochondria: A PHYSIOLOGICAL ROLE FOR SOD1 IN GUARDING AGAINST MITOCHONDRIAL OXIDATIVE DAMAGE*. Journal of Biological Chemistry 276:38084–38089. https://doi.org/10.1074/jbc.M105296200

17. Tainer JA, Getzoff ED, Richardson JS, Richardson DC (1983) Structure and mechanism of copper, zinc superoxide dismutase. Nature 306:284–287. https://doi.org/10.1038/306284a0

18. Reddi AR, Culotta VC (2013) SOD1 Integrates Signals from Oxygen and Glucose to Repress Respiration. Cell 152:224–235. https://doi.org/10.1016/j.cell.2012.11.046

19. Cobine PA, Pierrel F, Winge DR (2006) Copper trafficking to the mitochondrion and assembly of copper metalloenzymes. Biochimica et Biophysica Acta (BBA) - Molecular Cell Research 1763:759–772. https://doi.org/10.1016/j.bbamcr.2006.03.002

20. Tsukihara T, Aoyama H, Yamashita E, Tomizaki T, Yamaguchi H, Shinzawa-Itoh K, Nakashima R, Yaono R, Yoshikawa S (1996) The Whole Structure of the 13-Subunit Oxidized Cytochrome c Oxidase at 2.8 Å. Science 272:1136–1144. https://doi.org/10.1126/science.272.5265.1136

21. Carr HS, Winge DR (2003) Assembly of cytochrome c oxidase within the mitochondrion. Accounts of Chemical Research 36:309–316. https://doi.org/10.1021/ar0200807

22. Leary SC, Winge DR, Cobine PA (2009) "Pulling the plug" on cellular copper: The role of mitochondria in copper export. Biochimica et Biophysica Acta (BBA) - Molecular Cell Research 1793:146–153. https://doi.org/10.1016/j.bbamcr.2008.05.002

23. Aller SG, Unger VM (2006) Projection structure of the human copper transporter CTR1 at 6-Å resolution reveals a compact trimer with a novel channel-like architecture. Proceedings of the National Academy of Sciences 103:3627–3632. https://doi.org/10.1073/pnas.0509929103

24. Dancis A, Yuan DS, Haile D, Askwith C, Eide D, Moehle C, Kaplan J, Klausner RD (1994) Molecular characterization of a copper transport protein in S. cerevisiae: An unexpected role for copper in iron transport. Cell 76:393–402. https://doi.org/10.1016/0092-8674(94)90345-X

25. Gross C, Kelleher M, Iyer VR, Brown PO, Winge DR (2000) Identification of the Copper Regulon in *Saccharomyces cerevisiae* by DNA Microarrays*. Journal of Biological Chemistry 275:32310–32316. https://doi.org/10.1074/jbc.M005946200

26. Yamaguchi-Iwai Y, Serpe M, Haile D, Yang W, Kosman DJ, Klausner RD, Dancis A (1997) Homeostatic Regulation of Copper Uptake in Yeast via Direct Binding of MAC1 Protein to Upstream Regulatory Sequences of*FRE1* and *CTR1* *. Journal of Biological Chemistry 272:17711–17718. https://doi.org/10.1074/jbc.272.28.17711

27. De Feo CJ, Aller SG, Siluvai GS, Blackburn NJ, Unger VM (2009) Three-dimensional structure of the human copper transporter hCTR1. Proceedings of the National Academy of Sciences 106:4237–4242. https://doi.org/10.1073/pnas.0810286106

28. Eisses JF, Kaplan JH (2005) The Mechanism of Copper Uptake Mediated by Human CTR1: A MUTATIONAL ANALYSIS*. Journal of Biological Chemistry 280:37159–37168. https://doi.org/10.1074/jbc.M508822200

29. Xiao Z, Wedd AG (2002) A C-terminal domain of the membrane copper pump Ctr1 exchanges copper(I) with the copper chaperone Atx1. Chem Commun (Camb) 588–589. https://doi.org/10.1039/b111180a

30. Peña MMO, Puig S, Thiele DJ (2000) Characterization of the *Saccharomyces cerevisiae* High Affinity Copper Transporter Ctr3*. Journal of Biological Chemistry 275:33244–33251. https://doi.org/10.1074/jbc.M005392200

31. Hassett R, Dix DR, Eide DJ, Kosman DJ (2000) The Fe(II) permease Fet4p functions as a low affinity copper transporter and supports normal copper trafficking in Saccharomyces cerevisiae. Biochem J 351 Pt 2:477–484

32. Cohen A, Nelson H, Nelson N (2000) The Family of *SMF* Metal Ion Transporters in Yeast Cells*. Journal of Biological Chemistry 275:33388–33394. https://doi.org/10.1074/jbc.M004611200

33. Hassett R, Kosman DJ (1995) Evidence for Cu(II) Reduction as a Component of Copper Uptake by *Saccharomyces cerevisiae*(∗). Journal of Biological Chemistry 270:128–134. https://doi.org/10.1074/jbc.270.1.128

34. Fu D, Beeler TJ, Dunn TM (1995) Sequence, mapping and disruption of CCC2, a gene that cross-complements the Ca2+-sensitive phenotype of csg1 mutants and encodes a P-type ATPase belonging to the Cu2+-ATPase subfamily. Yeast 11:283–292. https://doi.org/10.1002/yea.320110310

35. Yuan DS, Stearman R, Dancis A, Dunn T, Beeler T, Klausner RD (1995) The Menkes/Wilson disease gene homologue in yeast provides copper to a ceruloplasmin-like oxidase required for iron uptake. Proceedings of the National Academy of Sciences 92:2632–2636. https://doi.org/10.1073/pnas.92.7.2632

36. Banci L, Bertini I, Ciofi-Baffoni S, Huffman DL, O'Halloran TV (2001) Solution Structure of the Yeast Copper Transporter Domain Ccc2a in the Apo and Cu(I)-loaded States*. Journal of Biological Chemistry 276:8415–8426. https://doi.org/10.1074/jbc.M008389200

37. Huffman DL, O'Halloran TV (2001) Function, Structure, and Mechanism of Intracellular Copper Trafficking Proteins. Annual Review of Biochemistry 70:677–701. https://doi.org/10.1146/annurev.biochem.70.1.677

38. Banci L, Bertini I, Cantini F, Felli IC, Gonnelli L, Hadjiliadis N, Pierattelli R, Rosato A, Voulgaris

P (2006) The Atx1-Ccc2 complex is a metal-mediated protein-protein interaction. Nat Chem Biol 2:367–368. https://doi.org/10.1038/nchembio797

39. Cobine PA, Ojeda LD, Rigby KM, Winge DR (2004) Yeast Contain a Non-proteinaceous Pool of Copper in the Mitochondrial Matrix*. Journal of Biological Chemistry 279:14447–14455. https://doi.org/10.1074/jbc.M312693200

40. Cobine PA, Pierrel F, Bestwick ML, Winge DR (2006) Mitochondrial Matrix Copper Complex Used in Metallation of Cytochrome Oxidase and Superoxide Dismutase*. Journal of Biological Chemistry 281:36552–36559. https://doi.org/10.1074/jbc.M606839200

41. Vest KE, Leary SC, Winge DR, Cobine PA (2013) Copper Import into the Mitochondrial Matrix in *Saccharomyces cerevisiae* Is Mediated by Pic2, a Mitochondrial Carrier Family Protein*. Journal of Biological Chemistry 288:23884–23892. https://doi.org/10.1074/jbc.M113.470674

42. Palmieri F (2004) The mitochondrial transporter family (SLC25): physiological and pathological implications. Pflugers Arch - Eur J Physiol 447:689–709. https://doi.org/10.1007/s00424-003-1099-7

43. Vest KE, Wang J, Gammon MG, Maynard MK, White OL, Cobine JA, Mahone WK, Cobine PA (2016) Overlap of copper and iron uptake systems in mitochondria in Saccharomyces cerevisiae. Open Biol 6:150223. https://doi.org/10.1098/rsob.150223

44. Rees EM, Thiele DJ (2007) Identification of a Vacuole-associated Metalloreductase and Its Role in Ctr2-mediated Intracellular Copper Mobilization*. Journal of Biological Chemistry 282:21629–21638. https://doi.org/10.1074/jbc.M703397200

45. Rees EM, Lee J, Thiele DJ (2004) Mobilization of Intracellular Copper Stores by the Ctr2 Vacuolar Copper Transporter*. Journal of Biological Chemistry 279:54221–54229. https://doi.org/10.1074/jbc.M411669200

46. Pufahl RA, Singer CP, Peariso KL, Lin SJ, Schmidt PJ, Fahrni CJ, Culotta VC, Penner-Hahn JE, O'Halloran TV (1997) Metal ion chaperone function of the soluble Cu(I) receptor Atx1. Science 278:853–856. https://doi.org/10.1126/science.278.5339.853

47. Arnesano F, Banci L, Bertini I, Huffman DL, O'Halloran TV (2001) Solution Structure of the Cu(I) and Apo Forms of the Yeast Metallochaperone, Atx1,. Biochemistry 40:1528–1539. https://doi.org/10.1021/bi0014711

48. Huffman DL, O'Halloran TV (2000) Energetics of Copper Trafficking between the Atx1 Metallochaperone and the Intracellular Copper Transporter, Ccc2*. Journal of Biological Chemistry 275:18611–18614. https://doi.org/10.1074/jbc.C000172200

49. Portnoy ME, Rosenzweig AC, Rae T, Huffman DL, O'Halloran TV, Culotta VC (1999) Structure-Function Analyses of the ATX1 Metallochaperone*. Journal of Biological Chemistry 274:15041–15045. https://doi.org/10.1074/jbc.274.21.15041

50. Xiao Z, Loughlin F, George GN, Howlett GJ, Wedd AG (2004) C-Terminal Domain of the Membrane Copper Transporter Ctr1 from Saccharomyces cerevisiae Binds Four Cu(I) Ions as a Cuprous-Thiolate Polynuclear Cluster: Sub-femtomolar Cu(I) Affinity of Three Proteins Involved in Copper Trafficking. J Am Chem Soc 126:3081–3090. https://doi.org/10.1021/ja0390350

51. Oxygen-induced maturation of SOD1: a key role for disulfide formation by the copper chaperone CCS - PMC. https://www.ncbi.nlm.nih.gov/pmc/articles/PMC1150991/. Accessed 30 Mar 2024

52. Schmidt PJ, Rae TD, Pufahl RA, Hamma T, Strain J, O'Halloran TV, Culotta VC (1999) Multiple Protein Domains Contribute to the Action of the Copper Chaperone for Superoxide Dismutase*. Journal of Biological Chemistry 274:23719–23725. https://doi.org/10.1074/jbc.274.34.23719

53. Lamb AL, Wernimont AK, Pufahl RA, Culotta VC, O'Halloran TV, Rosenzweig AC (1999) Crystal structure of the copper chaperone for superoxide dismutase. Nat Struct Biol 6:724–729. https://doi.org/10.1038/11489

54. Lamb AL, Torres AS, O'Halloran TV, Rosenzweig AC (2000) Heterodimer formation between superoxide dismutase and its copper chaperone. Biochemistry 39:14720–14727. https://doi.org/10.1021/bi002207a

55. Culotta VC, Klomp LWJ, Strain J, Casareno RLB, Krems B, Gitlin JD (1997) The Copper Chaperone for Superoxide Dismutase*. Journal of Biological Chemistry 272:23469–23472. https://doi.org/10.1074/jbc.272.38.23469

56. Schmidt PJ, Kunst C, Culotta VC (2000) Copper Activation of Superoxide Dismutase 1 (SOD1) *in Vivo*. Journal of Biological Chemistry 275:33771–33776. https://doi.org/10.1074/jbc.M006254200

57. Garber Morales J, Holmes-Hampton GP, Miao R, Guo Y, Münck E, Lindahl PA (2010) Biophysical Characterization of Iron in Mitochondria Isolated from Respiring and Fermenting Yeast. Biochemistry 49:5436–5444. https://doi.org/10.1021/bi100558z

58. Glerum DM, Shtanko A, Tzagoloff A (1996) Characterization of COX17, a Yeast Gene Involved in Copper Metabolism and Assembly of Cytochrome Oxidase*. Journal of Biological Chemistry 271:14504–14509. https://doi.org/10.1074/jbc.271.24.14504

59. Banci L, Bertini I, Ciofi-Baffoni S, Janicka A, Martinelli M, Kozlowski H, Palumaa P (2008) A Structural-Dynamical Characterization of Human Cox17*. Journal of Biological Chemistry 283:7912–7920. https://doi.org/10.1074/jbc.M708016200

60. Banci L, Bertini I, Cefaro C, Ciofi-Baffoni S, Gallo A (2011) Functional Role of Two Interhelical Disulfide Bonds in Human Cox17 Protein from a Structural Perspective*. Journal of Biological Chemistry 286:34382–34390. https://doi.org/10.1074/jbc.M111.246223

61. Banci L, Bertini I, Ciofi-Baffoni S, Hadjiloi T, Martinelli M, Palumaa P (2008) Mitochondrial copper(I) transfer from Cox17 to Sco1 is coupled to electron transfer. Proceedings of the National Academy of Sciences 105:6803–6808. https://doi.org/10.1073/pnas.0800019105

62. Horng Y-C, Cobine PA, Maxfield AB, Carr HS, Winge DR (2004) Specific Copper Transfer from the Cox17 Metallochaperone to Both Sco1 and Cox11 in the Assembly of Yeast Cytochrome *c* Oxidase*. Journal of Biological Chemistry 279:35334–35340. https://doi.org/10.1074/jbc.M404747200

63. Abajian C, Rosenzweig AC (2006) Crystal structure of yeast Sco1. J Biol Inorg Chem 11:459–466. https://doi.org/10.1007/s00775-006-0096-7

64. Schulze M, Rödel G (1988) SCO1, a yeast nuclear gene essential for accumulation of mitochondrial

cytochrome c oxidase subunit II. Mol Gen Genet 211:492–498. https://doi.org/10.1007/BF00425706

65. Nittis T, George GN, Winge DR (2001) Yeast Sco1, a Protein Essential for Cytochrome *c*Oxidase Function Is a Cu(I)-binding Protein*. Journal of Biological Chemistry 276:42520–42526. https://doi.org/10.1074/jbc.M107077200

66. Horng Y-C, Leary SC, Cobine PA, Young FBJ, George GN, Shoubridge EA, Winge DR (2005) Human Sco1 and Sco2 Function as Copper-binding Proteins*. Journal of Biological Chemistry 280:34113–34122. https://doi.org/10.1074/jbc.M506801200

67. Glerum DM, Shtanko A, Tzagoloff A (1996) *SCO1* and *SCO2* Act as High Copy Suppressors of a Mitochondrial Copper Recruitment Defect in *Saccharomyces cerevisiae**. Journal of Biological Chemistry 271:20531–20535. https://doi.org/10.1074/jbc.271.34.20531

68. Beers J, Glerum DM, Tzagoloff A (2002) Purification and Characterization of Yeast Sco1p, a Mitochondrial Copper Protein*. Journal of Biological Chemistry 277:22185–22190. https://doi.org/10.1074/jbc.M202545200

69. Carr HS, George GN, Winge DR (2002) Yeast Cox11, a Protein Essential for Cytochrome *c*Oxidase Assembly, Is a Cu(I)-binding Protein*. Journal of Biological Chemistry 277:31237–31242. https://doi.org/10.1074/jbc.M204854200

70. Hiser L, Di Valentin M, Hamer AG, Hosler JP (2000) Cox11p Is Required for Stable Formation of the CuBand Magnesium Centers of Cytochrome c Oxidase. Journal of Biological Chemistry 275:619–623. https://doi.org/10.1074/jbc.275.1.619

71. Khalimonchuk O, Bestwick M, Meunier B, Watts TC, Winge DR (2010) Formation of the redox cofactor centers during Cox1 maturation in yeast cytochrome oxidase. Mol Cell Biol 30:1004–1017. https://doi.org/10.1128/MCB.00640-09

72. Khalimonchuk O, Bird A, Winge DR (2007) Evidence for a Pro-oxidant Intermediate in the Assembly of Cytochrome Oxidase. Journal of Biological Chemistry 282:17442–17449. https://doi.org/10.1074/jbc.m702379200

73. Horn D, Barrientos A (2008) Mitochondrial copper metabolism and delivery to cytochrome c oxidase. IUBMB Life 60:421–429. https://doi.org/10.1002/iub.50

74. Bode M, Woellhaf MW, Bohnert M, van der Laan M, Sommer F, Jung M, Zimmermann R, Schroda M, Herrmann JM (2015) Redox-regulated dynamic interplay between Cox19 and the copper-binding protein Cox11 in the intermembrane space of mitochondria facilitates biogenesis of cytochrome c oxidase. Mol Biol Cell 26:2385–2401. https://doi.org/10.1091/mbc.E14-11-1526

75. Ghosh A, Pratt AT, Soma S, Theriault SG, Griffin AT, Trivedi PP, Gohil VM (2016) Mitochondrial disease genes COA6, COX6B and SCO2 have overlapping roles in COX2 biogenesis. Hum Mol Genet 25:660–671. https://doi.org/10.1093/hmg/ddv503

76. Pacheu-Grau D, Bareth B, Dudek J, Juris L, Vögtle F-N, Wissel M, Leary SC, Dennerlein S, Rehling P, Deckers M (2015) Cooperation between COA6 and SCO2 in COX2 Maturation during Cytochrome c Oxidase Assembly Links Two Mitochondrial Cardiomyopathies. Cell Metabolism 21:823–833. https://doi.org/10.1016/j.cmet.2015.04.012

77. Stroud DA, Maher MJ, Lindau C, Vögtle F-N, Frazier AE, Surgenor E, Mountford H, Singh AP, Bonas M, Oeljeklaus S, Warscheid B, Meisinger C, Thorburn DR, Ryan MT (2015) COA6 is a mitochondrial complex IV assembly factor critical for biogenesis of mtDNA-encoded COX2. Human Molecular Genetics 24:5404–5415. https://doi.org/10.1093/hmg/ddv265

78. Gross DP, Burgard CA, Reddehase S, Leitch JM, Culotta VC, Hell K (2011) Mitochondrial Ccs1 contains a structural disulfide bond crucial for the import of this unconventional substrate by the disulfide relay system. Mol Biol Cell 22:3758–3767. https://doi.org/10.1091/mbc.E11-04-0296

79. Horn D, Al-Ali H, Barrientos A (2008) Cmc1p is a conserved mitochondrial twin CX9C protein involved in cytochrome c oxidase biogenesis. Mol Cell Biol 28:4354–4364. https://doi.org/10.1128/MCB.01920-07

80. Wegner SV, Sun F, Hernandez N, He C (2011) The tightly regulated copper window in yeast. Chem Commun 47:2571–2573. https://doi.org/10.1039/c0cc04292g

81. Culotta VC, Howard WR, Liu XF (1994) CRS5 encodes a metallothionein-like protein in Saccharomyces cerevisiae. Journal of Biological Chemistry 269:25295–25302. https://doi.org/10.1016/s0021-9258(18)47246-8

82. Winge DR, Nielson KB, Gray WR, Hamer DH (1985) Yeast metallothionein. Sequence and metal-binding properties. Journal of Biological Chemistry 260:14464–14470. https://doi.org/10.1016/s0021-9258(17)38592-7

83. Jensen LT, Howard WR, Strain JJ, Winge DR, Culotta VC (1996) Enhanced Effectiveness of Copper Ion Buffering by CUP1 Metallothionein Compared with CRS5 Metallothionein in Saccharomyces cerevisiae. Journal of Biological Chemistry 271:18514–18519. https://doi.org/10.1074/jbc.271.31.18514

84. Gralla EB, Thiele DJ, Silar P, Valentine JS (1991) ACE1, a copper-dependent transcription factor, activates expression of the yeast copper, zinc superoxide dismutase gene. Proc Natl Acad Sci U S A 88:8558–8562. https://doi.org/10.1073/pnas.88.19.8558

85. Dameron CT, Winge DR, George GN, Sansone M, Hu S, Hamer D (1991) A copper-thiolate polynuclear cluster in the ACE1 transcription factor. Proc Natl Acad Sci U S A 88:6127–6131. https://doi.org/10.1073/pnas.88.14.6127

86. Ooi CE, Rabinovich E, Dancis A, Bonifacino JS, Klausner RD (1996) Copper-dependent degradation of the Saccharomyces cerevisiae plasma membrane copper transporter Ctr1p in the apparent absence of endocytosis. The EMBO Journal 15:3515–3523. https://doi.org/10.1002/j.1460-2075.1996.tb00720.x

87. Lin S-J, Pufahl RA, Dancis A, O'Halloran TV, Culotta VC (1997) A Role for the Saccharomyces cerevisiae ATX1 Gene in Copper Trafficking and Iron Transport. Journal of Biological Chemistry 272:9215–9220. https://doi.org/10.1074/jbc.272.14.9215

88. Liu XF, Elashvili I, Gralla EB, Valentine JS, Lapinskas P, Culotta VC (1992) Yeast lacking superoxide dismutase. Isolation of genetic suppressors. Journal of Biological Chemistry 267:18298–18302. https://doi.org/10.1016/s0021-9258(19)36959-5

89. Adamo GM, Brocca S, Passolunghi S, Salvato B, Lotti M (2012) Laboratory evolution of copper

tolerant yeast strains. Microb Cell Fact 11:1–1. https://doi.org/10.1186/1475-2859-11-1

90. Foster AW, Dainty SJ, Patterson CJ, Pohl E, Blackburn H, Wilson C, Hess CR, Rutherford JC, Quaranta L, Corran A, Robinson NJ (2014) A chemical potentiator of copper-accumulation used to investigate the iron-regulons of Saccharomyces cerevisiae. Mol Microbiol 93:317–330. https://doi.org/10.1111/mmi.12661

91. Reeder NL, Kaplan J, Xu J, Youngquist RS, Wallace J, Hu P, Juhlin KD, Schwartz JR, Grant RA, Fieno A, Nemeth S, Reichling T, Tiesman JP, Mills T, Steinke M, Wang SL, Saunders CW (2011) Zinc pyrithione inhibits yeast growth through copper influx and inactivation of iron-sulfur proteins. Antimicrob Agents Chemother 55:5753–5760. https://doi.org/10.1128/AAC.00724-11

92. Turski ML, Brady DC, Kim HJ, Kim B-E, Nose Y, Counter CM, Winge DR, Thiele DJ (2012) A novel role for copper in Ras/mitogen-activated protein kinase signaling. Mol Cell Biol 32:1284–1295. https://doi.org/10.1128/MCB.05722-11

93. Beaudoin J, Ekici S, Daldal F, Ait-Mohand S, Guérin B, Labbé S (2013) Copper transport and regulation in Schizosaccharomyces pombe. Biochem Soc Trans 41:1679–1686. https://doi.org/10.1042/BST2013089

94. Beaudoin J, Thiele DJ, Labbé S, Puig S (2011) Dissection of the relative contribution of the Schizosaccharomyces pombe Ctr4 and Ctr5 proteins to the copper transport and cell surface delivery functions. Microbiology (Reading) 157:1021–1031. https://doi.org/10.1099/mic.0.046854-0

95. Okada M, Miura T, Nakabayashi T (2017) Comparison of extracellular Cys/Trp motif between Schizosaccharomyces pombe Ctr4 and Ctr5. Journal of Inorganic Biochemistry 169:97–105. https://doi.org/10.1016/j.jinorgbio.2017.01.009

96. Plante S, Ioannoni R, Beaudoin J, Labbé S (2014) Characterization of Schizosaccharomyces pombe copper transporter proteins in meiotic and sporulating cells. J Biol Chem 289:10168–10181. https://doi.org/10.1074/jbc.M113.543678

97. Hlynialuk CJ, Ling B, Baker ZN, Cobine PA, Yu LD, Boulet A, Wai T, Hossain A, El Zawily AM, McFie PJ, Stone SJ, Diaz F, Moraes CT, Viswanathan D, Petris MJ, Leary SC (2015) The Mitochondrial Metallochaperone SCO1 Is Required to Sustain Expression of the High-Affinity Copper Transporter CTR1 and Preserve Copper Homeostasis. Cell Reports 10:933–943. https://doi.org/10.1016/j.celrep.2015.01.019

Chapter 2: Identification of Residues Define SLC25A3 Transport Specificity

From Xinyu Zhu, Aren Boulet, Katherine M Buckley, Casey B Phillips, Micah G Gammon, Laura E Oldfather, Stanley A Moore, Scot C Leary, Paul A Cobine (2021) "Mitochondrial copper and phosphate transporter specificity was defined early in the evolution of eukaryotes", *eLife* 10:e64690.

Abstract

Mitochondrial matrix contains a copper pool that is required for metallation of proteins that are essential for various cellular physiologies including cytochrome *c* oxidase and copper-zinc superoxide dismutase. In mammals, the mitochondrial carrier family protein SLC25A3 translocate both copper and phosphate into the matrix, while in *Saccharomyces cerevisiae* the transport of these substrates is partitioned across two paralogs: PIC2 and MIR1. To dissect the transport specificity of SLC25A3, we explored the evolutionary relationships of the yeast orthologs across the eukaryotic tree of life. Phylogenetic analyses revealed that PIC2-like and MIR1-like orthologs are present in all major eukaryotic supergroups, indicating an ancient gene duplication created these paralogs. To link this phylogenetic signal to protein function, we used structural modeling and site-directed mutagenesis to identify residues involved in copper and phosphate transport. Based on these analyses, we generated an L175A variant of mouse SLC25A3 that retains the ability to transport copper but not phosphate. This work highlights the utility of using an evolutionary framework to uncover amino acids involved in substrate recognition by mitochondrial carrier family proteins.

Introduction

Mitochondrial carrier family (MCF/SLC25) proteins comprise the largest family of mitochondrial inner membrane (IM) proteins and are responsible for transporting numerous substrates, including Krebs cycle intermediates, nucleoside di- and triphosphates for energy metabolism and nucleotide replication, amino acids for degradation or maintenance of the urea cycle, and essential metals such as copper (Cu) and iron [1, 2]. Structurally, MCF transporters consist of a conserved fold with three repeats that contain two transmembrane helices connected by a short α-helical loop [3, 4]. The repeated structural elements and variable copy numbers across eukaryotic phyla (53 in humans and 35 in yeast) suggest that this complex gene family arose through multiple duplication events followed by neofunctionalization as substrate needs changed. From an evolutionary perspective, one hypothesis is that protein families with multiple substrates (e.g., enzymes and transporters) arose as generalists that duplicated to evolve specificity over time [5, 6]. However, the evolutionary history of the MCF/SLC25 family with respect to substrate specificity remains largely unexplored.

Our current mechanistic understanding of MCF activity is based on in vitro transport assays, phenotypic observations made in mutant cells, and structures of the ADP-ATP carrier [4, 7]. This MCF transporter adopts two conformational states: the cytoplasmic, or c-state, which is open to the intermembrane space (IMS), and the matrix, or m-state, which is open to the matrix [8, 9]. All MCFs have six transmembrane helices with conserved motifs that allow for formation of salt bridges and the close packing of helices that are critical to the mechanism of transport [4].

Cu is required in mitochondria for the stability and activity of the IM-embedded enzyme cytochrome c oxidase (COX) and the IMS-localized superoxide dismutase. The Cu used in the

assembly of these enzymes comes from a pool in the mitochondrial matrix [10]. *PIC2* has been identified as a mitochondrial Cu transporter in *Saccharomyces cerevisiae* [11]. Mutant yeast strains lacking *PIC2* (Δ*pic2*) are deficient in COX activity and have lower mitochondrial Cu levels than isogenic wild-type (WT) strains [11]. Silver (Ag^+) is an isoelectronic with Cu and has been widely used as a tool to interrogate Cu homeostasis [12]. In yeast, inclusion of Ag^+ in the growth medium restricts Cu uptake and results in a mitochondrial Cu deficiency [11]. This competition assay allowed us to identify yeast strains that could not overcome the Cu limitations imposed by Ag^+ when grown on non-fermentable carbon sources. We also exploited the toxicity of Ag^+ uptake to assay the Cu transport activity of these MCFs when expressed in *Lactococcus lactis* [11, 13, 14]. Expression of MCFs in *L. lactis* has been used extensively to assess transport activity because the proteins are readily expressed and inserted into the cytoplasmic membrane [15–18]. The expression of a Cu-transporting MCF (e.g., *PIC2*) in *L. lactis* reduces the minimal inhibitory concentration of Ag^+ required for growth arrest.

Although *PIC2* has also been implicated in phosphate transport [19–22], the primary phosphate-transporting MCF in yeast is *MIR1* [20, 23]. *PIC2* expression can complement Δ*mir1* phenotypes and mitochondria from Δ*mir1*Δ*pic2* yeast strains regain phosphate transport activity when *PIC2* is overexpressed [19], suggesting that phosphate can be a *PIC2* substrate. However, it is unlikely that this transport activity is physiologically relevant under normal conditions as *PIC2* deletion does not result in phosphate deficiency phenotypes in yeast. Based on these findings, we predict that while yeast PIC2 and MIR1 have specialized to transport specific substrates, *PIC2* retains some promiscuity for both Cu and phosphate transport. In contrast, humans express a single paralog of PIC2/MIR1, SLC25A3, which serves as the major mitochondrial transporter of both Cu and phosphate [13, 24]. Cells lacking SLC25A3 exhibit a

Cu-dependent COX assembly defect [13]. Additionally, SLC25A3 transports Cu when recombinantly expressed and reconstituted in liposomes or when heterologously expressed in *L. lactis* [13]. Similarly, both phenotypic and biochemical assays confirm that SLC25A3 is the major phosphate transporter in mammalian mitochondria [21, 24, 25].

These findings highlight a major unanswered question in our understanding of MCFs. Specifically, what differences enable the transport of single versus multiple substrates? Using newly available phylogenomic data from diverse lineages that span the major eukaryotic supergroups, we used an evolutionary framework to infer residues in the PIC2-MIR1 MCF subfamily that likely mediate substrate selection and transport. By coupling phylogenetic analyses with biochemical assays, we have uncovered residues required for transport of Cu and phosphate. Further, we demonstrate that Cu transport to the mitochondrial matrix is directly responsible for the COX deficiency observed in cells lacking SLC25A3.

Materials and Methods

Yeast strains, culture conditions, and standard methods

Yeast strains used in this study were BY4741 (*MATa, leu2*Δ*, met15*Δ*, ura3*Δ*, his3*Δ) parental and the isogenic kanMX4- containing mutant, purchased from Invitrogen. All cultures were grown in YP (1% yeast extract, 2% peptone) medium or synthetic defined medium with 1-2% glucose added as a carbon source. Copper sulfate was added the medium when increased copper conditions were required. All cells were grown in a shaking incubator at 30 °C.

Expression in *L. lactis*

L. lactis cells transformed with vector (pNZ8148 [MoBiTec]) alone or pNZ8148 carrying yeast MIR1, PIC2, or site-directed PIC2 mutants were grown overnight at 30°C in M17 medium with 0.5% glucose and 10 µg/mL chloramphenicol. To determine Ag^+ toxicity, cells were grown in a 96-well plate containing M17 medium plus 1 ng/mL nisin and increasing concentrations of Ag^+ (0-250 µM) or AsO_4^{3-} (0-2.5 mM). Controls containing M17 without nisin or M17 plus Ag^+ or AsO_4^{3-} without nisin were included. Optical density at 600 nm was used to assess growth after 24 hr. Percent growth was quantified by comparing to the optical density of the same genotype in nisin alone.

Immunoblot and activity assays

This study used monoclonal antibodies raised against COX1 (Abcam ab14734), a rabbit polyclonal antibody TOM40 (ProteinTech 18409-1-AP), and a rabbit polyclonal antibody raised against the Keyhole limpet hemocyanin conjugated SLC25A3 peptide CRMQVDPQKYKGIFNGSVTLKED (Pacific Immunology). For *L. lactis* extracts, we used rabbit polyclonal antibody raised against a PIC2 peptide [11]. COX activity was determined by monitoring the decrease in absorbance at 550 nm of chemically reduced cytochrome *c* in the presence of whole cell or mitochondrial extracts [26]. All activities were normalized to protein concentration, then converted to percentage of maximum control value.

Elemental analysis

Samples were digested in 40% nitric acid by boiling for 1 hr in capped, acid washed tubes, diluted in ultra-pure, metal-free water, and analyzed by ICP-OES (Perkin Elmer, Optima 7300DV) versus acid-washed blanks. Concentrations were determined from a standard curve constructed with serial dilutions of two commercially available mixed metal standards (Optima).

Blanks of nitric acid with and without ‘metal-spikes’ were analyzed to ensure reproducibility.

Ligand uptake assay

Isolated, intact mitochondria were incubated with CuL complex for variable time points and removed from solution by centrifugation. Resultant supernatants were separated on silica-coated TLC plates (GE Healthcare) using a mixture of 90% ethanol and 10% acetic acid. TLC plates were analyzed for fluorescence on an ImageQuant LAS 4000 (GE Healthcare) using the Cy2 detection filter set (EX 492/5, EM 510/5). Bands were quantified using ImageJ.

Fluorescence anisotropy

CuL was diluted to give a fluorescence intensity of ~30 AU using an excitation maximum of 320 nm and emission maximum of 400 nm (slit widths were set to 5 nm). Inclusion bodies and MCF protein incorporated into liposomes were added in 1-5 µL increments. Anisotropy was measured using a PerkinElmer Life Sciences LS55 spectrofluorimeter.

Miscellaneous methods

Western blots were performed using mouse anti-His (Invitrogen) followed by Cy3-conjugated goat anti-mouse (GenScript). Blots were observed using an ImageQuant LAS 4000 (GE Healthcare). Egg yolk phospholipids were prepared using the Folch method of extraction in methanol and chloroform.

Results

MIR1 does not transport Cu

To determine if MIR1 can transport Cu in addition to phosphate, we exploited the fact that MCF proteins insert into the cytoplasmic membrane of *L. lactis* in an active state and that Cu transport activity in this system can be detected by growth arrest in the presence of Ag^{+} [11, 17] (Figure 2.1A). This assay was also used to assess phosphate transport by quantifying the growth rates of *L. lactis* strains expressing MCF genes in the presence of the toxic phosphate mimetic arsenate (AsO_4^{3-}). The plasmid carries MCFs is transformed into *L. lactis*, then nisin is added to the media to induce the expression of the transformed MCFs. In the presence of 80 µM Ag^{+}, the growth of *L. lactis* expressing *PIC2*, but not *MIR1* or an empty vector (EV), was significantly inhibited (Figure 2.1B). In contrast, the growth of *L. lactis* expressing *MIR1* or *PIC2* was inhibited to the same extent when cultured in 1.6 mM AsO_4^{3-} relative to a control strain harboring the EV (Figure 2.1C). These data show that in *L. lactis MIR1* is capable of transporting the phosphate mimetic AsO_4^{3-} but not the Cu mimetic Ag^{+}.

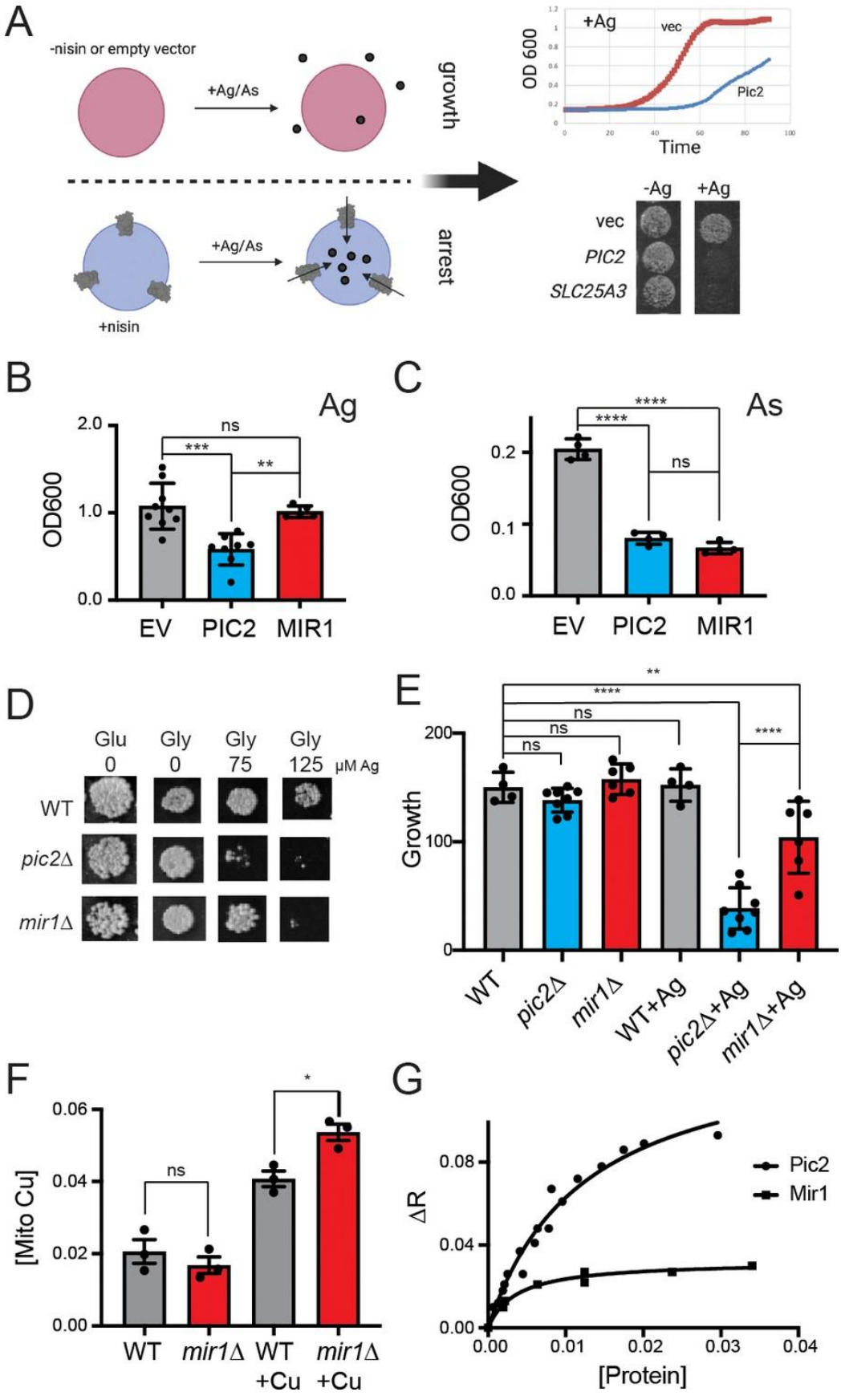
A
-nisin or empty vector
+Ag/As
growth
+Ag
vec
Pic2
OD 600
Time
+Ag/As
arrest
+nisin
-Ag
+Ag
vec
PIC2
SLC25A3
B
Ag
OD600
ns
***
**
EV
PIC2
MIR1
C
As
OD600
****
****
ns
EV
PIC2
MIR1
D
Glu 0
Gly 0
Gly 75
Gly 125
µM Ag
WT
pic2Δ
mir1Δ
E
Growth
ns
ns
ns
****
**
WT
pic2Δ
mir1Δ
WT+Ag
pic2Δ+Ag
mir1Δ+Ag
F
[Mito Cu]
ns
*
WT
mir1Δ
WT +Cu
mir1Δ +Cu
G
ΔR
Pic2
Mir1
[Protein]

Figure 2.1: *S. cerevisiae* MIR1 does not transport Cu.

(**A**) Schematic representation of the *L. lactis* expression system used to quantify transport characteristics. Survival is determined by the growth rate in liquid culture or by visual inspection of cells grown on agar plates containing Ag^+ or AsO_4^{3-} in the presence of the inducer nisin. (**B**) Quantification of the growth of *L. lactis* expressing empty vector (EV), *S. cerevisiae* PIC2, or *S. cerevisiae* MIR1 after 12 hr in 80 µM Ag^+-containing media (n > 5). (**C**) Quantification of the growth of *L. lactis* expressing EV, PIC2, or MIR1 after 12 hr in 1.6 mM AsO_4^{3-}-containing media (n = 5). (**D**) Wild-type (WT), *pic2*Δ, or *mir1*Δ yeast grown in rich medium with a fermentable (Glu: glucose) or a non-fermentable (glycerol: Gly) carbon source in the absence (0) or presence of Ag^+ (75 or 125 µM). All strains were spotted on media as a 10^{-3} dilution of OD_{600} of 1. (**E**) Densitometry measurements of serial dilutions (10, 10^2, 10^3, 10^4) of cells in **D** on Glu, Gly, and Gly plus 75 µM Ag (WT n = 4, *pic2*Δ n = 8, *mir1*Δ n = 6). (**F**) Cu content of purified intact mitochondria from *mir1*Δ cells assayed by Inductively coupled plasma - optical emission spectrometry (ICP-OES) and compared with that of parental WT cells. Both strains were grown in YP medium with glucose as a carbon source containing 10 µM bathocuproinedisulfonic acid (BCS) or 100 µM Cu (+Cu) (n = 3). (**G**) Fluorescence anisotropy (FA) of CuL (Ex320, Em400) upon the addition of reconstituted PIC2 or MIR1 in proteoliposomes prepared from extracted egg yolk lipids. Control FA of equal quantity of lipids without protein added was subtracted from each data point. Protein concentrations were determined by Bradford assay, and curves are fit with a nonlinear regression that assumes a single binding site. In all panels, data are plotted as the mean ± standard deviation of the measurements and a one-way ANOVA was used for statistical analysis; ns: not statistically significant; *p<0.05, **p<0.01, ***p<0.001, ****p<0.0001.

Consistent with the previous results [11], we find that the growth of yeast lacking *PIC2* is severely compromised on a non-fermentable carbon source in the presence of 75 μM Ag^+ due to a Cu deficiency in mitochondria (Figure 2.1 D, E). In contrast, yeast lacking *MIR1*only exhibited a mild growth defect relative to the isogenic WT strain at this Ag^+ concentration (Figure 2.1 D, E). Exposure to 125 μM Ag^+ led to a growth defect in both *mir1*Δ and *pic2*Δ yeast but not in the isogenic WT strain (Figure 2.1 D). To further establish that MIR1 is incapable of Cu transport activity, we quantified mitochondrial Cu levels by inductively coupled optical emission spectroscopy. Cu levels in mitochondria from *mir1*Δ yeast cells were similar to those isolated from WT cells (Figure 2.1 F). In yeast mitochondria, Cu is stably bound by a fluorescent, non-proteinaceous ligand (CuL). Previously we used fluorescence anisotropy to investigate the binding of this fluorescent complex to purified *PIC2* and SLC25A3 [11, 13, 14]. The decreased levels of anisotropy observed for purified MIR1 compared to PIC2 showed limited interaction with the CuL complex and MIR1 (Figure 2.1 G). Thus, while the growth assays indicate that *MIR1* deletion can produce a Cu-dependent respiration defect at high Ag^+ concentrations, our biochemical data suggest that MIR1 does not transport Cu. Therefore, both MIR1 and PIC2 transport phosphate but only PIC2 can transport Cu.

Mitochondrial Cu and phosphate carriers duplicated early in the evolution of eukaryotes

It is not surprising that MCF proteins are present across all eukaryotes given their fundamental roles in maintaining cellular physiology. We hypothesize that Cu transport to mitochondria was an important consideration in eukaryo-genesis as it is required to maintain the activity of the electron transport chain and provide an advantage to the ancestral eukaryote [27]. Conservation of this activity across diverse organisms may provide a phylogenetic signal with which to resolve residues that dictate *PIC2* and *MIR1* substrate specificities. One hypothesis is that because ancient proteomes were smaller the transporters in these organisms were generalists that gained specificity as a consequence of gene duplication and subsequent sub-functionalization [5, 6, 28, 29].

To provide evolutionary context for the existing experimental data, which has nearly all been collected from mammals and yeast, we performed a phylogenetic analysis on MCF transporters from a broad range of eukaryotic lineages. We selected a set of 47 taxa that spanned the supergroups within the eukaryotic Tree of Life (eToL) [30]. Only taxa with complete nuclear and mitochondrial genome sequences were included to accurately enumerate gene duplications and losses, and to ensure that apparent losses were not due to incomplete datasets. From these genomes, a total of 2447 putative MCF family members were identified based on the presence of a mitochondrial carrier domain (PFAM domain PF00153). To distinguish *PIC2-MIR1* orthologs from other members of the MCF family, phylogenetic trees were constructed using the MCF proteins from each taxon as well as the complete set of yeast and human MCF proteins. Candidate sequences that clustered with *PIC2* or *MIR1* were retained for further analyses (92 of 2447 MCF sequences).

The amino acid sequences of these potential Cu and/or phosphate transporting proteins were aligned and subsequently used to reconstruct the evolutionary history of *PIC2-MIR1* orthologs across eukaryotes (Figure 2.2). Of the 92 sequences, 47 clustered with *S. cerevisiae PIC2* and are referred to as PIC2-like while 42 clustered with *S. cerevisiae MIR1* and are defined as MIR1-like. The remaining three sequences were more closely related to PIC2-MIR1 than other MCFs but nonetheless fell outside of these two well-supported clades (Figure 2.2).

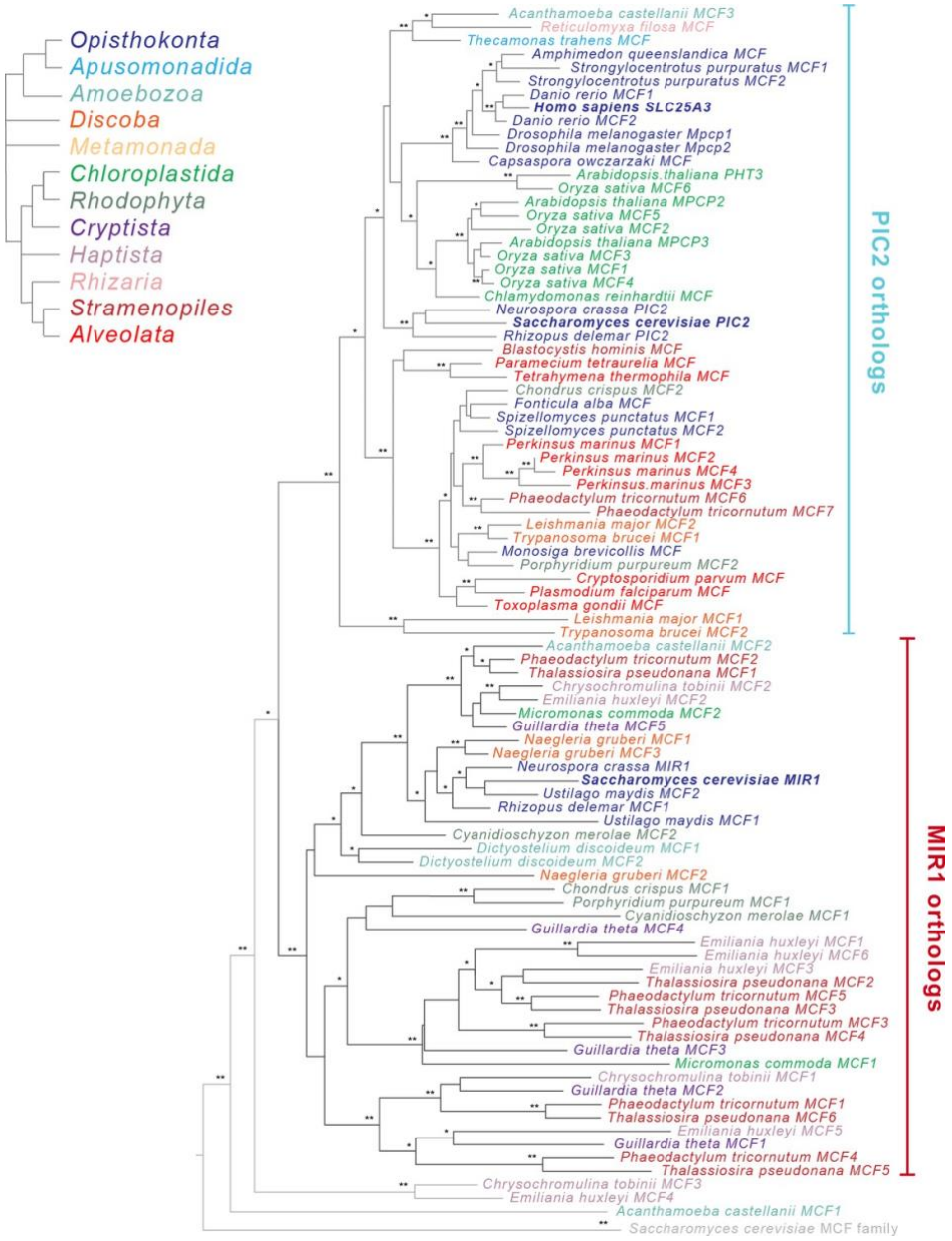

Figure 2.2: Phylogenetic analysis of the PIC2/MIR1 orthologs from 47 taxa reveals two major clades.

Amino acid sequences of the eukaryotic MIR1/PIC2/SLC25A3 orthologs were aligned with the complete set of mitochondrial carrier family (MCF) proteins from *S. cerevisiae*. The maximum-likelihood tree shown was constructed in iQ-TREE using a general codon exchange matrix for nuclear genes with amino acid frequencies determined empirically from the data and seven rate categories (LG+F+R7). Support for the nodes was calculated using 1000 replications and is indicated as follows: **>95%; *>75%. Taxa names for the MIR1/PIC2/SLC25A3 sequences are color-coded according to the eukaryotic Tree of Life supergroups as indicated; the *S. cerevisiae* MCF outgroup sequences (gray) have been collapsed to a single branch.

To estimate the timing of gene duplications and losses within eukaryotes, we overlaid the presence and/or absence of PIC2-like or MIR1-like sequences onto the established eToL tree (Figure 2.3 A). Recent phylogenomic analyses indicate that extant eukaryotes form nine supergroups [30]. Species from seven of these groups were included in this analysis: Amorphea, Discoba, Archaeplastida, TSAR (Telonemids, Stramenopiles, Alveolates, and Rhizaria), Haptista, Cryptista, and Metamonada. Two additional groups, CRuMs (Collodictyonids, Rigifilida, and Mantamonas) and Hemimastigophora, were not included due to the lack of complete nuclear genome sequences. *PIC2-MIR1* orthologs were present in each taxon analyzed except for those from Metamonada, which are anaerobic protists that secondarily lost mitochondria [31, 32]. This broad phylogenetic conservation suggests that the two paralogs were present within the last common eukaryotic ancestor (Figure 2.3 A).

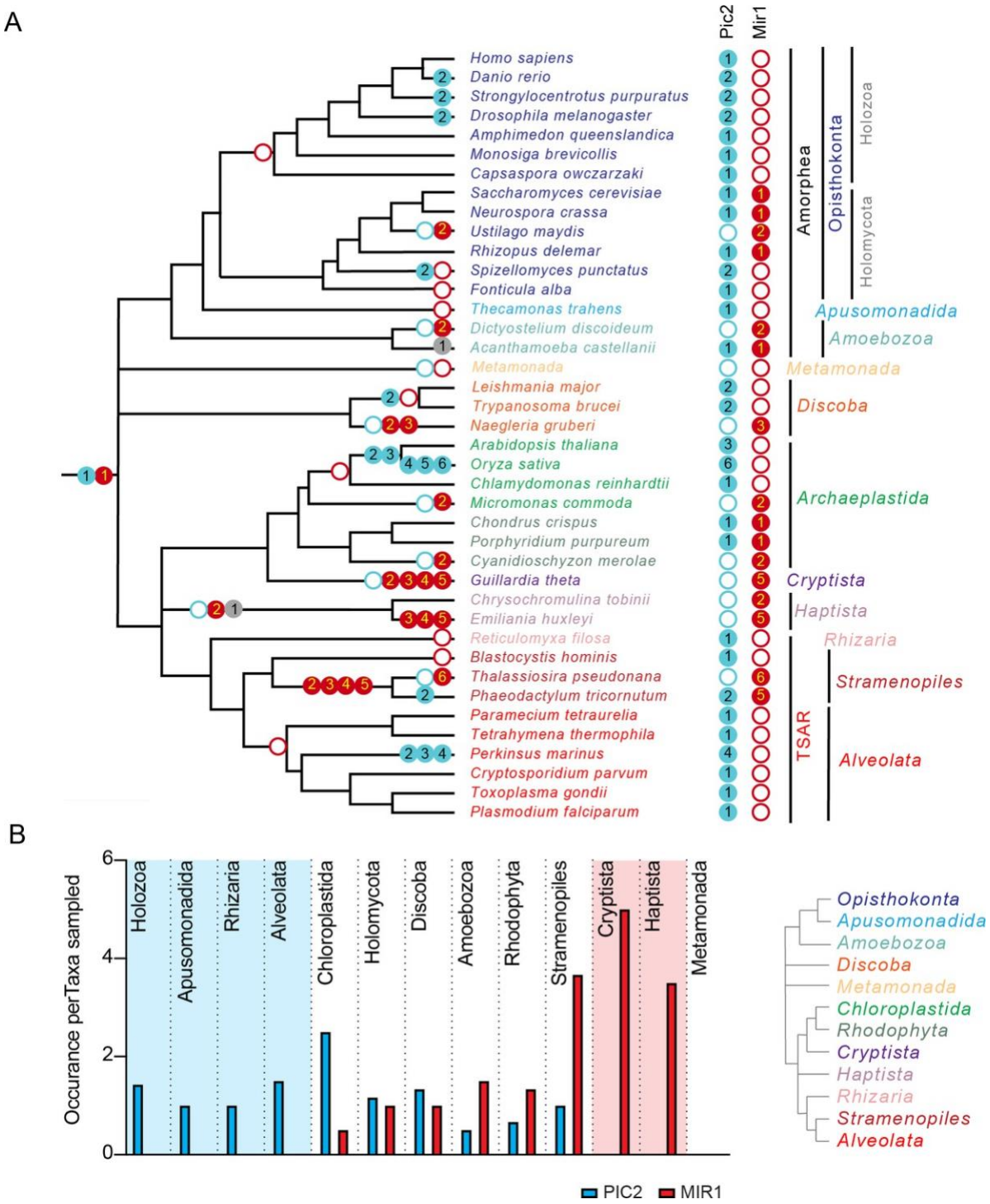

Figure 2.3: The PIC2/MIR1 family of mitochondrial carrier family transporters is ancient within eukaryotes.

(A) Using the presence or absence of orthologs within the eukaryotic lineages, we inferred the evolutionary timings of gene duplications (solid circles) and losses (hollow circles) of the PIC2-like (blue), MIR1-like (red), and other (gray) sequences. (B) The average number of PIC2 and MIR1 orthologs identified in the sampled taxa from eight of the nine eukaryotic supergroups.

Given the ancient origin of *PIC2* and *MIR1,* we first analyzed the presence and absence of orthologs within Amorphea, which consists of the opisthokonts (animals, fungi, and yeast), apusomonads, and amoebae [30]. MIR1-like sequences are absent from Holozoan taxa with this lineage retaining only *PIC2*-like transporters (Figure 2.3 A, B). In contrast, the fungal lineages (Holomycota) exhibit more variability in the numbers of *PIC2*-like and *MIR1*-like sequences (Figure 2.3 B). Single orthologs of each type are present in *S. cerevisiae* and the closely related *Neurospora crassa*. The only Amorphea taxa that lost *PIC2* are *Ustilago maydis* and *Dictyostelium discoideum,* which both have a *MIR1*duplication. Outside the Amorphea, the gene copy number of the *PIC2-MIR1* orthologs is more variable, which may reflect different evolutionary pressures on these transporters across lineages. Several lineages have lost either *PIC2* or *MIR1* and retained multiple copies of the remaining paralog (e.g., *PIC2*-like transporters within Chloroplastida and the alveolate *Perkinsus marinus* or the MIR1 duplications in Cryptista and Stramenopile lineages; Figure 2.3). This raises the possibility that, to compensate for the loss of the *MIR1* transporter, *PIC2* duplicated and convergently evolved additional substrate specificities. While there may be other constraints on this evolution, the loss of a *PIC2* ortholog is always accompanied by duplication of the *MIR1* ortholog. In contrast, a *PIC2*-like MCF is retained in all species that have a single *PIC2-MIR1* ortholog, indicating that the loss of *MIR1* does not always coincide with *PIC2* duplication.

Structural modeling of PIC2 suggests appropriate spatial organization of conserved residues that may coordinate Cu transport

We hypothesize that specific residues in *PIC2*-like proteins that confer the ability to transport Cu are absent in *MIR1*-like proteins, while amino acids conserved across *PIC2*- and *MIR1*-like proteins are required for both Cu and phosphate transport. To predict residues involved in substrate specificity, we modeled the *PIC2* sequence onto the c-state and m-state structures of the ADP/ATP carrier [8, 9]. To quantify sequence conservation at the level of individual residues independently of the evolutionary histories of the proteins, Shannon entropy was calculated for each position within an alignment of the *PIC2*-like sequences (Figure 2.4 A, B). Shannon entropy is one of the simplest and most common measures of conservation that can be calculated from multiple sequence alignments [33]. The Shannon entropy was calculated for each residue within alignments of the *PIC2*-like sequences and compared to the values determined from the complete *PIC2-MIR1* grouping. By integrating the structural models and phylogenetic analyses, we were able to visualize conserved residues as a surface representation (Figure 2.4 C–E). The *PIC2*-like orthologs show high conservation (Shannon entropy <0.5 suggesting that the residue is maintained across all forms of the protein in the multiple sequence alignment) in the aqueous binding pocket, while alignment with the complete *PIC2-MIR1* family further reveals a smaller subset of conserved residues. This analysis also detects conserved patches extending into the IMS and outside the aqueous binding pocket in the lipid bilayer that may be required for interactions with other components of the IM (Figure 2.4 D, E).

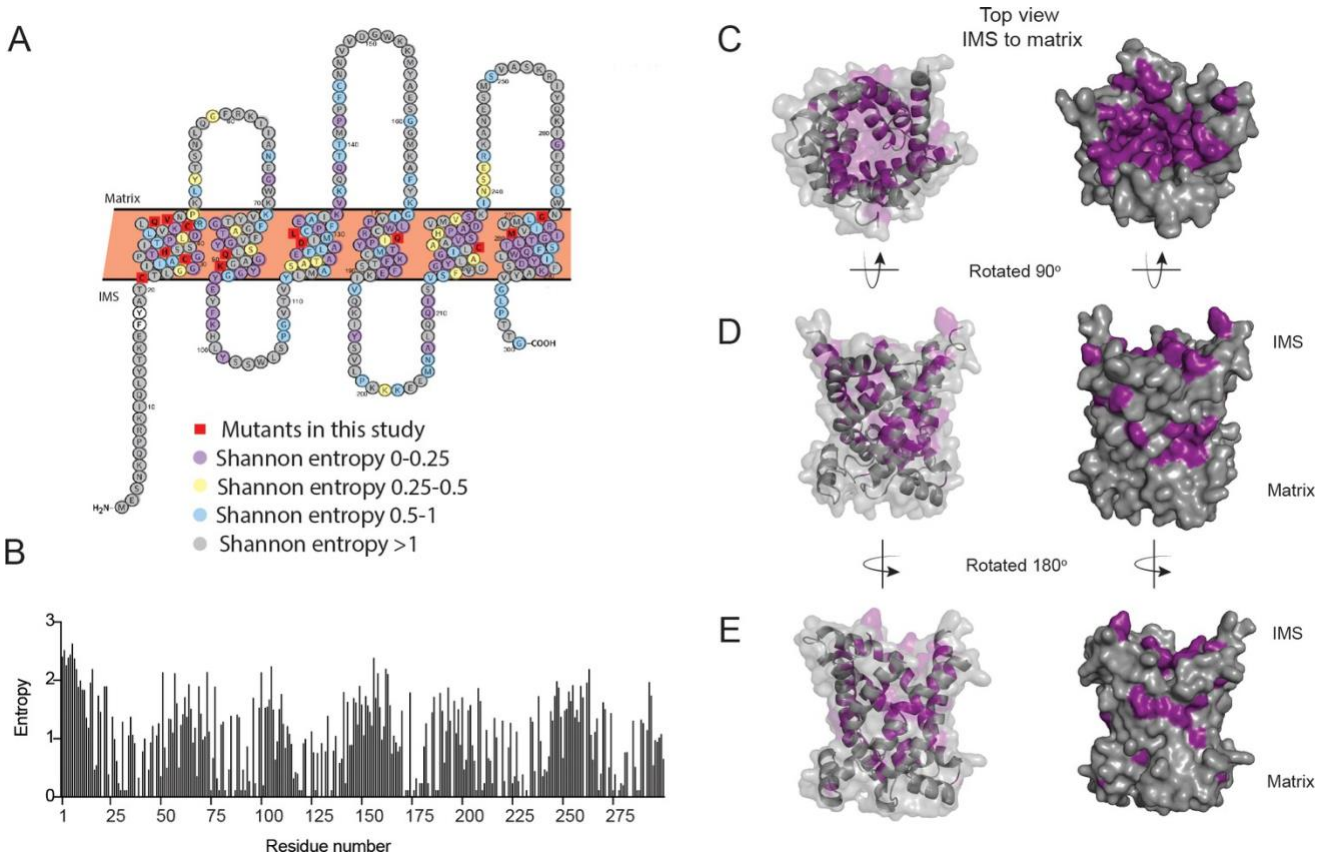

Figure 2.4: Conservation of residues in PIC2.

(**A**) A Protter representation of the *PIC2* amino acid sequence was generated and colored based on Shannon entropy scores for conservation of a given residue. (**B**) The Shannon entropy for each residue in *PIC2* based on all sequences in the *PIC2*-specific clade. (**C**) Structure of *PIC2* in the c-state viewed from the intermembrane space side, with conserved residues (Shannon entropy <0.5) highlighted in purple and all other residues shown in gray. (**D**) A 90° rotation of the structure to view it from side, and (**E**) a 180° rotation to view it from the opposite side.

To identify residues that mediate Cu transport, we initially focused on the well-established Cu-binding ligands Cys, His, and Met. Analysis of the *PIC2-MIR1* ortholog trees showed that histidine 33 (all residues are numbered according to the yeast *PIC2* sequence) is conserved in both the *PIC2* and *MIR1* clades (Figure 2.5). Cysteine 29 is conserved in the PIC2 clade and most *MIR1* proteins but is replaced with alanine in the *MIR1*-like transporters from lineages with multiple duplications (*Emiliania huxleyi, Thalassiosira pseudonana*, and *Phaeodactylum tricornutum*) (Figure 2.5). Cysteine 21 and Cys225 are strictly conserved among PIC2 orthologs, but not among MIR1 orthologs (Figure 2.5). Cysteine 44 is conserved in the *PIC2*-like clade, while *MIR1*-like orthologs have a conserved threonine in the equivalent position (Figure 2.5). The *PIC2*-like transporters that lack Cys44 are the *P. marinus*duplications, one of two copies of *PIC2* in *P. tricornutum*, and the single copy of *PIC2* in *N. crassa*. Analysis of the structural models revealed that Cys21, Cys29, Cys44, and His33 are positioned along one side of the aqueous binding pocket (Figure 2.5), whereas Cys225 is on the opposite side of this pocket. Cysteine 225 is positioned to interact with the peptide backbone of Cys182 (based on the alignments, this residue is only a cysteine in *S. cerevisiae*), which faces away from the aqueous binding pocket. Together, these data suggest that Cys21, Cys29, Cys44, and His33 may combine to form transient sites that bind Cu directly as it moves through the IM.

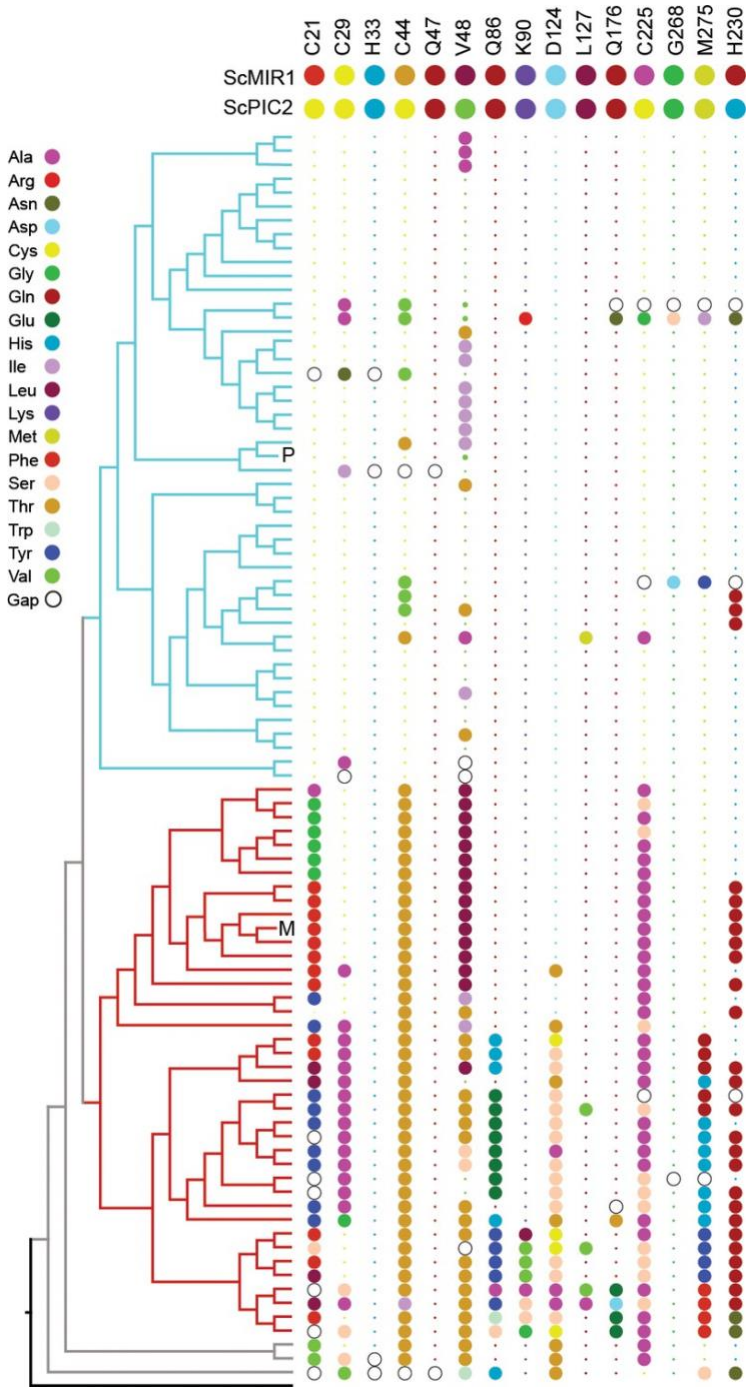

Figure 2.5: Conservation of selected residues in the PIC2/MIR1 family of transporters.

The tree topology is identical to that shown in Figure 2.2. Amino acids are colored according to the key, and insertion/deletion events that lead to gaps within the alignment are indicated by the hollow circles. P indicates position of *S. cerevisiae* PIC2, and M indicates *S. cerevisiae MIR1*. Small dots indicate that the residue is identical to that of *PIC2* (shown at the top), and large dots indicate differences.

Mutating structural elements and conserved contact points cause differential transport defects

To assess the functional importance of the Cys-His residues in Cu and/or phosphate transport, we altered these residues in the context of *S. cerevisiae PIC2* and expressed the mutants in *L. lactis*. To verify expression, protein content was assessed in *L. lactis* cells expressing the mutants versus EV controls. Although the levels of heterologous expression were too low to observe using Sypro Ruby, the mutant proteins were readily detectable upon immunoblot analysis (Figure 2.6 A). To assay Cu transport, we cultured each variant in media containing an Ag^{+} concentration that inhibited growth of *L. lactis* expressing WT *PIC2* but not of cells harboring an EV (Figure 2.1 A, Figure 2.6). *L. lactis* expressing C21A, C29A, H33A, C44A, and C225A *PIC2* mutants showed equal expression levels to WT *PIC2* (Figure 2.6 A) but displayed Ag^{+} resistance relative to *L. lactis* expressing WT *PIC2* (all $p<0.012$) (Figure 2.6 B), with the most resistance observed in the H33A mutant. However, these mutants also exhibited a growth defect relative to cells with an EV, suggesting that residue transport activity is present. Similarly, when Ag^{+} was replaced with AsO_4^{3-} to assess phosphate transport, *L. lactis* expressing each of the five *PIC2* mutants displayed increased resistance to AsO_4^{3-} (Figure 2.6 C), suggesting that these mutations also limit its transport.

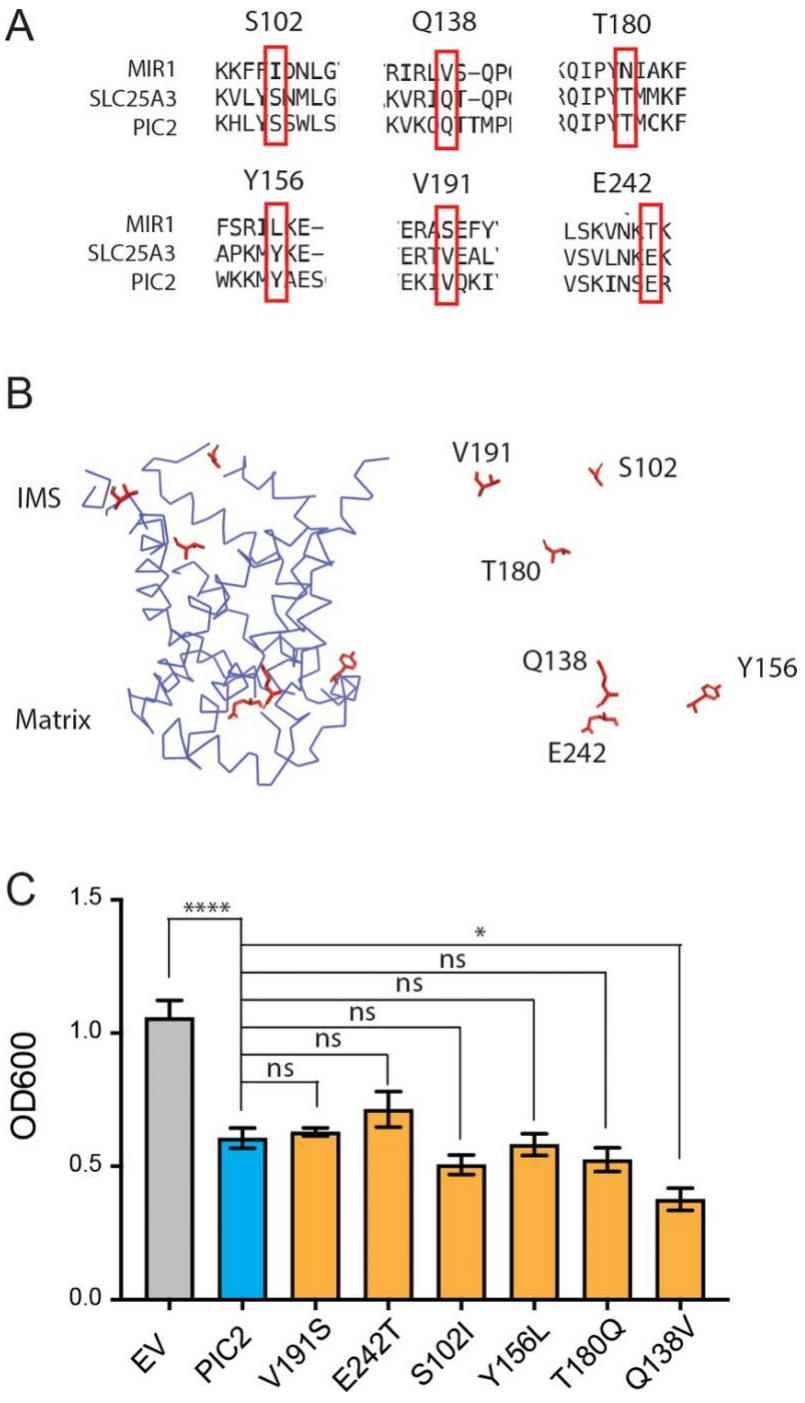

Figure 2.6: Substitution of PIC2 residues for MIR1 residues.

(**A**) Alignment of amino acid sequences from MIR1, PIC2, and SLC25A3. (**B**) Model of the c-state of PIC2 with residues mutated highlighted in sticks format and with the backbone cartoon representation removed. (**C**) Growth of *L. lactis* expressing empty vector (EV), wild-type PIC2 (WT), or a given PIC2 variant in which each of the listed residues was converted to an alanine in Ag^{+}-containing media. Each bar represents the median of six independent cultures with 95% confidence interval as error bars (*p<0.05, **p<0.01, ***p<0.001, ****p<0.0001 based on one-way ANOVA relative to PIC2 wild-type control).

Computational analyses predict that *S. cerevisiae* MCF transporters have three contact sites for substrate binding [3]. In *PIC2*, the proposed phosphate substrate contact points are Gln86 and Lys90 in transmembrane helix (TMH) 2, Gln176 in TMH4, and Met275 in TMH6 [3, 4, 8] (Figure 2.4). These residues are largely conserved in both the *PIC2*-like and *MIR1*-like clades (Figure 2.5), as is expected for transporters that share a substrate. We mutated each of these residues to alanine and assessed transport activity as described above. When expressed in *L. lactis*, the Q86A and Q176A mutants were expressed at WT levels (Figure 2.6 A) and were more resistant to Ag^{+} than WT *PIC2* (Figure 2.6 B) but less resistant than cells expressing EV. In contrast, the K90A and M275A mutants exhibited comparable Ag^{+} sensitivity to WT *PIC2* ($p>0.05$), suggesting that these substitutions do not affect Cu transport (Figure 2.6 B). The addition of AsO_4^{3-} to the media only inhibited the growth of cells expressing WT *PIC2*; cells expressing Q86A, K90A, Q176A, and M275A all grew at similar rates as cells expressing the EV (Figure 2.6 C).

Finally, we interrogated the functional significance of a subset of residues that were selected based on sequence conservation and our structural model: Gln47, Val48, Asp124, Leu127, and Gly268 (Figure 2.4 A). With very few exceptions, Gln47 is conserved among eukaryotic *PIC2-MIR1* orthologs (Figure 2.4 A, B and Figure 2.5). Val48 is part of a group of residues that appear to close the aqueous binding pocket in the c-state Asp124 interacts with Gln176 and is conserved among all *PIC2*-like orthologs and those transporters most closely related to yeast *MIR1* (Figure 2.5). Leu127 is conserved in all orthologs and interacts with Gln86 (Figure 2.4 A, B, Figure 2.5). Gly268 is maintained throughout the evolution of this protein family (Figure 2.4A, Figure 2.5). The Q47A variant was unstable in *L. lactis* (Figure 2.6 A), suggesting that it has been maintained across evolution for structural stability. The V48A variant

did not affect protein expression (Figure 2.6) or AsO_4^{3-} resistance. However, it did result in a significant difference in Ag^+ resistance compared to WT *PIC2* (Figure 2.6 B, C). The D124A *PIC2* mutant was stably expressed in *L. lactis* and more resistant to Ag^+ than WT *PIC2* (Figure 2.6 A) but less resistant than cells expressing EV, suggesting that it harbored residual Cu transport activity. When expressed in *L. lactis*, the L127A PIC2 variant showed WT expression (Figure 2.6 A) and equivalent susceptibility to Ag^+ as WT *PIC2* but was resistant to AsO_4^{3-} (Figure 2.6 B, C), indicating that this single substitution interferes with phosphate transport but does not prevent Cu transport. Finally, the G268A variant was unstable in *L. lactis* (Figure 2.6 A), suggesting that the increased resistance to Ag^+ and AsO_4^{3-} associated with the expression of this variant was due to decreased levels of the protein (Figure 2.6 B, C). We also tested a series of mutants that exchanged the residues found in yeast *PIC2* and mammalian SLC25A3 with those found in *MIR1*. Conversion of the *PIC2* residues Ser102, Tyr156, Thr180, Gln138, Glu242, and Val191 to the equivalent residues in *MIR1* did not affect the ability to transport Ag^+ (Figure 2.6). Collectively, the data from the *L. lactis* assays show that mutating individual residues can impair the transport of both substrates, or Cu or phosphate alone.

Mitochondrial transport of phosphate but not Cu is compromised in a Leu175 mutant of SLC25A3

Based on the His33 and Leu127 *PIC2* mutant data from *L. lactis*, we investigated the transport activity of the equivalent variants in murine SLC25A3 (His75 and Leu175). Consistent with the failure of the H33A *PIC2* mutant to transport Ag^+ or AsO_4^{3-} in *L. lactis*, expression of the H75A SLC25A3 variant in immortalized mouse embryonic fibroblasts (MEFs) with floxed (WT) or collapsed (KO) *Slc25a3* alleles did not rescue the COX deficiency of the knock-out (KO) cells (Figure 2.7 A, B). Conversely, expression of the L175A SLC25A3 variant was able to reverse

the COX defect (Figure 2.7 B). Immunoblot analysis showed that the L175A mutant was present in mitochondria and increased steady-state COX1 levels (Figure 2.7 C). Consistent with our previous studies using a mitochondrially targeted Cu sensor [13, 34], we found that total mitochondrial Cu content was significantly reduced in KO MEFs and increased in KO MEFs expressing the L175A variant (Figure 2.7 D).

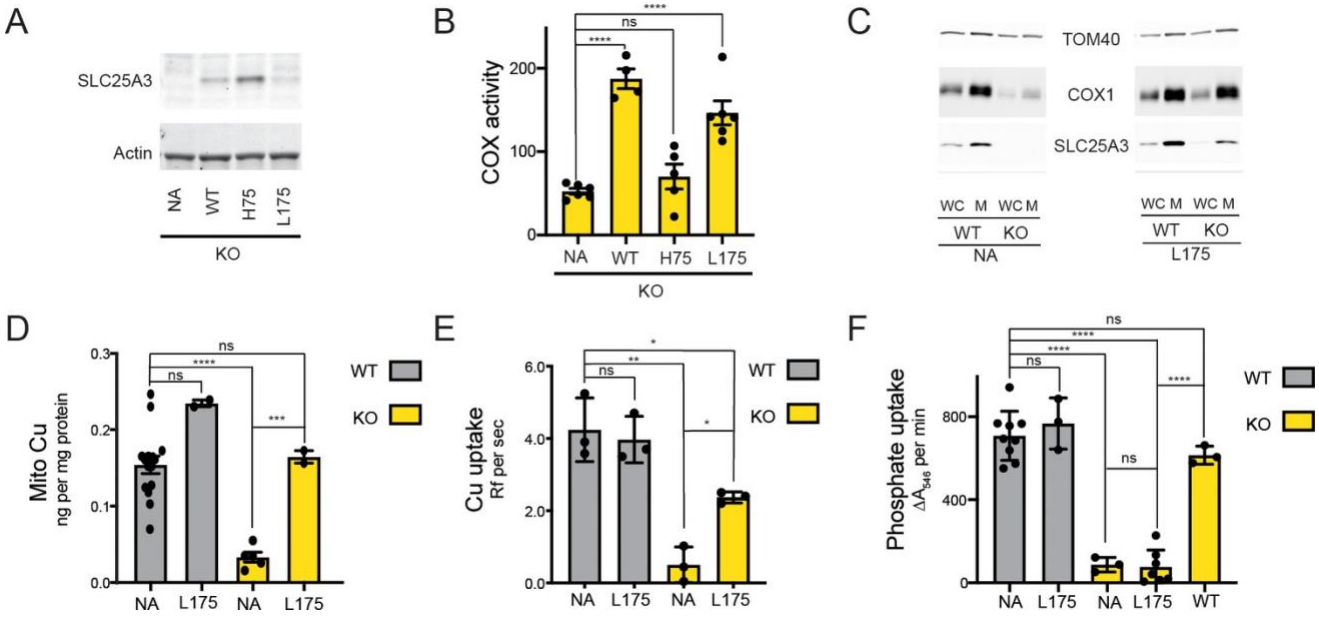

Figure 2.7: The SLC25A3 L175A variant restores mitochondrial Cu levels and rescues the cytochrome c oxidase (COX) deficiency in KO MEFs.

(**A**) Immunoblot analysis of SLC25A3 abundance in *Slc25a3 KO* MEFs alone or those transduced with wild-type SLC25A3 (WT), a H75A variant (H75), or a L175A variant (L175). Actin served as an internal loading control. (**B**) COX activity in KO MEFs alone (n = 6) or transduced with WT SLC25A3 (n = 4), a H75A variant (H75) (n = 5), or a L175A variant (L175) (n = 6). ns, $p>0.05$, ****, $p<0.0001$ based on a one-way ANOVA. (**C**) Immunoblot analysis of SLC25A3, TOM40, and COX1 abundance in whole cells (WC) or isolated mitochondrial (M) from WT or KO MEFs alone (NA) or transduced with the SLC25A3 L175A variant (L175). (**D**) Total Cu levels in mitochondria from WT or KO cells as in (**C**), determined by ICP-OES. (**E**) Cu uptake in mitochondrially derived liposomes created by the membranes of mitochondria in (**C**) with additional lipids. Liposomes contain Phen Green to monitor the uptake of Cu. (**F**) Mitochondrial swelling rate in the presence of phosphate as a measure of phosphate uptake.

Reconstitution of MCF proteins in liposomes has been used extensively to assess substrate transport and specificity [21, 35–39]. Liposomes created from mitochondrial membranes of WT but not KO MEFs were able to transport Cu (Figure 2.7 E). The Cu transport defect in KO-derived liposomes was reversed upon expression of the L175A variant (Figure 2.7 E). To assess phosphate uptake, mitochondrial swelling in the presence of phosphate was measured [19, 24]. Intact mitochondria isolated from KO cells had a phosphate uptake defect compared to WT that was rescued by expressing WT SLC25A3 but not the L175A variant (Figure 2.7 F). Taken together, these data show that the L175A mutant is able to transport Cu but not phosphate in mitochondria and that this Cu transport activity is sufficient to rescue COX activity.

Discussion

The mechanisms that mediate MCF transporter specificity remain largely unknown. Although two recent studies have shown that single residue changes can modulate MCF substrate specificity [40, 41], the majority of investigations have focused on deficiencies in the transport of one substrate, and few have assessed substrate promiscuity. Here, we directly addressed this issue by focusing on Cu and phosphate transport, which, in mammals, is mediated by the single MCF transporter SLC25A3. Multiple studies clearly connect SLC25A3 to phosphate transport, and mutations in *SLC25A3* lead to skeletal muscle myopathy and heart disease in humans [13, 24, 42–45] and cardiac hypertrophy in mice[24]. MEFs derived from the heart-specific *Slc25a3* knockout mouse exhibit clear COX and SOD1 defects that can be rescued by overexpression of a *Slc25a3* cDNA or addition of Cu [13]. These data are complemented by in vitro assays in liposomes showing Cu transport by purified SLC25A3 and by Ag^+ growth arrest phenotypes associated with its expression in *L. lactis* [13]. The data presented in this study provide the first experimental evidence of a missense mutation that separates Cu and phosphate transport, and firmly establish that physiological defects in COX and SOD1 are due to impaired Cu transport rather than a secondary consequence of decreased phosphate transport.

Evolutionary history of mitochondrial Cu-phosphate transporters

Our evolutionary analyses of the Cu-phosphate transporters were prompted by the observation that *S. cerevisiae PIC2* and *MIR1* exhibit substrate specificity, whereas the mammalian ortholog SLC25A3 is responsible for the transport of both Cu and phosphate. Selection on genes with multiple functions can constrain diversity to avoid negative effects associated with losing one of these functions. Therefore, gene duplications serve as important

sources for evolutionary selection and refinement. Resulting duplications can be retained for the original function, specialized for new functions, refined to enhance an existing function or allow for increased expression by gene dosage; if none of these outcomes occur, the duplicate gene is lost [46–52]. In *S. cerevisiae*, *PIC2* and *MIR1* are partially redundant for phosphate transport [19]. However, mutation of *MIR1* in *S. cerevisiae* is sufficient to produce phosphate-related phenotypes suggesting that, under most conditions, the ability of *PIC2* to transport phosphate is unable to compensate for loss of *MIR1* function [13, 19]. Instead, the *PIC2* sequence appears to be optimized for Cu transport. Similarly, we show here that *MIR1* lacks clear Cu transport activity even though *mir1*Δ yeast exhibit increased susceptibility to Cu restriction compared to WT cells. Our phylogenetic analyses of *PIC2* and *MIR1* sequences suggest that the gene duplication that created these two orthologs was an ancient event, and that evolutionary interplay between these two substrate specificities may have occurred multiple times throughout eukaryotic evolution.

The loss of *MIR1* has occurred multiple times in eukaryotes, an event that is likely facilitated by the dual specificity of PIC2. *SLC25A3* is essential in mammals as the homozygous deletion is embryonic lethal. While mammals do express two SLC25A3 isoforms, isoform A is expressed primarily in heart and skeletal muscle whereas isoform B is expressed in all tissues [21, 24, 42]. Therefore, it is unlikely that the isoforms provide the functional redundancy that would be afforded via gene duplication or retention of *MIR1*.

Understanding Cu transport

Copper transport in eukaryotic cells has been an area of intense research since the discovery of cytosolic copper chaperones [53, 54], and the observation that there is vanishingly little freely available copper in the cytosol [55]. These early findings have been refined to

recognize that, in addition to proteins, multiple cytosolic ligands contribute to the regulation of metal trafficking and target binding [56]. The recruitment of Cu to mitochondria was initially attributed to COX17 due to its dual localization in cytosol and IMS [57]. However, COX is fully functional when COX17 is artificially restricted to the IMS by an inner membrane tether [58], suggesting that its critical role in holoenzyme assembly involves local, redox regulated delivery of Cu to the accessory proteins SCO1/2 and COX11 [59, 60]. Consistent with a mitochondrially restricted function for COX17 in Cu handling, yeast cells lacking this gene accumulate wild-type levels of Cu in mitochondria [61]. In fact, attempts to isolate a protein that delivers Cu to mitochondria led to the identification of a non-proteinaceous ligand (CuL) that accumulates in the matrix [26, 27, 62–64]. Although the molecular identity of this ligand remains unknown, its biophysical properties have been used to suggest that the ligand contributes to buffering cytosolic Cu and facilitating uptake of Cu into mitochondria [26, 64]. *PIC2* is able to transport both the CuL purified from the mitochondrial matrix as well as ionic Cu in both liposomes and the *L. lactis* system [65]. It is unclear if the transport of the CuL proceeds as an intact complex or if Cu is released from the ligand during transport. The ionic Cu in our transport assays is Cu^{+} due to presence of an exogenous reductant (*e.g.,* ascorbate) or the endogenous reductant menaquinone in *L. lactis* [66] and there is no experimental evidence for other metal ions being transported by PIC2. The transport of ionic Cu could be a mechanism to limit cytosolic accumulation of Cu during Cu-overload induced stress [27, 65]. Crosslinking and damage of mitochondrial membranes induced by Cu has been observed in models of Cu-overload, such as the Long-Evans Cinnamon rat [67].

In SLC25A3, the L175A mutation separates Cu and phosphate transport by fully restoring COX activity and mitochondrial Cu levels without rescuing phosphate transport. This

finding confirms that the COX defect in mutant cells is due to defective Cu transport, rather than reduced phosphate levels. Further, our data suggest that compromising the phosphate transport function of PIC2 is easier than inactivating its Cu transport function. Mutations in a series of cysteine and histidine residues lining the aqueous binding pocket of the c-state model decrease, but do not eliminate, Cu transport. The PIC2 structural model indicates that the Cys29 and His33 would be the most likely location to form a Cu-binding site. The cysteine positioned above that site (residue 21) may help recruit Cu from the IMS and present it to Cys29-His33. In the m-state model, the Cys29-His33 proximity is maintained and the next potential ligand, Cys44, is exposed allowing for potential relocation of the Cu.

To understand the transport of the CuL complex, we considered the net negative charge of the complex, which suggests that positively charged or hydrogen-bond donor residues within the aqueous binding pocket may stabilize this interaction, including those that participate in phosphate transport (Gln86 and Lys90) [26]. Though mutating Lys90 does not affect ionic Ag^+ transport in *L. lactis*, we nonetheless envision that this residue may be important to transport competency *in vivo* where the CuL is more abundant. Interestingly, in the m-state model of PIC2 the aromatic ring of the side chain of Tyr83 is located between the Cys29 and His33, raising the possibility that these residues could be used as direct ligands for ionic Cu transport and as a site for binding for the CuL through π-interactions with aromatic components of the ligand. NMR analysis of the CuL by proton and carbon spectrums shows the presence of an aromatic ring structure with proton chemical shifts of 6.5-8 ppm, and carbon chemical shifts of 110-175 ppm (Figure 2.8). The ring structure is consistent with the fluorescent properties of the CuL complex [64, 65]. The positioning of an aromatic ring between the Cys29-His33 site could mimic a hypothetical CuL-bound state (from the c-state), and the movement of the Tyr83 side chain into

this position during substrate transport could facilitate the release of the complex from the Cys29-His33 site towards the matrix (Figure 2.8). While we cannot differentiate between possible mechanisms of transport that include release of Cu to the matrix upon CuL binding or direct transport of the intact CuL complex, the transport of intact CuL may be expected as this is the major form of Cu found in mitochondria under normal conditions [26, 34, 64]. In addition, the anionic nature of the CuL complex may explain some of the promiscuity between Cu and phosphate as substrates of the same carrier.

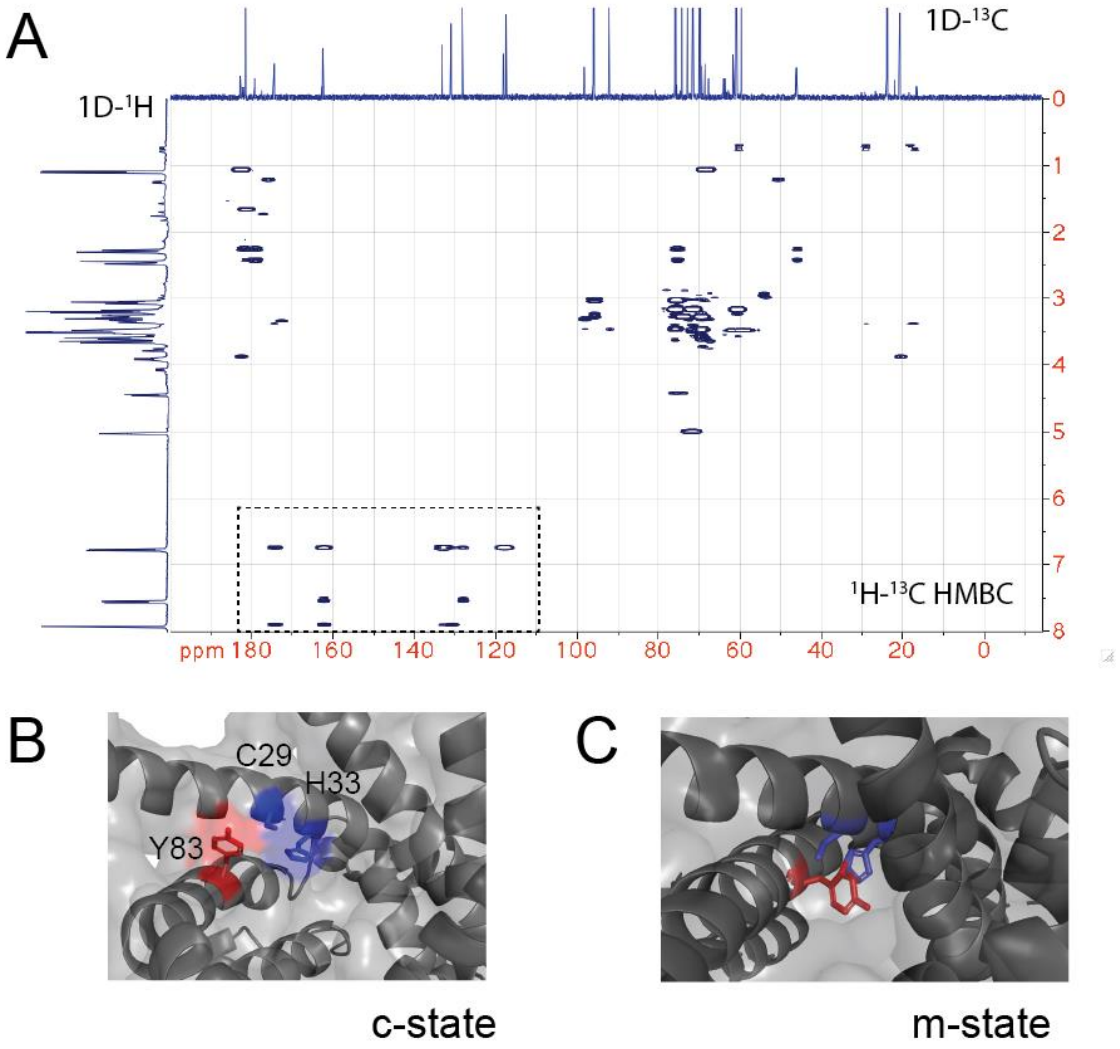

Figure 2.8: NMR of the CuL and role of Y83 in interactions with the proposed C29-H33 binding site.

A) ^{1}H-^{13}C HMBC spectrum of the purified CuL complex. The 1D ^{1}H and ^{13}C spectrum are shown. The box highlights the signals consistent with a benzene ring (Carbon shifts 110-175 ppm and Proton shifts 6.75-7.9 ppm) in the CuL. B) Enlargement of the C29-H33 region of c-state with C29, H33 and Y83 shown in sticks. C) Enlargement of the C29-H33 region of m-state with C29, H33 and Y83 shown in sticks with Y83 between the C29-H33 "replacing/occluding" a potential site for CuL binding.

Our phylogenetic analysis revealed nine taxa that lack a PIC2-like ortholog but have retained COX. Each of these taxa have multiple *MIR1*-like transporters (*Guillardia theta, Thalassiosira pseudonana, Emiliania huxleyi, Dictyostelium discoideum, Ustilago maydis, Cyanidioschyzon merolae, Chrysochromulina tobinii, Micromonas commoda,* and *Naegleria gruberi*). Alignment of these paralogs identified residues that are present in at least one of the duplicates and are shared with PIC2 (Figure 2.5). We hypothesize that these variants may have allowed MIR1 to secondarily gain Cu transport activity. One consistent difference we observe is a histidine found in PIC2 orthologs versus a glutamine found in MIR1 orthologs at position 230 (as numbered in PIC2). Both side chains stabilize the conformation of a possible cardiolipin binding site, by hydrogen bonding to peptide carbonyl oxygens. Additional experiments will be required to determine if this substitution affects substrate selectivity.

We favor an idea that *MIR1* duplication is a response to overcome the loss of PIC2 due to the basal polytomy among MCF subfamilies observed in our phylogenetic analyses of MCF proteins from each taxon. The lack of clear phylogenetic relationship to a second MCF group suggested that functional transitions are occurring within PIC2-MIR1 clades. However, this requires further investigation and an acknowledgement that other MCF transporters may have also acquired Cu transport activity. Indeed, in yeast we have shown that the MCF family member MRS3 serves as a secondary importer of mitochondrial Cu [14] . MRS3 is known as an iron transporter, but transport of Cu by MRS3 and its orthologs has been reported in studies using mitochondrially-derived vesicles from yeast and plants and in a reconstituted assay system [68–71]. MRS3 orthologs are not consistently recovered in a well-supported sister clade to the PIC2-MIR1 clade suggesting that this functional redundancy is the result of convergent evolution.

Understanding phosphate transport

Our biochemical data suggest that Lys90, Leu127 and Met275 are important for phosphate transport but are dispensable for Cu transport in *L. lactis*. The proposed mechanism of transport for MCFs based on the comparison of the c- and m-states of the ADP-ATP carrier suggests that even-numbered helices shift to allow transport/transition to the opposite state [4, 8]. The PIC2 structural model shows that Leu127 is located on helix 3 adjacent to a proline that kinks the helix, thereby altering helix-helix packing interactions with helix 2 (Figure 2.9). The Leu127 side chain interacts with the peptide backbone between Leu85 (Met in SLC25A3) and Gln86 in a knobs-into-holes interaction. We hypothesize that helix 2 reorients in the alanine substitution mutant especially in the vicinity of Gln86, changing the dynamics of that part of the structure. In the c-state, this change could shift the side chains of Gln86 and therefore Lys90 to a conformation that disrupts a phosphate binding site (Figure 2.9) and, by extension, decreases its rate of transport. Methionine 275 is part of the computationally-predicted conserved substrate contact point [3]. Based on its position in the c-state model below Lys90, Met275 is most likely involved in transport after phosphate enters deeper into the aqueous binding pocket of the protein.

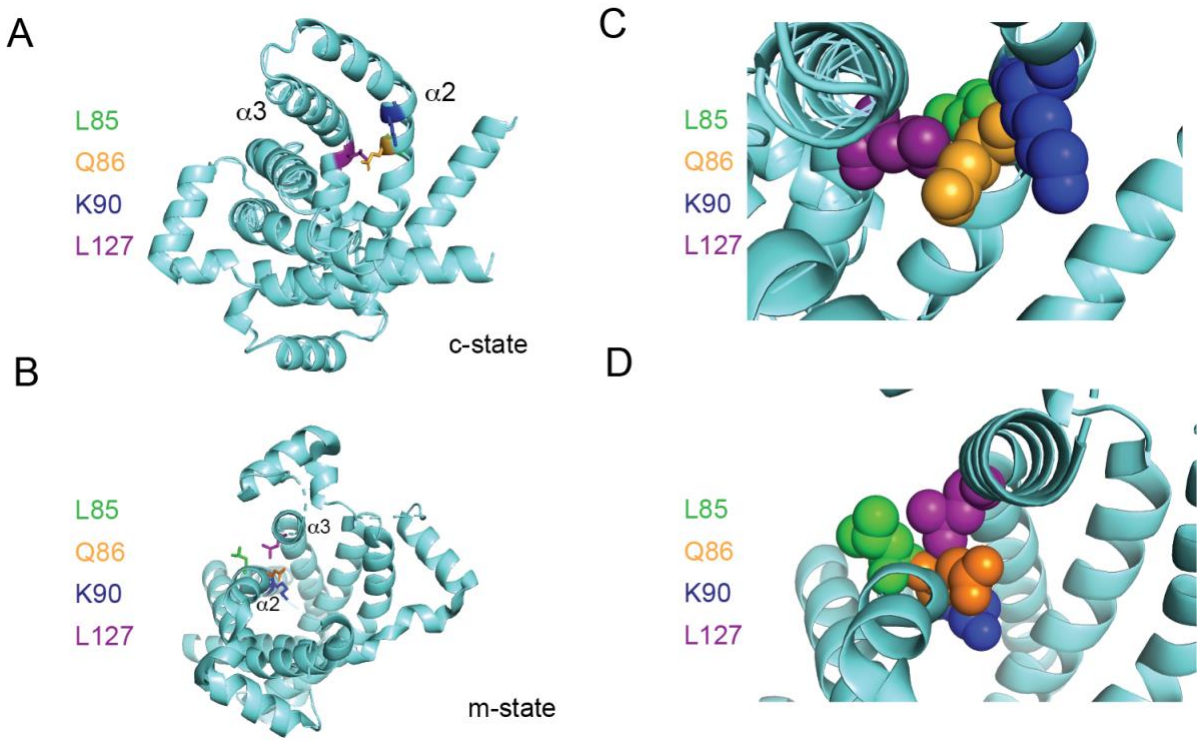

Figure 2.9: Positioning of Leu127 relative to adjacent residues on helix 2.

Ribbon diagrams of PIC2 *A)* c-state and *B)* m-state structures. The polypeptide is shown as a ribbon trace (aquamarine), the side chains as stick models. The Leu127 is colored purple to distinguish it from the adjacent Leu85 (green), Gln86 (orange) and Lys90 (blue) residues on helix 2 (a2). Enlargement of the Leu127 interaction with the surrounding residues shown as spheres in *C)* c-state and *D)* m-state.

Cu transport requires the formation of transient covalent bonds between the metal and ligands during transport, whereas phosphate transport relies on hydrogen bonding and salt bridges. These requirements may account for the fact that multiple mutations were able to inhibit the ability of PIC2 to transport phosphate. Other site-directed mutational studies of MIR1 have identified multiple residues that are required for phosphate transport [72–76], including His33, Thr44 and Lys90 (using PIC2 numbering). Consistent with these earlier studies, we observe decreased phosphate transport when mutating the corresponding residues in PIC2. In fact, previous studies of MIR1 function showed that mutation of Thr44 to cysteine partially inactivated phosphate transport [76] . This cysteine/threonine is clearly demarcated at the node between PIC2 and MIR1 clades, suggesting that it may be a critical change that weakened, but did not eliminate, phosphate transport in PIC2-like transporters (Figure 2.5). Three lineages (*O. sativa, S. punctatus* and *P. marinus*) lack MIR1-like transporters and have multiple PIC2-like transporters. In the case of rice, this could simply be due to the polyploid nature of its genome. In the chytrid *S. punctatus,* it may suggest that duplication enhances gene dosage. That is, additional copies compensate for less efficient phosphate transport. In contrast, the duplicated genes in *P. marinus* have undergone several notable changes; one variant has a large carboxy terminal truncation, 3 of the 4 variants have valine replacing cysteine at position 44 (as noted above from previous studies threonine at this position is optimal for phosphate transport) and histidine at position 230 is replaced by the glutamine that is found in more phosphate-selective transporters. These changes and gene dosage may be sufficient to overcome the loss of a MIR1-like transporter. Testing these hypotheses will require *in vitro* expression of multiple transporters to assess substrate selection.

Conclusions

Mitochondria function as a metabolic hub that controls physiology and disease by balancing the concentrations of multiple metabolites and essential elements [10, 77]. The MCF proteins play a critical role in regulating the import and export of these substrates [2, 78], and have been duplicated and specialized over evolutionary time to selectivity recognize and transport highly similar substrates. However, gene duplication has allowed for the retention of some carriers with multiple substrates. The evolutionary relationships among these carriers reveal aspects of transport mechanisms and the physiological demands of the organism. Our analysis of the Cu–phosphate MCF transporters shows that organisms deploy multiple strategies to recruit these substrates. We cannot determine a single characteristic that indicates an advantage or disadvantage of either strategy as unique patterns appear nested in different lineages. Metal transport to the mitochondrial matrix is required for Fe–S cluster assembly and COX assembly. Perhaps metal substrates are sufficiently simple that multiple MCFs are capable of transport. However, given the fatal disorders that result from too much or too little Cu or iron, it is unlikely that their transport is left to chance [79]. Storage in the mitochondrial matrix may have evolved as a mechanism to ensure Cu availability for COX assembly in an early endosymbiont that was subsequently retained during eukaryo-genesis [27]. Additional roles for Cu in the matrix remain to be determined. The recent discoveries that mitochondrial Cu can induce cell death through a pathway coined cuproptosis [80], disrupt essential processes such as Fe–S assembly [81, 82] and alter the stability of SOD1 in the cytosol [13] collectively suggest that understanding the physiological consequences of disrupting this Cu pool and its homoeostasis remains an important area of future research.

References

1. Palmieri F, Scarcia P, Monné M (2020) Diseases Caused by Mutations in Mitochondrial Carrier Genes SLC25: A Review. Biomolecules 10:655. https://doi.org/10.3390/biom10040655

2. Cunningham CN, Rutter J (2020) 20,000 picometers under the OMM: diving into the vastness of mitochondrial metabolite transport. EMBO Rep 21:e50071. https://doi.org/10.15252/embr.202050071

3. Robinson AJ, Overy C, Kunji ERS (2008) The mechanism of transport by mitochondrial carriers based on analysis of symmetry. Proc Natl Acad Sci U S A 105:17766–17771. https://doi.org/10.1073/pnas.0809580105

4. Ruprecht JJ, Kunji ERS (2020) The SLC25 Mitochondrial Carrier Family: Structure and Mechanism. Trends Biochem Sci 45:244–258. https://doi.org/10.1016/j.tibs.2019.11.001

5. Eick GN, Bridgham JT, Anderson DP, Harms MJ, Thornton JW (2017) Robustness of Reconstructed Ancestral Protein Functions to Statistical Uncertainty. Molecular Biology and Evolution 34:247–261. https://doi.org/10.1093/molbev/msw223

6. Eick GN, Colucci JK, Harms MJ, Ortlund EA, Thornton JW (2012) Evolution of Minimal Specificity and Promiscuity in Steroid Hormone Receptors. PLOS Genetics 8:e1003072. https://doi.org/10.1371/journal.pgen.1003072

7. Palmieri F (2004) The mitochondrial transporter family (SLC25): physiological and pathological implications. Pflugers Arch - Eur J Physiol 447:689–709. https://doi.org/10.1007/s00424-003-1099-7

8. Ruprecht JJ, King MS, Zögg T, Aleksandrova AA, Pardon E, Crichton PG, Steyaert J, Kunji ERS (2019) The Molecular Mechanism of Transport by the Mitochondrial ADP/ATP Carrier. Cell 176:435-447.e15. https://doi.org/10.1016/j.cell.2018.11.025

9. Pebay-Peyroula E, Dahout-Gonzalez C, Kahn R, Trezeguet V, Lauquin GJ-M, Brandolin G (2003) structure of mitochondrial ADP/ATP carrier in complex with carboxyatractyloside. Worldwide Protein Data Bank

10. Baker ZN, Cobine PA, Leary SC (2017) The mitochondrion: a central architect of copper homeostasis. Metallomics 9:1501–1512. https://doi.org/10.1039/c7mt00221a

11. Vest KE, Leary SC, Winge DR, Cobine PA (2013) Copper Import into the Mitochondrial Matrix in *Saccharomyces cerevisiae* Is Mediated by Pic2, a Mitochondrial Carrier Family Protein*. Journal of Biological Chemistry 288:23884–23892. https://doi.org/10.1074/jbc.M113.470674

12. Puchkova LV, Broggini M, Polishchuk EV, Ilyechova EY, Polishchuk RS (2019) Silver Ions as a Tool for Understanding Different Aspects of Copper Metabolism. Nutrients 11:1364. https://doi.org/10.3390/nu11061364

13. Boulet A, Vest KE, Maynard MK, Gammon MG, Russell AC, Mathews AT, Cole SE, Zhu X, Phillips CB, Kwong JQ, Dodani SC, Leary SC, Cobine PA (2018) The mammalian phosphate carrier SLC25A3 is a mitochondrial copper transporter required for cytochrome c oxidase

biogenesis. J Biol Chem 293:1887–1896. https://doi.org/10.1074/jbc.RA117.000265

14. Vest KE, Wang J, Gammon MG, Maynard MK, White OL, Cobine JA, Mahone WK, Cobine PA (2016) Overlap of copper and iron uptake systems in mitochondria in Saccharomyces cerevisiae. Open Biol 6:150223. https://doi.org/10.1098/rsob.150223

15. King MS, Boes C, Kunji ERS (2015) Membrane Protein Expression in Lactococcus lactis. Membrane Proteins—Production and Functional Characterization 77–97. https://doi.org/10.1016/bs.mie.2014.12.009

16. Monné M, Chan KW, Slotboom D-J, Kunji ERS (2005) Functional expression of eukaryotic membrane proteins in Lactococcus lactis. Protein Sci 14:3048–3056. https://doi.org/10.1110/ps.051689905

17. KUNJI E, CHAN K, SLOTBOOM D, FLOYD S, OCONNOR R, MONNE M (2005) Eukaryotic membrane protein overproduction in. Current Opinion in Biotechnology 16:546–551. https://doi.org/10.1016/j.copbio.2005.08.006

18. Kunji ERS, Slotboom D-J, Poolman B (2003) Lactococcus lactis as host for overproduction of functional membrane proteins. Biochimica et Biophysica Acta (BBA) - Biomembranes 1610:97–108. https://doi.org/10.1016/s0005-2736(02)00712-5

19. Hamel P, Saint-Georges Y, De Pinto B, Lachacinski N, Altamura N, Dujardin G (2004) Redundancy in the function of mitochondrial phosphate transport in Saccharomyces cerevisiae and Arabidopsis thaliana. Molecular Microbiology 51:307–317. https://doi.org/10.1046/j.1365-2958.2003.03810.x

20. Takabatake R, Siddique A-BM, Kouchi H, Izui K, Hata S (2001) Characterization of a Saccharomyces cerevisiae Gene That Encodes a Mitochondrial Phosphate Transporter--Like Protein. Journal of Biochemistry 129:827–833. https://doi.org/10.1093/oxfordjournals.jbchem.a002926

21. Fiermonte G, Dolce V, Palmieri F (1998) Expression in Escherichia coli, Functional Characterization, and Tissue Distribution of Isoforms A and B of the Phosphate Carrier from Bovine Mitochondria. Journal of Biological Chemistry 273:22782–22787. https://doi.org/10.1074/jbc.273.35.22782

22. Kolbe HV, Costello D, Wong A, Lu RC, Wohlrab H (1984) Mitochondrial phosphate transport. Large scale isolation and characterization of the phosphate transport protein from beef heart mitochondria. Journal of Biological Chemistry 259:9115–9120. https://doi.org/10.1016/s0021-9258(17)47273-5

23. Phelps A, Schobert CT, Wohlrab H (1991) Cloning and characterization of the mitochondrial phosphate transport protein gene from the yeast Saccharomyces cerevisiae. Biochemistry 30:248–252. https://doi.org/10.1021/bi00215a035

24. Kwong JQ, Davis J, Baines CP, Sargent MA, Karch J, Wang X, Huang T, Molkentin JD (2014) Genetic deletion of the mitochondrial phosphate carrier desensitizes the mitochondrial permeability transition pore and causes cardiomyopathy. Cell Death Differ 21:1209–1217. https://doi.org/10.1038/cdd.2014.36

25. Wohlrab H, Kolbe HVJ, Collins A (1986) [55] Isolation and reconstitution of the phosphate transport protein from mitochondria. Methods in Enzymology 697–705. https://doi.org/10.1016/s0076-6879(86)25057-0

26. Cobine PA, Ojeda LD, Rigby KM, Winge DR (2004) Yeast Contain a Non-proteinaceous Pool of Copper in the Mitochondrial Matrix*. Journal of Biological Chemistry 279:14447–14455. https://doi.org/10.1074/jbc.M312693200

27. Cobine PA, Moore SA, Leary SC (2021) Getting out what you put in: Copper in mitochondria and its impacts on human disease. Biochimica et Biophysica Acta (BBA) - Molecular Cell Research 1868:118867. https://doi.org/10.1016/j.bbamcr.2020.118867

28. Risso VA, Gavira JA, Mejia-Carmona DF, Gaucher EA, Sanchez-Ruiz JM (2013) Hyperstability and Substrate Promiscuity in Laboratory Resurrections of Precambrian β-Lactamases. Journal of the American Chemical Society 135:2899–2902. https://doi.org/10.1021/ja311630a

29. Risso VA, Gavira JA, Sanchez-Ruiz JM (2013) Thermostable and promiscuous Precambrian proteins. Environmental Microbiology 16:1485–1489. https://doi.org/10.1111/1462-2920.12319

30. Burki F, Roger AJ, Brown MW, Simpson AGB (2020) The New Tree of Eukaryotes. Trends in Ecology & Evolution 35:43–55. https://doi.org/10.1016/j.tree.2019.08.008

31. Karnkowska A, Treitli SC, Brzoň O, Novák L, Vacek V, Soukal P, Barlow LD, Herman EK, Pipaliya SV, Pánek T, Žihala D, Petrželková R, Butenko A, Eme L, Stairs CW, Roger AJ, Eliáš M, Dacks JB, Hampl V (2019) The Oxymonad Genome Displays Canonical Eukaryotic Complexity in the Absence of a Mitochondrion. Mol Biol Evol 36:2292–2312. https://doi.org/10.1093/molbev/msz147

32. Karnkowska A, Vacek V, Zubáčová Z, Treitli SC, Petrželková R, Eme L, Novák L, Žárský V, Barlow LD, Herman EK, Soukal P, Hroudová M, Doležal P, Stairs CW, Roger AJ, Eliáš M, Dacks JB, Vlček Č, Hampl V (2016) A Eukaryote without a Mitochondrial Organelle. Current Biology 26:1274–1284. https://doi.org/10.1016/j.cub.2016.03.053

33. Capra JA, Singh M (2007) Predicting functionally important residues from sequence conservation. Bioinformatics 23:1875–1882. https://doi.org/10.1093/bioinformatics/btm270

34. Dodani SC, Leary SC, Cobine PA, Winge DR, Chang CJ (2011) A targetable fluorescent sensor reveals that copper-deficient SCO1 and SCO2 patient cells prioritize mitochondrial copper homeostasis. J Am Chem Soc 133:8606–8616. https://doi.org/10.1021/ja2004158

35. Marobbio CMT, Punzi G, Pierri CL, Palmieri L, Calvello R, Panaro MA, Palmieri F (2015) Pathogenic potential of SLC25A15 mutations assessed by transport assays and complementation of Saccharomyces cerevisiae ORT1 null mutant. Molecular Genetics and Metabolism 115:27–32. https://doi.org/10.1016/j.ymgme.2015.03.003

36. Marobbio CMT, Agrimi G, Lasorsa FM, Palmieri F (2003) Identification and functional reconstitution of yeast mitochondrial carrier for S-adenosylmethionine. EMBO J 22:5975–5982. https://doi.org/10.1093/emboj/cdg574

37. Fiermonte G, Dolce V, David L, Santorelli FM, Dionisi-Vici C, Palmieri F, Walker JE (2003) The Mitochondrial Ornithine Transporter. Journal of Biological Chemistry 278:32778–32783.

https://doi.org/10.1074/jbc.m302317200

38. Cavero S, Vozza A, Del Arco A, Palmieri L, Villa A, Blanco E, Runswick MJ, Walker JE, Cerdán S, Palmieri F, Satrústegui J (2003) Identification and metabolic role of the mitochondrial aspartate-glutamate transporter in Saccharomyces cerevisiae. Molecular Microbiology 50:1257–1269. https://doi.org/10.1046/j.1365-2958.2003.03742.x

39. Catalina-Rodriguez O, Kolukula VK, Tomita Y, Preet A, Palmieri F, Wellstein A, Byers S, Giaccia AJ, Glasgow E, Albanese C, Avantaggiati ML (2012) The mitochondrial citrate transporter, CIC, is essential for mitochondrial homeostasis. Oncotarget 3:1220–1235. https://doi.org/10.18632/oncotarget.714

40. Knight SAB, Yoon H, Pandey AK, Pain J, Pain D, Dancis A (2019) Splitting the functions of Rim2, a mitochondrial iron/pyrimidine carrier. Mitochondrion 47:256–265. https://doi.org/10.1016/j.mito.2018.12.005

41. King MS, Tavoulari S, Mavridou V, King AC, Mifsud J, Kunji ERS (2020) A Single Cysteine Residue in the Translocation Pathway of the Mitosomal ADP/ATP Carrier from Cryptosporidium parvum Confers a Broad Nucleotide Specificity. Int J Mol Sci 21:8971. https://doi.org/10.3390/ijms21238971

42. Seifert EL, Gál A, Acoba MG, Li Q, Anderson-Pullinger L, Golenár T, Moffat C, Sondheimer N, Claypool SM, Hajnóczky G (2016) Natural and Induced Mitochondrial Phosphate Carrier Loss: DIFFERENTIAL DEPENDENCE OF MITOCHONDRIAL METABOLISM AND DYNAMICS AND CELL SURVIVAL ON THE EXTENT OF DEPLETION. J Biol Chem 291:26126–26137. https://doi.org/10.1074/jbc.M116.744714

43. Bhoj EJ, Li M, Ahrens-Nicklas R, Pyle LC, Wang J, Zhang VW, Clarke C, Wong LJ, Sondheimer N, Ficicioglu C, Yudkoff M (2015) Pathologic Variants of the Mitochondrial Phosphate Carrier SLC25A3: Two New Patients and Expansion of the Cardiomyopathy/Skeletal Myopathy Phenotype With and Without Lactic Acidosis. JIMD Rep 19:59–66. https://doi.org/10.1007/8904_2014_364

44. Mayr JA, Zimmermann FA, Horváth R, Schneider H-C, Schoser B, Holinski-Feder E, Czermin B, Freisinger P, Sperl W (2011) Deficiency of the mitochondrial phosphate carrier presenting as myopathy and cardiomyopathy in a family with three affected children. Neuromuscular Disorders 21:803–808. https://doi.org/10.1016/j.nmd.2011.06.005

45. Mayr JA, Merkel O, Kohlwein SD, Gebhardt BR, Böhles H, Fötschl U, Koch J, Jaksch M, Lochmüller H, Horváth R, Freisinger P, Sperl W (2007) Mitochondrial phosphate-carrier deficiency: a novel disorder of oxidative phosphorylation. Am J Hum Genet 80:478–484. https://doi.org/10.1086/511788

46. Kuang MC, Hutchins PD, Russell JD, Coon JJ, Hittinger CT (2016) Ongoing resolution of duplicate gene functions shapes the diversification of a metabolic network. Elife 5:e19027. https://doi.org/10.7554/eLife.19027

47. Conant GC, Birchler JA, Pires JC (2014) Dosage, duplication, and diploidization: clarifying the interplay of multiple models for duplicate gene evolution over time. Current Opinion in Plant Biology 19:91–98. https://doi.org/10.1016/j.pbi.2014.05.008

48. Sandegren L, Andersson DI (2009) Bacterial gene amplification: implications for the evolution of

antibiotic resistance. Nature Reviews Microbiology 7:578–588. https://doi.org/10.1038/nrmicro2174

49. Conant GC, Wolfe KH (2007) Increased glycolytic flux as an outcome of whole-genome duplication in yeast. Mol Syst Biol 3:129–129. https://doi.org/10.1038/msb4100170

50. Hittinger CT, Carroll SB (2007) Gene duplication and the adaptive evolution of a classic genetic switch. Nature 449:677–681. https://doi.org/10.1038/nature06151

51. Zhang J, Zhang Y, Rosenberg HF (2002) Adaptive evolution of a duplicated pancreatic ribonuclease gene in a leaf-eating monkey. Nature Genetics 30:411–415. https://doi.org/10.1038/ng852

52. Force A, Lynch M, Pickett FB, Amores A, Yan YL, Postlethwait J (1999) Preservation of duplicate genes by complementary, degenerative mutations. Genetics 151:1531–1545. https://doi.org/10.1093/genetics/151.4.1531

53. Robinson NJ, Winge DR (2010) Copper metallochaperones. Annu Rev Biochem 79:537–562. https://doi.org/10.1146/annurev-biochem-030409-143539

54. Pufahl RA, Singer CP, Peariso KL, Lin SJ, Schmidt PJ, Fahrni CJ, Culotta VC, Penner-Hahn JE, O'Halloran TV (1997) Metal ion chaperone function of the soluble Cu(I) receptor Atx1. Science 278:853–856. https://doi.org/10.1126/science.278.5339.853

55. Rae TD, Schmidt PJ, Pufahl RA, Culotta VC, O'Halloran TV (1999) Undetectable intracellular free copper: The requirement of a copper chaperone for superoxide dismutase. Science 284:805–808. https://doi.org/10.1126/science.284.5415.805

56. Waldron KJ, Rutherford JC, Ford D, Robinson NJ (2009) Metalloproteins and metal sensing. Nature 460:823–830. https://doi.org/10.1038/nature08300

57. Glerum DM, Shtanko A, Tzagoloff A (1996) Characterization of COX17, a Yeast Gene Involved in Copper Metabolism and Assembly of Cytochrome Oxidase*. Journal of Biological Chemistry 271:14504–14509. https://doi.org/10.1074/jbc.271.24.14504

58. Maxfield AB, Heaton DN, Winge DR (2004) Cox17 Is Functional When Tethered to the Mitochondrial Inner Membrane. Journal of Biological Chemistry 279:5072–5080. https://doi.org/10.1074/jbc.m311772200

59. Banci L, Bertini I, Ciofi-Baffoni S, Janicka A, Martinelli M, Kozlowski H, Palumaa P (2008) A Structural-Dynamical Characterization of Human Cox17*. Journal of Biological Chemistry 283:7912–7920. https://doi.org/10.1074/jbc.M708016200

60. Horng Y-C, Cobine PA, Maxfield AB, Carr HS, Winge DR (2004) Specific Copper Transfer from the Cox17 Metallochaperone to Both Sco1 and Cox11 in the Assembly of Yeast Cytochrome *c* Oxidase*. Journal of Biological Chemistry 279:35334–35340. https://doi.org/10.1074/jbc.M404747200

61. Cobine PA, Ojeda LD, Rigby KM, Winge DR (2004) Yeast Contain a Non-proteinaceous Pool of Copper in the Mitochondrial Matrix. Journal of Biological Chemistry 279:14447–14455. https://doi.org/10.1074/jbc.m312693200

62. Vest KE, Zhu X, Cobine PA (2019) Copper Disposition in Yeast. Clinical and Translational Perspectives on WILSON DISEASE 115–126. https://doi.org/10.1016/b978-0-12-810532-0.00012-4

63. Vest KE, Cobine PA (2011) Copper in Mitochondria. Encyclopedia of Inorganic and Bioinorganic Chemistry 1–12. https://doi.org/10.1002/9781119951438.eibc2155

64. Cobine PA, Pierrel F, Bestwick ML, Winge DR (2006) Mitochondrial Matrix Copper Complex Used in Metallation of Cytochrome Oxidase and Superoxide Dismutase*. Journal of Biological Chemistry 281:36552–36559. https://doi.org/10.1074/jbc.M606839200

65. Vest KE, Leary SC, Winge DR, Cobine PA (2013) Copper import into the mitochondrial matrix in Saccharomyces cerevisiae is mediated by Pic2, a mitochondrial carrier family protein. J Biol Chem 288:23884–23892. https://doi.org/10.1074/jbc.M113.470674

66. Abicht HK, Gonskikh Y, Gerber SD, Solioz M (2013) Non-enzymic copper reduction by menaquinone enhances copper toxicity in Lactococcus lactis IL1403. Microbiology 159:1190–1197. https://doi.org/10.1099/mic.0.066928-0

67. Zischka H, Lichtmannegger J, Schmitt S, Jägemann N, Schulz S, Wartini D, Jennen L, Rust C, Larochette N, Galluzzi L, Chajes V, Bandow N, Gilles VS, DiSpirito AA, Esposito I, Goettlicher M, Summer KH, Kroemer G (2011) Liver mitochondrial membrane crosslinking and destruction in a rat model of Wilson disease. J Clin Invest 121:1508–1518. https://doi.org/10.1172/JCI45401

68. Brazzolotto X, Pierrel F, Pelosi L (2014) Three conserved histidine residues contribute to mitochondrial iron transport through mitoferrins. Biochem J 460:79–89. https://doi.org/10.1042/BJ20140107

69. Froschauer EM, Schweyen RJ, Wiesenberger G (2009) The yeast mitochondrial carrier proteins Mrs3p/Mrs4p mediate iron transport across the inner mitochondrial membrane. Biochimica et Biophysica Acta (BBA) - Biomembranes 1788:1044–1050. https://doi.org/10.1016/j.bbamem.2009.03.004

70. Christenson ET, Gallegos AS, Banerjee A (2018) In vitro reconstitution, functional dissection, and mutational analysis of metal ion transport by mitoferrin-1. Journal of Biological Chemistry 293:3819–3828. https://doi.org/10.1074/jbc.M117.817478

71. Jain A, Dashner ZS, Connolly EL (2019) Mitochondrial Iron Transporters (MIT1 and MIT2) Are Essential for Iron Homeostasis and Embryogenesis in Arabidopsis thaliana. Front Plant Sci 10:1449–1449. https://doi.org/10.3389/fpls.2019.01449

72. Wohlrab H, Annese V, Haefele A (2002) Single Replacement Constructs of All Hydroxyl, Basic, and Acidic Amino Acids Identify New Function and Structure-Sensitive Regions of the Mitochondrial Phosphate Transport Protein. Biochemistry 41:3254–3261. https://doi.org/10.1021/bi0117551

73. Briggs C, Mincone L, Wohlrab H (1999) Replacements of Basic and Hydroxyl Amino Acids Identify Structurally and Functionally Sensitive Regions of the Mitochondrial Phosphate Transport Protein. Biochemistry 38:5096–5102. https://doi.org/10.1021/bi982945n

74. Phelps A, Briggs C, Mincone L, Wohlrab H (1996) Mitochondrial Phosphate Transport Protein.

Replacements of Glutamic, Aspartic, and Histidine Residues Affect Transport and Protein Conformation and Point to a Coupled Proton Transport Path. Biochemistry 35:10757–10762. https://doi.org/10.1021/bi961052x

75. Wohlrab H, Briggs C (1994) Yeast Mitochondrial Phosphate Transport Protein Expressed in Escherichia coli. Site-Directed Mutations at Threonine-43 and at a Similar Location in the Second Tandem Repeat (Isoleucine-141). Biochemistry 33:9371–9375. https://doi.org/10.1021/bi00198a001

76. Phelps A, Wohlrab H (1991) Mitochondrial phosphate transport. The Saccharomyces cerevisiae (threonine 43 to cysteine) mutant protein explicitly identifies transport with genomic sequence. Journal of Biological Chemistry 266:19882–19885. https://doi.org/10.1016/s0021-9258(18)54864-x

77. Martínez-Reyes I, Chandel NS (2020) Mitochondrial TCA cycle metabolites control physiology and disease. Nat Commun 11:102–102. https://doi.org/10.1038/s41467-019-13668-3

78. Palmieri F, Scarcia P, Monné M (2020) Diseases Caused by Mutations in Mitochondrial Carrier Genes SLC25: A Review. Biomolecules 10:655. https://doi.org/10.3390/biom10040655

79. Xu W, Barrientos T, Andrews NC (2013) Iron and copper in mitochondrial diseases. Cell Metab 17:319–328. https://doi.org/10.1016/j.cmet.2013.02.004

80. Tsvetkov P, Detappe A, Cai K, Keys HR, Brune Z, Ying W, Thiru P, Reidy M, Kugener G, Rossen J, Kocak M, Kory N, Tsherniak A, Santagata S, Whitesell L, Ghobrial IM, Markley JL, Lindquist S, Golub TR (2019) Mitochondrial metabolism promotes adaptation to proteotoxic stress. Nat Chem Biol 15:681–689. https://doi.org/10.1038/s41589-019-0291-9

81. Vallières C, Holland SL, Avery SV (2017) Mitochondrial Ferredoxin Determines Vulnerability of Cells to Copper Excess. Cell Chem Biol 24:1228-1237.e3. https://doi.org/10.1016/j.chembiol.2017.08.005

82. Brancaccio D, Gallo A, Piccioli M, Novellino E, Ciofi-Baffoni S, Banci L (2017) [4Fe-4S] Cluster Assembly in Mitochondria and Its Impairment by Copper. Journal of the American Chemical Society 139:719–730. https://doi.org/10.1021/jacs.6b09567

Chapter 3: Identification of genetic interactors with mitochondrial copper transporters

Abstract

Saccharomyces cerevisiae use mitochondrial copper for various essential physiological processes including respiration, defense against oxidative stress and iron uptake. Copper is imported into the mitochondrial matrix as copper ligand complex (CuL) primarily through the mitochondrial carrier family members Pic2 and Mrs3. In screening for additional targets of mitochondrial copper, we identified 194 yeast genes that showed no growth phenotype as a single deletion mutant, but when combined with *pic2*Δ*, mrs3*Δ and *pic2*Δ*mrs3*Δ as double or triple mutants, either a proliferation phenotype or a germination defect was exhibited. We assessed multiple mutants that grew the worst on a non-fermentable carbon source under mild copper limitation condition for whole cell and mitochondrial metals content and cytochrome c oxidase activity. In addition, ten synthetic lethal interactors were analyzed, and among which *aco2*Δ*pic2*Δ was the only mutant whose germination phenotype was rescued by adding copper. The mutant grew poorly on the fermentable carbon source. The characterization of the single mutants of the viable candidates that exhibited the most severe growth defect showed *aco2*Δ is the most similar to *pic2*Δ.

Introduction

Copper (Cu) is essential for eukaryotes for survival. Given the redox active nature of the metal, Cu must be delivered to their correct subcellular destinations in a timely manner after being imported into the cells to avoid potential harm caused by inappropriate interactions and oxidative damage [1, 2]. There are many diseases associated with disrupted Cu homeostasis in mammals, including Menkes disease, Wilson disease and an array of neurological pathologies [3–6]. Elucidating the mechanisms of maintaining cellular Cu homeostasis at a molecular level will provide insights into the management and treatment of the related diseases.

Majority of the Cu are imported into the cell through Ctr1 [7–9]. Then, they are chelated by either Cu chaperone proteins or cysteine-rich metabolites [10–12]. A ligand has also been isolated and demonstrated to be able to bind Cu [13]. Once bound, Cu ions are directed to their targets. Within the cytosol, a protein-mediated delivery mechanism has been identified for copper. ATOX1 was the first discovered copper chaperon in the cytosol. It is a non-catalytic copper-binding protein that delivers Cu to the trans-Golgi vesicles via ATP7A/B, a P-type ATPase [14]. In humans, ATP7A loss-of-function mutation results in Cu deficiency and leads to Menkes disease, whereas any mutation causes dysfunctional ATP7B leads to Cu overload and Wilson disease [3]. Cu/Zn superoxide dismutase (SOD1) is another cytosol-localized protein that requires Cu to be activated. CCS inserts Cu into the newly synthesized apoprotein in the cytoplasm and then catalyzes the formation of an essential disulfide bond [12]. It interacts with Sod1 as a heterodimer via the SOD-like domain and transfers the metal ion to the disulfide-reduced apo-Sod1 [15]. CCS interacts with a partially folded conformation of apo, reduced Sod1 facilitates the insertion of copper and the formation of the disulfide bond in a reaction that is

dependent on oxygen [16]. The change in structure decreases the affinity of the interaction as disordered loops adopt a more rigid structure in the copper-bound, disulfide bonded folded protein. Impaired SOD activity has been linked to neuropathies such as amyotrophic lateral sclerosis and Parkinson's disease [5].

An important cuproenzyme found in mitochondria is cytochrome c oxidase (COX). It is embedded in the inner membrane of mitochondria, being the terminal electron acceptor of the electron transport chain, it mediates the transfer of the electrons from cytochrome c to oxygen to produce water [17]. COX is required for respiration and contributes to the formation of membrane potential in mitochondria. Cu is found in the catalytic core of the enzyme that is surrounded by subunits COX1 and COX2 [18]. The assembly of the enzyme, including cofactor insertion, requires the coordination of more 30 different accessory proteins [19]. Previous studies showed the proper assembly and activation of COX is linked to an anionic mitochondrial Cu pool. Any diminished Cu availability in this pool, either by deleting the mitochondrial Cu importer, SLC25A1, or chelating mitochondrial Cu, demolishes the expression of COX or renders the enzyme inactive [20]. This indicates the functional COX is dependent on mitochondrial Cu. However, the mechanism for Cu delivery to the mitochondrial is unclear [13].

It has been demonstrated that there is no free Cu is detected within the cell, most of the Cu exist as an anionic pool within the mitochondria [21]. It has been calculated that only 20% to 40% of the mitochondrial Cu are associated with COX. Organellar fractionation experiments showed that more than 70% of mitochondrial Cu is present as a soluble, anionic complex contained within a matrix-localized, bioavailable pool. This complex has been defined as the copper ligand (CuL) and its existence and localization have been confirmed by X-ray fluorescence imaging and Cu chelation studies [13]. The significancy of this mitochondrial CuL

pool is understudied. Tsvetkov et al. discovered a Cu inducible cell death mechanism and named it cuproptosis, where Cu is pharmacologically overloaded into mitochondria, causing lipoylated protein to be denatured and aggregated and ultimately lead to cell death [22, 23]. The process is dependent on the expression of ferredoxin, a small iron-sulfur cluster containing protein. Additional studies reported the similar phenomena exist in *Escherichia coli* [24, 25]. Given the endosymbiotic nature of the mitochondria, we hypothesize there are additional mitochondrial protein targets that Cu can bind to and affect cellular physiology [26].

Conditions for novel mitochondrial Cu binding targets screen

Saccharomyces cerevisiae is one of the ideal model systems to study the Cu homeostasis. It is unicellular with short doubling time and its genome has been fully sequenced [27]. The methods for its genetical manipulation are well-established, and phenotypes can be identified when yeast homologs of mammalian Cu-related genes are mutated under some conditions. Boone's lab developed a strategy that allows for high throughput yeast genetic screen called synthetic genetic array (SGA) [28]. In an SGA screen, double mutants of the query deletion and deletion mutation array (DMA) are systematic constructed for a global analysis of synthetic genetic interactions. To achieve this, a query mutation bearing the nourseothricin (clonNAT) resistance marker is created and crossed to the DMA, which is an ordered array of approximately 5000 viable gene deletion mutants (representing ~80% of all yeast genes) and carry the kanamycin resistance marker. Once crossed, the diploid strains undergo a series of selections for the meiotic progeny harboring both mutations. The haploid double mutants are then transferred to the plates under the screening conditions to be scored for fitness defects [28].

The phenotypes that are associated with disruption of Cu homeostasis are related to either

Cu toxicity or Cu deficiency. Cu toxicity can be induced by either adding Cu to the growth media; mutating genes encode Cu chelating proteins such as *CUP1* and *CRS5*, or deletion of Cu inducible transcription factor *ACE1* [29–31]. We have tested that wild type yeast strain can survive in rich media contain up to 8 mM Cu without showing any phenotype. There are two metallothioneins in yeast: Cup1 and Crs5. They are cysteine-rich proteins capable of binding multiple copper atoms to prevent redox cycling or inappropriate binding interactions. *CUP1* is a highly expressed, duplicated gene in yeast and is responsible for a significant proportion of the copper resistance in yeast. Cup1 has unique cysteine spacing and is considered a copper-specific metallothionein [32]. Crs5 has different cysteine arrangement that is more like other eukaryotic metallothionein, it plays a less significant role in protection of the cells against copper toxicity. Once intracellular Cu reaches toxic levels, Ace1 induces the transcription of *CUP1* and *CRS5* [33]. Cu deficiency can be induced by either limiting Cu availability to the cells, deleting Cu transporters, or mutating transcriptional factors that induce the expression of Cu transporters. Bathocuproine disulfonic acid (BCS) is the extracellular Cu chelator that binds with Cu and prevents it from importing into the cell. Ctr1 is a high-affinity Cu transport protein embedded in the plasma membrane, it transports Cu in the cuprous form, so an extracellular metalloreductase (Fre1) is required for efficient Cu transport [34]. Ctr3 is an additional Cu importer in the plasma membrane that was discovered as in a genetic screen to identify suppressors of defects in yeast lacking CTR1 [35]. Yeast also uses a series of low-affinity Cu transporters such as Fet4 and Smf1 [36–38]. A common feature for both low and high-affinity transport is that Cu(I) is used specifically as a substrate. Thus, cells need cell surface reductases or an exogenous reductant to uptake necessary Cu. The export pathway for Cu in yeast has yet discovered and the only equivalent of export is import into the vacuole. Cu is contained in the vacuole in the cuprous

form as a metalloreductase (Fre6) is required for mobilization of Cu into the cytosol via Ctr2, a homolog of Ctr1 [39]. The deletion of CTR2 causes hyperaccumulation of copper in the vacuole. Ctr2 is demonstrated to be a copper transporter by mutation analysis that showed it can function as a high-affinity copper transporter when localized to the plasma membrane [40].

Most characterized phenotypes associate to Cu deficiency in yeast are related to three major cuproproteins: Fet3, Sod1, and COX. The multicopper oxidase Fet3 converts ferrous iron to ferric iron and is required for high-affinity iron transport in yeast. Cu cofactor in Fet3 mediates the oxidation of the substrate and the reduction of oxygen to water [41]. For high-affinity iron transport to proceed, ferrous iron must be oxidized to ferric. Under Cu deficient conditions, the cells are susceptible to iron deficiency as well. Therefore, with dysfunctional Fet3 due to low Cu, yeast cells require supplemental iron to be added to the medium. The ferroxidase family can have multiple substrates, and in addition to oxidizing iron, and Fet3 has been shown to oxidize cuprous copper at the plasma membrane [34]. This has been suggested to be responsible for copper stress phenotypes associated with overexpression of Fet3. A high level of Fet3 presumably induces cycling between Cu(I) and Cu(II) leading to lipid damage and toxicity[36]. Sod1 is a homo-dimeric free radical scavenging enzyme that destroys superoxide radicals and protects cells from oxidative stress via a copper-mediated disproportionation reaction [15]. Sod1 is expressed predominantly in the cytoplasm of yeast, but a small percentage of the protein is found in the mitochondrial intermembrane space [42]. The monomer structure consists of an eight-stranded beta-barrel that binds a copper ion and a zinc ion that play both catalytic and structural roles [43]. With limited Cu availability, Sod1 deficiencies can cause phenotypes such as amino-acid auxotrophy and reduced growth rate under aerobic conditions. COX is a multimeric protein complex that contains two copper centers, a binuclear Cu_A site and

a heme *a3*-Cu_B site [44]. It has been shown that the anionic mitochondrial pool within the matrix is required for the active COX [13]. Without functional COX, the yeast cells lose the ability to grow on the media with non-fermentable carbon sources such as lactate-glycerol and acetate.

The inner membrane of the mitochondria is impermeable to most ions and molecules, and the transport of metabolic substrates such as oxaloacetate, citrate, GTP and ATP into and out of the matrix are mediated by mitochondrial carrier family protein (MCF) [45, 46]. In yeast, MCF members Pic2 and Mrs3 are the transporters that import Cu into mitochondrial matrix [47, 48]. Yeast strains with a deletion of *PIC2* show copper-dependent growth defects, and mitochondria from these cells have lower total mitochondrial copper. Importantly, Pic2 expressed in *Lactococcus lactis* was able to transport copper [49]. The iron transporting MCF, Mrs3, also contributes to copper import into mitochondria. Deletion of both *PIC2* and *MRS3* in yeast did not eliminate Cu accumulation in the matrix, indicating additional Cu transports likely exist [48]. The insertion of the Cu cofactors into COX and Sod1 occur in the intermembrane space; however, the mechanism for the export of copper from the matrix to the intermembrane space is still unknown [13].

To identify additional mitochondrial Cu binding targets, we chose the condition of non-fermentable carbon source lactate-glycerol with mild limited Cu availability. We used *pic2*Δ, *mrs3*Δ and *pic2*Δ*mrs3*Δ as query strains to create haploid double or triple mutants to look for genetic interactors that show lethality or fitness defects.

Materials and Methods

Yeast strains, culture conditions, and standard methods

The yeast strains used in this study were BY4741 (*MATa, leu2*Δ, *met15*Δ, *ura3*Δ, *his3*Δ) and the isogenic kanMX4- containing mutant from Invitrogen. The query strains are constructed in

Y8205 background (*MATα, can1*Δ*::STE2pr-Sp_his5 lyp1*Δ*::STE3pr-LEU2 his3*Δ *leu2*Δ *ura3*Δ). Query strains were constructed by transforming the PCR products of the amplified clonNAT cassette with overhangs of 55 base pair specific to the upstream and downstream of the gene of interest into Y8205 [28]. Transformants are selected on YP medium with 1% glucose and 100 µg/L clonNAT. Correct targeting of the deletion cassette is verified by PCR. Query strains used in this study are *pic2*Δ (*MATα, pic2*Δ*::clonNAT can1*Δ*::STE2pr-Sp_his5 lyp1*Δ *::STE3pr-LEU2 his3*Δ *leu2*Δ *ura3*Δ*), mrs3*Δ (*MATα, mrs3*Δ*::URA3 can1*Δ*::STE2pr-Sp_his5 lyp1*Δ *::STE3pr-LEU2 his3*Δ *leu2*Δ *ura3*Δ) and *pic2*Δ*mrs3*Δ (*MATα, pic2*Δ*::clonNAT mrs3*Δ*::URA3 can1*Δ*::STE2pr-Sp_his5 lyp1*Δ *::STE3pr-LEU2 his3*Δ *leu2*Δ *ura3*Δ). clonNAT cassette is carried in plasmid p4339 (pCRII-TOPO::natRMX4).

All cultures were grown in YP (1% yeast extract, 2% peptone) medium or synthetic defined media (with selective amino acids excluded) with the appropriate filter sterilized carbon source added. Metal concentrations were varied by using Bio101 yeast nitrogen base (Sunrise, Inc). If required, further copper chelation was achieved by adding bathocuproine disulfonic acid (BCS). Exogenous copper was provided by adding $CuSO_4$. All strains were incubated at 30 °C.

Screen for novel mitochondrial Cu binding targets

DMA and query strains are pinned onto omni plate containing YP media with 2% glucose with the pinning tool to the same position, each plate contains up to 384 strains. After incubation for 48 hours at 30^{o}C, resultant diploid cells were selected for on medium containing clonNAT and G418. The heterozygous diploids are then transferred to plates with sporulation medium to induce sporulation and the formation of haploid meiotic spore progeny. MATa meiotic progeny were then selected for by synthetic medium lacking histidine. The selected spores were then germinated on medium with canavanine, thialysine, G418, and clonNAT with or without uracil.

This condition allowed selection for meiotic progenies with double or triple mutations. The germinated progenies were then grown under the selected conditions for further analyses.

Tetrad Dissection

A tipful of sporulated zygotes were suspended in 50 µl of water with 50 U of lyticase (Sigma-Aldrich L2524) and incubated in 30ºC water bath for 30 minutes. Digested tetrads were then gently transferred onto a dried plate YP medium with 1% glucose. Individual spores from the same tetrad were separated with glass fiber needle under a microscope. The dissected spored were incubated in 30ºC for 48 hours before further analyses.

Elemental analysis

Samples were digested in concentrated metal-free nitric acid by heating at 95ºC for 1 h in capped acid-washed tubes, diluted in ultra-pure, metal-free water, and analyzed by ICP-OES (PerkinElmer Life Sciences, Optima 7300DV) versus acid-washed blanks. Concentrations were determined from a standard curve constructed with serial dilutions of two commercially available mixed metal standards (Optima).

Mitochondria isolation

Mitochondria were isolated as described previously. Briefly, lyticase was used to create spheroplasts that were gently ruptured in a glass Dounce homogenizer. After the spheroplasts were lysed, crude mitochondria were isolated by differential centrifugation in the presence of 0.5 mm phenylmethylsulfonyl fluoride. Cell debris was pelleted at 1,500 × g, mitochondria and microsomes were pelleted at 12,000 × g; the supernatant represented the post-mitochondrial fraction. The crude mitochondria were then loaded onto a discontinuous Nycodenz gradient (16% on 22%) and centrifuged at 150,000 × g for 1 h. The intact mitochondria recovered from the gradient interface were washed in isotonic buffer and pelleted at 12,000 × g before analysis.

Mitochondria were quantified using standard Bradford protein reagents.

Enzyme assay

COX activity was determined by monitoring the decrease in absorbance at 550 nm of chemically reduced cytochrome c in the presence of cell or mitochondrial extracts. Cytochrome c (Sigma # C2506) is prepared at 20 mg in 50 mL of assay buffer (40 mM KH_2PO_4, pH 6.7, 0.5% Tween 20). The A550 nm (using water to zero instrument at A550 nm) is read ($A_{initial}$). The A550 nm is read with cytochrome c solution and recorded as (A_{red}). Next 5 mg dithionite is directly added to the cuvette to achieve and measure the maximum reduction (A_{max}). Percentage reduced is calculated by A_{red}-$A_{initial}/A_{max}$ samples of >90% reduction is used for the assay. If samples are <90% reduced additional dithionite is added and A_{red} re-measured until >90% is achieved. After preparing reduced cytochrome c, mitochondrial (or of whole cells) samples are added and rate of decrease in absorbance at 550nm is measured.

The rates are re-measured in the presence of potassium cyanide (inhibits cytochrome c oxidase activity) to determine any background rate. Activity can be calculated as ΔAbs/min/ microgram protein.

Quantification of the growth

After 48 hours of incubation at 30°C, the plates were scanned and converted to binary with ImageJ. The growth of each mutant was quantified with the measurement function in ImageJ. A box with fixed size was placed around the colony, and average pixel count within that box was measured as the quantified growth of the mutant colony (Figure 3.1). The process was repeated for all colonies on the plates. After all mutant growths were quantified, a Z-score was assigned to each one of them.

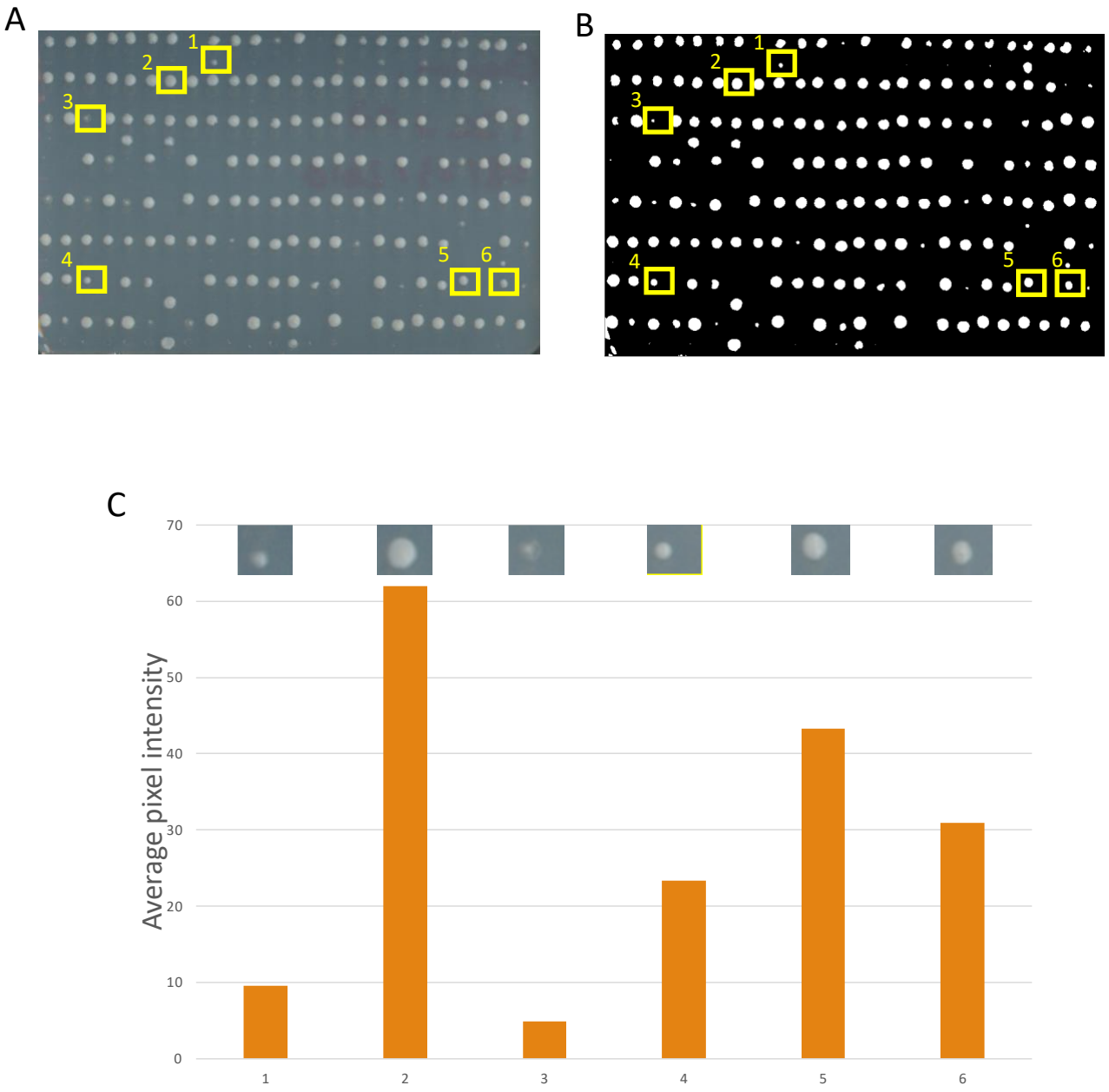

Figure 3.1: Quantification of the Mutant Growth.

Each plate contains up to 384 mutant strains. The equal loading and placement of the culture is ensured by the pinning tool, each pin carries 5 µL of the culture and places it to the precisely the same location across different plates to track their growth. A) After incubation on the selected media for 48 hours at 30°C, the plate is scanned. The six colonies on this plate are used to demonstrate the quantification of the mutants in the experiment. B) the image of the plate is converted to binary. To quantify the growth of each mutant, a box with 2025 pixels is placed around it and the average pixel intensity is measured. C) the growth score of a mutant is represented by the measured average intensity. The quantified growth matches visual observation.

Calculate Z-score for each strain

The z-score is a dimensionless quantity that indicates the number of standard deviations by which an event is above or below the mean value. Values above the mean have positive z-scores, while values below the mean have negative z-scores. The z-scores were calculated by subtracting the mean growth from the raw score, then dividing the difference by the standard deviation:

$$z - score = \frac{x - \mu}{\sigma}$$

where x is the quantified growth, μ is the mean of quantified growth of all mutants, and σ is the standard deviation of the quantified mutant growth.

Results

194 Genes Interact with MCF Translocate Cu

Selected double mutants (DMA x *pic2*Δ, DMA x *mrs3*Δ) and triple mutants (DMA x *pic2*Δ*mrs3*Δ) were transferred to the rich media containing 2% non-fermentable carbon source lactate-glycerol with 5 µM BCS added to create a mild Cu limitation condition (n=2). The double and triple mutants were incubated at 30 ºC. Plates were scanned and the mutant growths were quantified after 48 hours. Strains were then returned to the incubator and allowed to keep growing for up to five days to validate the synthetic lethal interactions. After quantification, the Z-score is calculated and assigned to each mutant.

There were 194 genes that had z-scores of less than -1 as double mutant with *pic2*Δ and *mrs3*Δ and as triple mutant with *pic2*Δ*mrs3*Δ, suggesting these are the potential genetic interactors of MCFs responsible for Cu transport. Analysis of these genes with gene ontology (GO) term revealed no enrichment in cellular functions, processes, or localization.

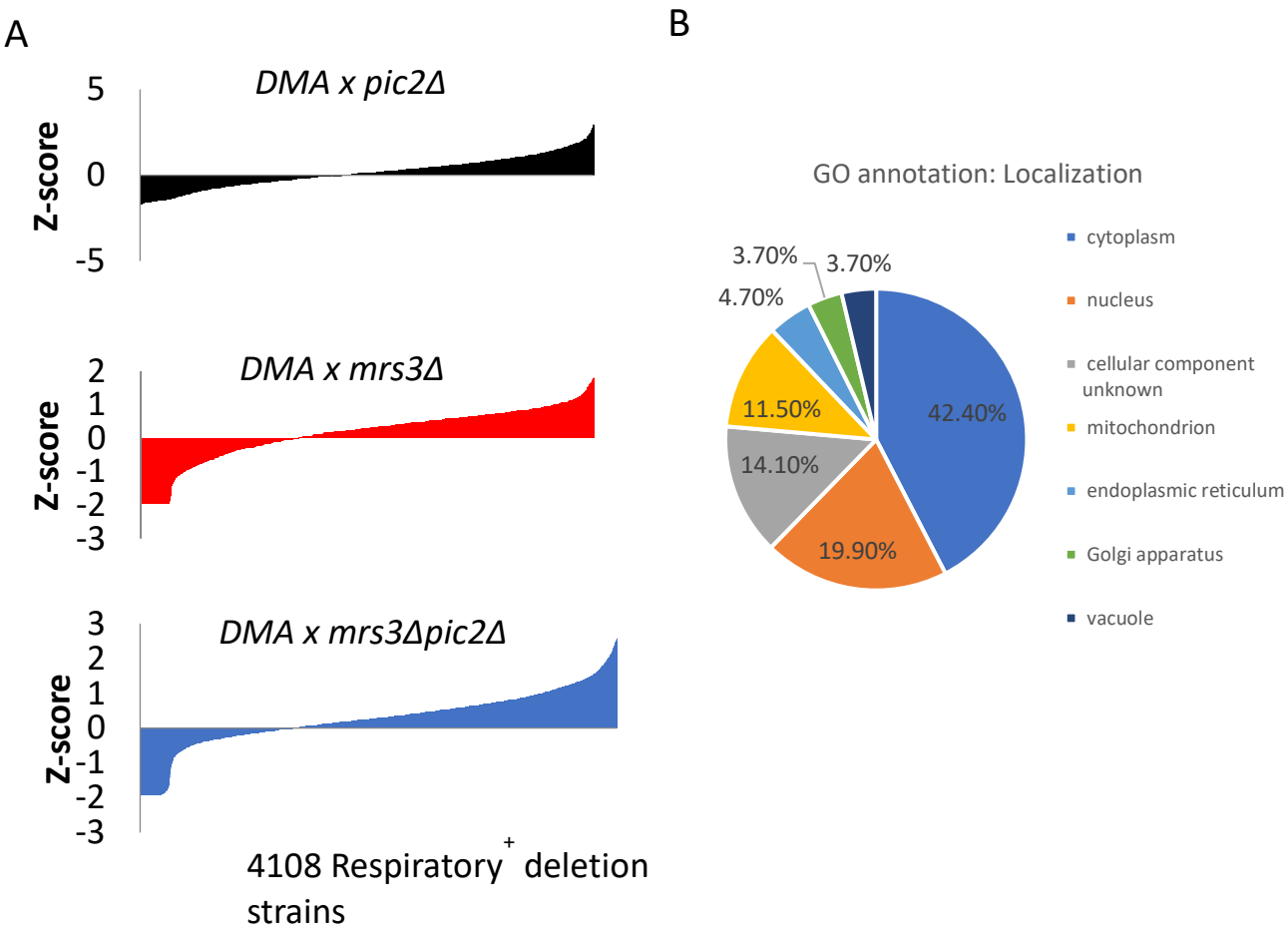

Figure 3.2: SGA yield 194 potential interactors with MCF responsible for Cu transport.

The DMA of over 4,000 single deletion mutants were crossed with *pic2*Δ, *mrs3*Δ, and *pic2*Δ*mrs3*Δ. The double and triple mutants were selected and grown on rich media with non-fermentable carbon source, lactate glycerol, and mild Cu limiting condition with 5 µM BCS. After incubation for 48 hours, the growth of each mutant was quantified, and a z-score was calculated for each colony. A) The distribution of z-scores for all double and triple mutants. 194 genes have z-score of less than -1 when deleted with *pic2*Δ, *mrs3*Δ, and *pic2*Δ*mrs3*Δ. B) these 194 genes were analyzed with GO term for cellular localization, process, and function. The figure shows the GO analysis for cellular localization of the potential interactors as an example. GO term analyses showed no enrichment of the candidates in cellular localization, process, or function.

Synthetic Lethal Interactors with Cu transporting MCFs

There are two types of outcomes can be expected from the SGA: 1) the double or triple mutants can germinate but show a growth defect when grown under the selected screening conditions. These are synthetic sick candidates. 2) the double or triple mutants that are not able to germinate, termed synthetic lethal candidates. The synthetic sick candidates show the additive phenotypes to the known Cu related pathways, suggest the additional components to these pathways. Whereas the synthetic lethal interactors may reveal the genes that are novel in Cu homeostasis.

There were 32 synthetic lethal interactors identified from the screen. These are the ones scored less than 5 on germination plates when crossed with *pic2*Δ*, mrs3*Δ, and *pic2*Δ*mrs3*Δ. In another words, the ones that were not viable as double or triple mutants. Out of these 32 candidates, 22 mutants have physiological roles that prevented germination, i.e. mating defect, sporulation defect or amino acid auxotroph. There are ten synthetic lethal candidates left to be analyzed further. These ten candidates are *ncr1*Δ*, ykr070w*Δ*, pyc2*Δ*, yea4*Δ*, ynr068c*Δ*, uL1b*Δ*, rib1*Δ*, mhf2*Δ*, bud16*Δ, and *aco2*Δ.

Ncr1 is a vacuolar membrane protein involved in sterol trafficking, it mediates transits of sterol through biosynthetic vacuolar protein sorting pathway; cells lacking *NCR1* accumulate long chain bases [50–52]. Ykr070w is a putative protein of unknown function, it is detected as a highly purified mitochondria protein in high-throughput studies [53, 54]. Pyc2 is one of the isoforms of pyruvate carboxylase, it localizes to cytoplasm and converts pyruvate to oxaloacetate [55, 56]. *YEA4* encodes uridine diphosphate-N-acetylglucosamine transporter, it is required for cell wall chitin synthesis, and Yea4 it is localized to the endoplasmic reticulum [57]. Ynr068c is a putative protein of unknown function [58]. uL1b is a component of the ribosomal 60S subunit,

ribosomes containing uL1b are more efficient in translation of respiration-related proteins. *uL1B* is homologous to mammalian ribosomal protein uL10 and bacterial L1, and *uL1a*Δ*uL1b*Δ double mutant is lethal [59–61]. Rib1 catalyzes the first step of the riboflavin biosynthesis pathway [62–64]. *MHF2* is orthologous to human centromere constitutive-associated network subunit CENP-X, it encodes the components in the hetero-tetrameric MHF histone-fold complex. In humans the MHF complex interacts with both DNA and Mph1 ortholog FANCM to stabilize and remodel blocked replication forks and repair damaged DNA [65–67]. Bud16 is a putative pyridoxal kinase localizes to cytosol and peroxisomes that is involved in synthesizing pyridoxal 5'-phosphate, the active form of vitamin B6 [68–70]. It is required for genome integrity. Aco2 is a putative mitochondrial aconitase isozyme that is required for the TCA cycle. The expression of *ACO2* is induced during growth on glucose, by amino acid starvation via Gcn4p, and repressed on ethanol [53, 71, 72].

To test whether adding Cu rescues the lethal phenotype, we obtained the sporulated progenies of *pic2*Δ and candidate deletion diploids, placed them on the germination media with the two selection markers, G418 and clonNAT, with 100 µM of $CuSO_4$, after incubation at 30°C for 48 hours, *aco2*Δ*pic2*Δ double mutant was the only candidate whose lethality was rescued by Cu supplementation (Figure 3.3).

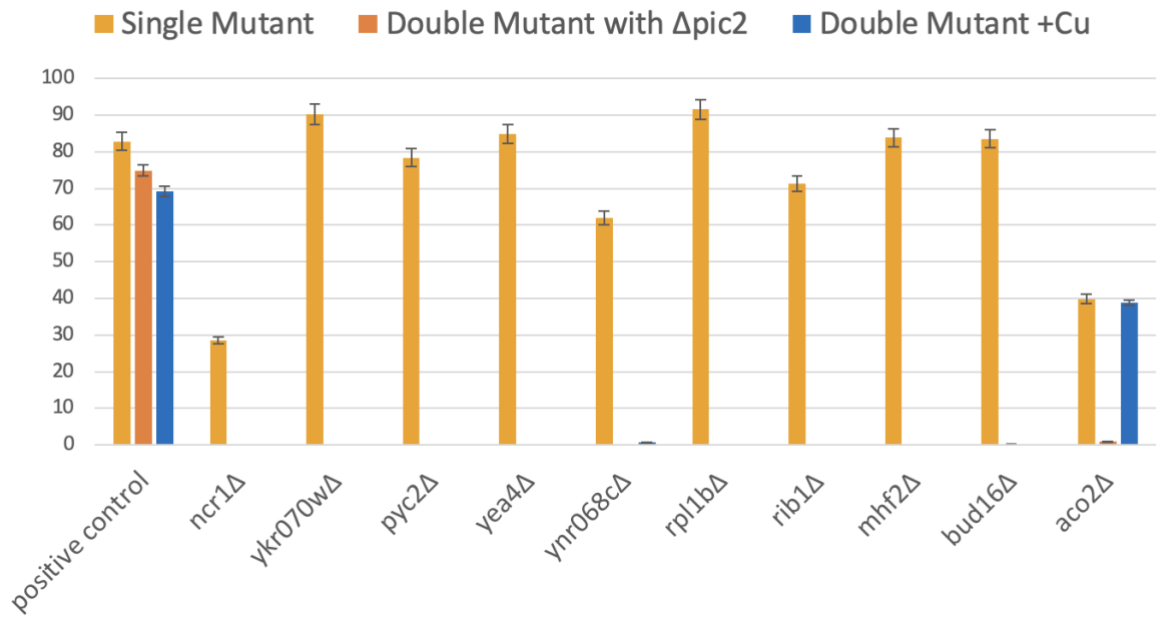

Figure 3.3: *pic2*Δ*aco2*Δ lethality is rescued by Cu supplementation.

Comparison between the quantified growth of synthetic lethal candidates as single mutant, double mutant with *pic2*Δ and double mutant with *pic2*Δ with 100 µM $CuSO_4$ added to the germination media. The mutant (*yor120w*Δ) with average growth is served as the positive control. Quantified growth showed the mutants are viable as single mutant but lethal when combined with picΔ as double mutant. The lethality of *pic2*Δ*aco2*Δ is the only one rescued with 100 µM of $CuSO_4$ was added to the germination media.

Characterization of the Top Candidates

We measured the COX activity and evaluated the ionomic profiles of *aco2*Δ and the single mutants of 10 synthetically sick candidates that grew the worst as double mutants with *pic2*Δ to examine whether they share any similar characteristics with *pic2*Δ and the deletion mutation of its homolog, *mir1*Δ. For ionome profile, we measured cellular Ca, Cu, Fe, K, Mg, Mn, Na, P, and Zn content with inductively coupled plasma – optical emission spectroscopy. We combined the ionomic data and COX activity to generate a heat map and performed principal component analysis (PCA).

Among the analyzed candidates, the heat map indicated *aco2*Δ had the most similar ionomic profile and COX activity to *pic2*Δ, and the next closest candidate. *pic2*Δ, *mir1*Δ, and *aco2*Δ showed a highly consistent trend in Cu content but divergent profiles for COX activity, Fe, K, and Na content. The single mutants of 10 selected candidates showed a similar trend in terms of ionomic profile and COX activity with the exception of *hop2*Δ, which exhibited a different COX activity with the rest of the single mutants.

Driven by primary component of cellular Ca content and secondary component of cellular Cu content, the PCA clustered the 10 selected mutants together, while *pic2*Δ, *aco2*Δ, and *mir1*Δ formed another distinct cluster. Further suggesting *aco2*Δ and *pic2*Δ share very similar characteristics.

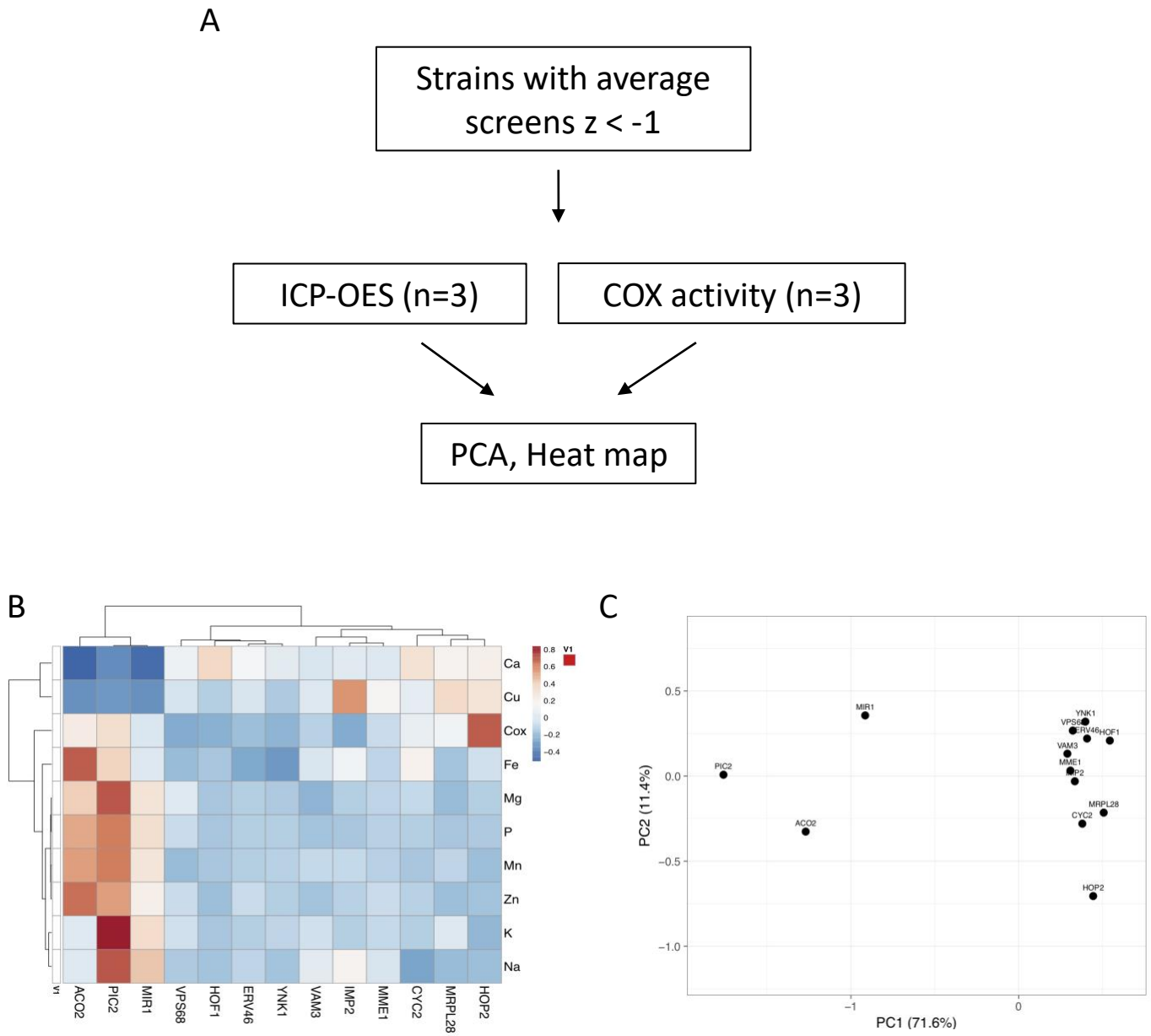

Figure 3.4: Characterization of the single mutants of selected candidates

A) The viable candidates showed the most severe growth defect when combined with *pic2*Δ, *aco2*Δ, and mutant of PIC2 homolog, *mir1*Δ were measured for the COX activity and cellular element content. The collected data were used to generate a heat map and perform PCA. B) the heat map showed *aco2*Δ and *pic2*Δ are closely related while C) PCA clustered *pic2*Δ, *aco2*Δ, and *mir1*Δ together, suggesting they share a high level of similarity.

Conclusion

Cu is required for many critical cellular functions in eukaryotes to survive, it can cause damage to the cells if not handled properly. Therefore, Cu must be delivered to their subcellular destinations in a timely manner after being imported into the cells [1]. Cells adopt a complicated yet highly efficient molecular system to maintain Cu homeostasis and avoid any potential harmful effects it might cause [13]. This system controls the import of Cu into the cell, distribution of Cu to the correct targets at the right time and storage of unused Cu and keep them in a non-redox active form [73]. Any disruption in this system may cause imbalanced cellular Cu homeostasis that leads to diseases at organismal level or even death [22, 23].

Previous studies discovered a soluble anionic Cu pool within the mitochondrial matrix that is required for metalation and activation of mitochondrially localized enzymes. In *S. cerevisiae*, this pool is replenished primarily by MCFs Pic2 and Mrs3, while in mammals the major transporter that is responsible for importing Cu into mitochondria is SLC25A3 [74]. It has been estimated that 10% of mitochondrial Cu is associated with cupro-enzymes that localized to the mitochondria [13]. In addition to that, pharmaceutically induced Cu accumulation in mitochondria causes lipoylated TCA enzymes to be aggregated and denatured, and ultimately leads to cell death [22]. This discovery coincides with other studies that showed overloading of Cu in *E. coli* causes protein aggregations and induces cell death [24, 25]. Collectively, this evidence suggests there are additional targets for Cu to bind within the mitochondria. In this study, we proposed to identify additional protein targets within the mitochondria for Cu binding. We used SGA to screen yeast genes by generating double or triple mutants of mitochondrial transporters and DMA [28]. 194 potential interactors were identified, among which 162 showed

synthetic sickness and 32 were synthetic lethal that failed to germinate as double or triple mutants. GO term analyses did not reveal an obvious connection between these candidates. We then examined the synthetic lethal interactors and 22 of them had a known role preventing them from germinating. We transferred the diploid progenies produced by crossing of the remaining 10 candidates and *pic2*Δ to germination media with added Cu, and *aco2*Δ*pic2*Δ was the only strain whose lethality was reversed.

Further biochemical and ionomic analyses of a selected group of candidates showed the *aco2*Δ resembled the profile of *pic2*Δ. Therefore, we chose this candidate for the further analyses and the results is presented in the next chapter.

References

1. Beaudoin J, Ekici S, Daldal F, Ait-Mohand S, Guérin B, Labbé S (2013) Copper transport and regulation in Schizosaccharomyces pombe. Biochem Soc Trans 41:1679–1686. https://doi.org/10.1042/BST2013089

2. Boal AK, Rosenzweig AC (2009) Structural biology of copper trafficking. Chem Rev 109:4760–4779. https://doi.org/10.1021/cr900104z

3. Yuan DS, Stearman R, Dancis A, Dunn T, Beeler T, Klausner RD (1995) The Menkes/Wilson disease gene homologue in yeast provides copper to a ceruloplasmin-like oxidase required for iron uptake. Proceedings of the National Academy of Sciences 92:2632–2636. https://doi.org/10.1073/pnas.92.7.2632

4. Barber RG, Grenier ZA, Burkhead JL (2021) Copper Toxicity Is Not Just Oxidative Damage: Zinc Systems and Insight from Wilson Disease. Biomedicines 9:316. https://doi.org/10.3390/biomedicines9030316

5. Trist BG, Fifita JA, Freckleton SE, Hare DJ, Lewis SJG, Halliday GM, Blair IP, Double KL (2018) Accumulation of dysfunctional SOD1 protein in Parkinson's disease is not associated with mutations in the SOD1 gene. Acta Neuropathol 135:155–156. https://doi.org/10.1007/s00401-017-1779-6

6. Nikseresht S, Hilton JBW, Kysenius K, Liddell JR, Crouch PJ (2020) Copper-ATSM as a Treatment for ALS: Support from Mutant SOD1 Models and Beyond. Life (Basel) 10:271. https://doi.org/10.3390/life10110271

7. Aller SG, Unger VM (2006) Projection structure of the human copper transporter CTR1 at 6-Å resolution reveals a compact trimer with a novel channel-like architecture. Proceedings of the National Academy of Sciences 103:3627–3632. https://doi.org/10.1073/pnas.0509929103

8. De Feo CJ, Aller SG, Siluvai GS, Blackburn NJ, Unger VM (2009) Three-dimensional structure of the human copper transporter hCTR1. Proceedings of the National Academy of Sciences 106:4237–4242. https://doi.org/10.1073/pnas.0810286106

9. Eisses JF, Kaplan JH (2005) The Mechanism of Copper Uptake Mediated by Human CTR1: A MUTATIONAL ANALYSIS*. Journal of Biological Chemistry 280:37159–37168. https://doi.org/10.1074/jbc.M508822200

10. Arnesano F, Banci L, Bertini I, Huffman DL, O'Halloran TV (2001) Solution Structure of the Cu(I) and Apo Forms of the Yeast Metallochaperone, Atx1,. Biochemistry 40:1528–1539. https://doi.org/10.1021/bi0014711

11. Huffman DL, O'Halloran TV (2000) Energetics of Copper Trafficking between the Atx1 Metallochaperone and the Intracellular Copper Transporter, Ccc2*. Journal of Biological Chemistry 275:18611–18614. https://doi.org/10.1074/jbc.C000172200

12. Carroll MC, Girouard JB, Ulloa JL, Subramaniam JR, Wong PC, Valentine JS, Culotta VC (2004) Mechanisms for activating Cu- and Zn-containing superoxide dismutase in the absence of the CCS Cu chaperone. Proceedings of the National Academy of Sciences of the United States of America

101:5964–5969. https://doi.org/10.1073/pnas.0308298101

13. Cobine PA, Ojeda LD, Rigby KM, Winge DR (2004) Yeast Contain a Non-proteinaceous Pool of Copper in the Mitochondrial Matrix*. Journal of Biological Chemistry 279:14447–14455. https://doi.org/10.1074/jbc.M312693200

14. Banci L, Bertini I, Cantini F, Felli IC, Gonnelli L, Hadjiliadis N, Pierattelli R, Rosato A, Voulgaris P (2006) The Atx1-Ccc2 complex is a metal-mediated protein-protein interaction. Nat Chem Biol 2:367–368. https://doi.org/10.1038/nchembio797

15. Schmidt PJ, Kunst C, Culotta VC (2000) Copper Activation of Superoxide Dismutase 1 (SOD1) *in Vivo*. Journal of Biological Chemistry 275:33771–33776. https://doi.org/10.1074/jbc.M006254200

16. Gross DP, Burgard CA, Reddehase S, Leitch JM, Culotta VC, Hell K (2011) Mitochondrial Ccs1 contains a structural disulfide bond crucial for the import of this unconventional substrate by the disulfide relay system. Mol Biol Cell 22:3758–3767. https://doi.org/10.1091/mbc.E11-04-0296

17. Liebschner D, Afonine PV, Baker ML, Bunkóczi G, Chen VB, Croll TI, Hintze B, Hung LW, Jain S, McCoy AJ, Moriarty NW, Oeffner RD, Poon BK, Prisant MG, Read RJ, Richardson JS, Richardson DC, Sammito MD, Sobolev OV, Stockwell DH, Terwilliger TC, Urzhumtsev AG, Videau LL, Williams CJ, Adams PD (2019) Macromolecular structure determination using X-rays, neutrons and electrons: recent developments in Phenix. Acta Crystallogr D Struct Biol 75:861–877. https://doi.org/10.1107/S2059798319011471

18. Carr HS, Winge DR (2003) Assembly of cytochrome c oxidase within the mitochondrion. Accounts of Chemical Research 36:309–316. https://doi.org/10.1021/ar0200807

19. Leary SC, Winge DR, Cobine PA (2009) "Pulling the plug" on cellular copper: The role of mitochondria in copper export. Biochimica et Biophysica Acta (BBA) - Molecular Cell Research 1793:146–153. https://doi.org/10.1016/j.bbamcr.2008.05.002

20. Baker ZN, Cobine PA, Leary SC (2017) The mitochondrion: a central architect of copper homeostasis. Metallomics 9:1501–1512. https://doi.org/10.1039/c7mt00221a

21. Rae TD, Schmidt PJ, Pufahl RA, Culotta VC, O'Halloran TV (1999) Undetectable intracellular free copper: The requirement of a copper chaperone for superoxide dismutase. Science 284:805–808. https://doi.org/10.1126/science.284.5415.805

22. Tsvetkov P, Coy S, Petrova B, Dreishpoon M, Verma A, Abdusamad M, Rossen J, Joesch-Cohen L, Humeidi R, Spangler RD, Eaton JK, Frenkel E, Kocak M, Corsello SM, Lutsenko S, Kanarek N, Santagata S, Golub TR (2022) Copper induces cell death by targeting lipoylated TCA cycle proteins. Science 375:1254–1261. https://doi.org/10.1126/science.abf0529

23. Cobine PA, Brady DC (2022) Cuproptosis: Cellular and molecular mechanisms underlying copper-induced cell death. Molecular Cell 82:1786–1787. https://doi.org/10.1016/j.molcel.2022.05.001

24. Wiebelhaus N, Zaengle-Barone JM, Hwang KK, Franz KJ, Fitzgerald MC (2021) Protein folding stability changes across the proteome reveal targets of Cu toxicity in E. coli. ACS Chem Biol 16:214–224. https://doi.org/10.1021/acschembio.0c00900

25. Zuily L, Lahrach N, Fassler R, Genest O, Faller P, Sénèque O, Denis Y, Castanié-Cornet M-P,

Genevaux P, Jakob U, Reichmann D, Giudici-Orticoni M-T, Ilbert M (2022) Copper Induces Protein Aggregation, a Toxic Process Compensated by Molecular Chaperones. mBio 13:e03251-21. https://doi.org/10.1128/mbio.03251-21

26. Martin WF, Garg S, Zimorski V (2015) Endosymbiotic theories for eukaryote origin. Philosophical Transactions of the Royal Society B: Biological Sciences 370:. https://doi.org/10.1098/rstb.2014.0330

27. Engel SR, Dietrich FS, Fisk DG, Binkley G, Balakrishnan R, Costanzo MC, Dwight SS, Hitz BC, Karra K, Nash RS, Weng S, Wong ED, Lloyd P, Skrzypek MS, Miyasato SR, Simison M, Cherry JM (2013) The Reference Genome Sequence of Saccharomyces cerevisiae: Then and Now. G3 (Bethesda) 4:389–398. https://doi.org/10.1534/g3.113.008995

28. Tong AHY, Boone C (2006) Synthetic genetic array analysis in Saccharomyces cerevisiae. Methods Mol Biol 313:171–192. https://doi.org/10.1385/1-59259-958-3:171

29. Jensen LT, Howard WR, Strain JJ, Winge DR, Culotta VC (1996) Enhanced Effectiveness of Copper Ion Buffering by CUP1 Metallothionein Compared with CRS5 Metallothionein in Saccharomyces cerevisiae. Journal of Biological Chemistry 271:18514–18519. https://doi.org/10.1074/jbc.271.31.18514

30. Culotta VC, Howard WR, Liu XF (1994) CRS5 encodes a metallothionein-like protein in Saccharomyces cerevisiae. Journal of Biological Chemistry 269:25295–25302. https://doi.org/10.1016/s0021-9258(18)47246-8

31. Brown KR, Keller GL, Pickering IJ, Harris HH, George GN, Winge DR (2002) Structures of the cuprous-thiolate clusters of the Mac1 and Ace1 transcriptional activators. Biochemistry 41:6469–6476. https://doi.org/10.1021/bi0160664

32. Thiele DJ, Wright CF, Walling MJ, Hamer DH (1987) Function and Regulation of Yeast Copperthionein. In: Kägi JHR, Kojima Y (eds) Metallothionein II: Proceedings of the «Second International Meeting on Metallothionein and Other Low Molecular Weight Metalbinding Proteins», Zürich, August 21–24, 1985. Birkhäuser, Basel, pp 423–429

33. Thiele DJ (1988) ACE1 Regulates Expression of the Saccharomyces cerevisiae Metallothionein Gene. Molecular and Cellular Biology 8:2745–2752. https://doi.org/10.1128/mcb.8.7.2745-2752.1988

34. Shi X, Stoj C, Romeo A, Kosman DJ, Zhu Z (2003) Fre1p Cu2+ Reduction and Fet3p Cu1+ Oxidation Modulate Copper Toxicity in *Saccharomyces cerevisiae**. Journal of Biological Chemistry 278:50309–50315. https://doi.org/10.1074/jbc.M307019200

35. Peña MMO, Puig S, Thiele DJ (2000) Characterization of the *Saccharomyces cerevisiae* High Affinity Copper Transporter Ctr3*. Journal of Biological Chemistry 275:33244–33251. https://doi.org/10.1074/jbc.M005392200

36. Askwith C, Eide D, Van Ho A, Bernard PS, Li L, Davis-Kaplan S, Sipe DM, Kaplan J (1994) The *FET3* gene of S. cerevisiae encodes a multicopper oxidase required for ferrous iron uptake. Cell 76:403–410. https://doi.org/10.1016/0092-8674(94)90346-8

37. Hassett R, Dix DR, Eide DJ, Kosman DJ (2000) The Fe(II) permease Fet4p functions as a low

affinity copper transporter and supports normal copper trafficking in Saccharomyces cerevisiae. Biochem J 351 Pt 2:477–484

38. Cohen A, Nelson H, Nelson N (2000) The Family of *SMF* Metal Ion Transporters in Yeast Cells*. Journal of Biological Chemistry 275:33388–33394. https://doi.org/10.1074/jbc.M004611200

39. Rees EM, Thiele DJ (2007) Identification of a Vacuole-associated Metalloreductase and Its Role in Ctr2-mediated Intracellular Copper Mobilization*. Journal of Biological Chemistry 282:21629–21638. https://doi.org/10.1074/jbc.M703397200

40. Rees EM, Lee J, Thiele DJ (2004) Mobilization of Intracellular Copper Stores by the Ctr2 Vacuolar Copper Transporter*. Journal of Biological Chemistry 279:54221–54229. https://doi.org/10.1074/jbc.M411669200

41. Davis-Kaplan SR, Askwith CC, Bengtzen AC, Radisky D, Kaplan J (1998) Chloride is an allosteric effector of copper assembly for the yeast multicopper oxidase Fet3p: An unexpected role for intracellular chloride channels. Proceedings of the National Academy of Sciences of the United States of America 95:13641–13645. https://doi.org/10.1073/pnas.95.23.13641

42. Sturtz LA, Diekert K, Jensen LT, Lill R, Culotta VC (2001) A Fraction of Yeast Cu,Zn-Superoxide Dismutase and Its Metallochaperone, CCS, Localize to the Intermembrane Space of Mitochondria: A PHYSIOLOGICAL ROLE FOR SOD1 IN GUARDING AGAINST MITOCHONDRIAL OXIDATIVE DAMAGE*. Journal of Biological Chemistry 276:38084–38089. https://doi.org/10.1074/jbc.M105296200

43. Oxygen-induced maturation of SOD1: a key role for disulfide formation by the copper chaperone CCS - PMC. https://www.ncbi.nlm.nih.gov/pmc/articles/PMC1150991/. Accessed 30 Mar 2024

44. Khalimonchuk O, Bestwick M, Meunier B, Watts TC, Winge DR (2010) Formation of the redox cofactor centers during Cox1 maturation in yeast cytochrome oxidase. Mol Cell Biol 30:1004–1017. https://doi.org/10.1128/MCB.00640-09

45. Ruprecht JJ, Kunji ERS (2020) The SLC25 Mitochondrial Carrier Family: Structure and Mechanism. Trends in Biochemical Sciences 45:244–258. https://doi.org/10.1016/j.tibs.2019.11.001

46. Cavero S, Vozza A, Del Arco A, Palmieri L, Villa A, Blanco E, Runswick MJ, Walker JE, Cerdán S, Palmieri F, Satrústegui J (2003) Identification and metabolic role of the mitochondrial aspartate-glutamate transporter in Saccharomyces cerevisiae. Molecular Microbiology 50:1257–1269. https://doi.org/10.1046/j.1365-2958.2003.03742.x

47. Vest KE, Cobine PA (2011) Copper in Mitochondria. Encyclopedia of Inorganic and Bioinorganic Chemistry 1–12. https://doi.org/10.1002/9781119951438.eibc2155

48. Vest KE, Wang J, Gammon MG, Maynard MK, White OL, Cobine JA, Mahone WK, Cobine PA (2016) Overlap of copper and iron uptake systems in mitochondria in Saccharomyces cerevisiae. Open Biol 6:150223. https://doi.org/10.1098/rsob.150223

49. Vest KE, Leary SC, Winge DR, Cobine PA (2013) Copper Import into the Mitochondrial Matrix in *Saccharomyces cerevisiae* Is Mediated by Pic2, a Mitochondrial Carrier Family Protein*. Journal of Biological Chemistry 288:23884–23892. https://doi.org/10.1074/jbc.M113.470674

50. Eising S, Esch B, Wälte M, Vargas Duarte P, Walter S, Ungermann C, Bohnert M, Fröhlich F (2022) A lysosomal biogenesis map reveals the cargo spectrum of yeast vacuolar protein targeting pathways. Journal of Cell Biology 221:e202107148. https://doi.org/10.1083/jcb.202107148

51. Zhang S, Ren J, Li H, Zhang Q, Armstrong JS, Munn AL, Yang H (2004) Ncr1p, the Yeast Ortholog of Mammalian Niemann Pick C1 Protein, is Dispensable for Endocytic Transport. Traffic 5:1017–1030. https://doi.org/10.1111/j.1600-0854.2004.00241.x

52. Malathi K, Higaki K, Tinkelenberg AH, Balderes DA, Almanzar-Paramio D, Wilcox LJ, Erdeniz N, Redican F, Padamsee M, Liu Y, Khan S, Alcantara F, Carstea ED, Morris JA, Sturley SL (2004) Mutagenesis of the putative sterol-sensing domain of yeast Niemann Pick C–related protein reveals a primordial role in subcellular sphingolipid distribution. Journal of Cell Biology 164:547–556. https://doi.org/10.1083/jcb.200310046

53. Huh W-K, Falvo JV, Gerke LC, Carroll AS, Howson RW, Weissman JS, O'Shea EK (2003) Global analysis of protein localization in budding yeast. Nature 425:686–691. https://doi.org/10.1038/nature02026

54. Reinders J, Zahedi RP, Pfanner N, Meisinger C, Sickmann A (2006) Toward the Complete Yeast Mitochondrial Proteome: Multidimensional Separation Techniques for Mitochondrial Proteomics. J Proteome Res 5:1543–1554. https://doi.org/10.1021/pr050477f

55. Bricker DK, Taylor EB, Schell JC, Orsak T, Boutron A, Chen Y-C, Cox JE, Cardon CM, Van Vranken JG, Dephoure N, Redin C, Boudina S, Gygi SP, Brivet M, Thummel CS, Rutter J (2012) A Mitochondrial Pyruvate Carrier Required for Pyruvate Uptake in Yeast, Drosophila, and Humans. Science 337:96–100. https://doi.org/10.1126/science.1218099

56. Brewster NK, Val DL, Walker ME, Wallace JC (1994) Regulation of Pyruvate Carboxylase Isozyme (PYC1, PYC2) Gene Expression in *Saccharomyces cerevisiae* during Fermentative and Nonfermentative Growth. Archives of Biochemistry and Biophysics 311:62–71. https://doi.org/10.1006/abbi.1994.1209

57. Roy SK, Chiba Y, Takeuchi M, Jigami Y (2000) Characterization of Yeast Yea4p, a Uridine Diphosphate-*N*-acetylglucosamine Transporter Localized in the Endoplasmic Reticulum and Required for Chitin Synthesis*. Journal of Biological Chemistry 275:13580–13587. https://doi.org/10.1074/jbc.275.18.13580

58. Novoselova TV, Zahira K, Rose R-S, Sullivan JA (2012) Bul Proteins, a Nonredundant, Antagonistic Family of Ubiquitin Ligase Regulatory Proteins. Eukaryotic Cell 11:463–470. https://doi.org/10.1128/ec.00009-12

59. Venema J, Tollervey D (1999) Ribosome Synthesis in Saccharomyces cerevisiae. Annual Review of Genetics 33:261–311. https://doi.org/10.1146/annurev.genet.33.1.261

60. Zhao Y, Sohn J-H, Warner JR (2003) Autoregulation in the Biosynthesis of Ribosomes. Molecular and Cellular Biology 23:699–707. https://doi.org/10.1128/MCB.23.2.699-707.2003

61. Li B, Nierras CR, Warner JR (1999) Transcriptional Elements Involved in the Repression of Ribosomal Protein Synthesis. Molecular and Cellular Biology 19:5393–5404. https://doi.org/10.1128/MCB.19.8.5393

62. Oltmanns O, Bacher A (1972) Biosynthesis of Riboflavine in Saccharomyces cerevisiae: the Role of Genes rib1 and rib7. Journal of Bacteriology 110:818–822. https://doi.org/10.1128/jb.110.3.818-822.1972

63. Buitrago M-J, Gonzalez GA, Saiz JE, Revuelta JL (1993) Mapping of the RIB1 and RIB7 genes involved in the biosynthesis of riboflavin in Saccharomyces cerevisiae. Yeast 9:1099–1102. https://doi.org/10.1002/yea.320091009

64. Richter G, Fischer M, Krieger C, Eberhardt S, Lüttgen H, Gerstenschläger I, Bacher A (1997) Biosynthesis of riboflavin: characterization of the bifunctional deaminase-reductase of Escherichia coli and Bacillus subtilis. Journal of Bacteriology 179:2022–2028. https://doi.org/10.1128/jb.179.6.2022-2028.1997

65. Yang H, Zhang T, Tao Y, Wu L, Li H, Zhou J, Zhong C, Ding J (2012) *Saccharomyces Cerevisiae* MHF Complex Structurally Resembles the Histones (H3-H4)2 Heterotetramer and Functions as a Heterotetramer. Structure 20:364–370. https://doi.org/10.1016/j.str.2011.12.012

66. Schleiffer A, Maier M, Litos G, Lampert F, Hornung P, Mechtler K, Westermann S (2012) CENP-T proteins are conserved centromere receptors of the Ndc80 complex. Nat Cell Biol 14:604–613. https://doi.org/10.1038/ncb2493

67. Yan Z, Delannoy M, Ling C, Daee D, Osman F, Muniandy PA, Shen X, Oostra AB, Du H, Steltenpool J, Lin T, Schuster B, Décaillet C, Stasiak A, Stasiak AZ, Stone S, Hoatlin ME, Schindler D, Woodcock CL, Joenje H, Sen R, de Winter JP, Li L, Seidman MM, Whitby MC, Myung K, Constantinou A, Wang W (2010) A Histone-Fold Complex and FANCM Form a Conserved DNA-Remodeling Complex to Maintain Genome Stability. Molecular Cell 37:865–878. https://doi.org/10.1016/j.molcel.2010.01.039

68. Kanellis P, Gagliardi M, Banath JP, Szilard RK, Nakada S, Galicia S, Sweeney FD, Cabelof DC, Olive PL, Durocher D (2007) A Screen for Suppressors of Gross Chromosomal Rearrangements Identifies a Conserved Role for PLP in Preventing DNA Lesions. PLOS Genetics 3:e134. https://doi.org/10.1371/journal.pgen.0030134

69. Yifrach E, Holbrook-Smith D, Bürgi J, Othman A, Eisenstein M, van Roermund CW, Visser W, Tirosh A, Rudowitz M, Bibi C, Galor S, Weill U, Fadel A, Peleg Y, Erdmann R, Waterham HR, Wanders RJA, Wilmanns M, Zamboni N, Schuldiner M, Zalckvar E (2022) Systematic multi-level analysis of an organelle proteome reveals new peroxisomal functions. Molecular Systems Biology 18:e11186. https://doi.org/10.15252/msb.202211186

70. Ni L, Snyder M (2001) A Genomic Study of the Bipolar Bud Site Selection Pattern inSaccharomyces cerevisiae. MBoC 12:2147–2170. https://doi.org/10.1091/mbc.12.7.2147

71. Sickmann A, Reinders J, Wagner Y, Joppich C, Zahedi R, Meyer HE, Schönfisch B, Perschil I, Chacinska A, Guiard B, Rehling P, Pfanner N, Meisinger C (2003) The proteome of Saccharomyces cerevisiae mitochondria. Proceedings of the National Academy of Sciences 100:13207–13212. https://doi.org/10.1073/pnas.2135385100

72. Natarajan K, Meyer MR, Jackson BM, Slade D, Roberts C, Hinnebusch AG, Marton MJ (2001) Transcriptional Profiling Shows that Gcn4p Is a Master Regulator of Gene Expression during Amino Acid Starvation in Yeast. Molecular and Cellular Biology 21:4347–4368. https://doi.org/10.1128/MCB.21.13.4347-4368.2001

73. Heuchel R, Radtke F, Georgiev O, Stark G, Aguet M, Schaffner W (1994) The transcription factor MTF-1 is essential for basal and heavy metal-induced metallothionein gene expression. The EMBO Journal 13:2870–2875. https://doi.org/10.1002/j.1460-2075.1994.tb06581.x

74. Boulet A, Vest KE, Maynard MK, Gammon MG, Russell AC, Mathews AT, Cole SE, Zhu X, Phillips CB, Kwong JQ, Dodani SC, Leary SC, Cobine PA (2018) The mammalian phosphate carrier SLC25A3 is a mitochondrial copper transporter required for cytochrome c oxidase biogenesis. J Biol Chem 293:1887–1896. https://doi.org/10.1074/jbc.RA117.000265

Chapter 4: Copper Regulates Aconitase Activity through Metalloallostery

Abstract

Copper (Cu) is required for many important cellular functions in eukaryotes; however, it becomes toxic to cells when mis-regulated. In *Saccharomyces cerevisiae,* Cu serves as a cofactor for various enzymes including cytochrome *c* oxidase, superoxide dismutase and multi-copper oxidase. Recent studies focus on elucidating the role of Cu as a metalloallostery regulator in different signaling pathways. We discovered a novel copper-rescuable phenotype in yeast that cannot be explained by the known role of Cu. *ACO1* and *ACO2* are two aconitase homologs in *S. cerevisiae*. Aco1 is a TCA cycle enzyme that catalyzes isomerization of citrate to isocitrate through cis-aconitate, while Aco2 is required for lysine biosynthesis in the α-aminoadipate pathway to dehydrate homocitrate and produce cis-homoaconitate. We discovered a slow growth phenotype in the *aco2*Δ*pic2*Δ*lyp1*Δ mutant that is exacerbated under copper limitation and rescued by copper supplementation. The rescue of the phenotype is dependent on the expression of *ACO1*. Given the structural similarities between the two homologs, we hypothesize that Cu binds to Aco1 and allosterically regulates substrate specificity. *in vitro* biochemical assays demonstrated the substrate specificity of Aco1 can be modulated by adding Cu.

Introduction

Copper (Cu) is essential for eukaryotes. Cells exploit the redox nature of the metal by using it as a cofactor for numerous enzymes involved in vital biological processes. The Cu homeostasis is meticulously maintained by the cells to avoid any adventitious effects it may cause [1, 2]. Disruption of Cu homeostasis is linked to multiple human diseases. Cu accumulation causes Wilson disease, idiopathic Cu toxicosis and endemic tyrolean infantile cirrhosis, while Cu deficiency is associated with Menkes disease, developmental defects and neuropathologies including amyotrophic lateral sclerosis and Parkinson's disease [3–7]. Delivery of Cu from the outside environment to their designated targets within the cell is a highly complicated process that requires concerted cooperation of multiple transporters, chaperone proteins and redox active metabolites [8].

Saccharomyces cerevisiae uses a combination of high- and low-affinity transports to import Cu [9–13]. Once inside the cell, Cu is delivered to the targets by the copper chaperones [14]. The proper insertion of Cu is guided by the increasing affinity in the target protein [15]. Cu must be distributed to the secretory pathway for insertion into enzymes required for high-affinity iron transport [16, 17], to cytosolic targets for insertion into superoxide dismutase for protection against oxidative stress [18, 19], and to mitochondria to be assembled into the terminal electron accepting complex in the energy-producing electron transport chain, cytochrome c oxidase complex [20–22]. The translocation of Cu into mitochondria in yeast is mediated by mitochondrial carrier family protein (MCF) members [23]. These carriers contain three transmembrane alpha-helical domains that form an opening across the membrane characterizing a conserved structure of these proteins. The carrier channel is closed by the salt bridges formed by

conserved PX[DE]XX[KR] motifs within the transmembrane alpha-helices. Upon substrate binding, the channel is opened to allow for translocation across the membrane [24].

The transport of transition metal into mitochondria is mediated by multiple MCF proteins. Pic2 was the first identified MCF to transfer copper into the matrix to replenish the mitochondrial Cu pool, which is required for metalation of cytochrome c oxidase and superoxide dismutase. Yeast strains with deleted PIC2 show Cu-dependent growth defects, and mitochondria from these cells have lower Cu content. Importantly, Pic2 expressed in *Lactococcus lactis* was able to transport copper. The mitochondrial iron-transporting protein Mrs3 has also been shown to contribute to copper import into mitochondria [23].

While the Cu delivery pathways has been extensively studied, the role of Cu in metalloallostery has recently drawn attention of researchers. Studies have shown Cu can transiently bind to and modulate the activities of enzymes involved in different signaling pathways, including mitogen-activated protein kinase (MAPK) signaling pathway, ULK1/2 in autophagic pathway, and PDE3B in lipolysis pathway [25]. The canonical MAPK pathway consists of the RAF-MEK-ERK signaling cascade and represents one of the most well-defined axes within eukaryotic cells that promotes cell proliferation. Mutated enzymes that constitutively activate this pathway are associated with human cancers [26]. Surface plasmon resonance and proximity-dependent biotin ligase studies identified a Cu chaperone for superoxide dismutase (CCS) as the Cu chaperone that selectively bound to and facilitated Cu transfer to MAP kinase kinase (MEK1), and in vitro assay showed that the kinase activity is enhanced with increased Cu-loaded CCS present in the reaction mixture [26]. Mutants of CCS that disrupt Cu(I) acquisition and exchange or a CCS small-molecule inhibitor were used and resulted in reduced Cu-stimulated MEK1 kinase activity. Cu is also to activate the autophagic kinases ULK1 and

ULK2 (ULK1/2) through a direct interaction [27]. ULK1/2 share a conserved Cu binding sequence with MEK1/2, and the ULK1/2 mutants losing Cu binding capacity results in reduced ULK1/2-dependent signaling and the formation of autophagosome complexes. ULK1/2 enzyme activity corresponds to the intracellular Cu content, increased Cu level is associated with starvation-induced autophagy and are sufficient to enhance ULK1 kinase activity and, in turn, autophagic flux. Cu also interacts with energetic metabolism signaling pathway [27]. Elevated liver Cu level and diminished lipid level was observed in *Atp7b*$^{-/-}$ mouse, where mutation of the copper exporter protein ATP7B results in excess copper accumulation in the liver. In contrast to the liver, the white adipose tissue (WAT) of Atp7b$^{-/-}$ mice has reduced Cu levels. Investigation of cyclic AMP (cAMP)-dependent lipolysis with β-adrenergic receptor agonist in Atp7b$^{-/-}$ WAT suggest Cu level influences lipolysis activity. Further mechanistic biochemical studies showed Cu binds to a key allosteric C768 site and inhibits the activity of isoform-specific phosphodiesterase 3B (PDE3B), which is responsible for cAMP-dependent lipolysis of triglycerides into fatty acids and glycerol [28]. This shows that reversible metal binding can cause a decrease in catalytic activity of the enzyme target. The studies mentioned above demonstrated that the overall enzyme activity can be either enhanced or inhibited with transient Cu binding. However, no previous studies reported the substrate specificity can be modulated by Cu metalloallostery.

Materials and Methods

Yeast strains, culture conditions, and standard methods

Yeast strains used were BY4741 (*MATa, leu2*Δ*, met15*Δ*, ura3*Δ*, his3*Δ) and isogenic kanMX4 mutant from Open Biosystems (Huntsville, AL). Double mutants were constructed by homologous recombination of the *URA3MX* cassette at the *MRS3* locus. The Y8205 (*MATα,*

can1Δ::STE2pr-Sp_his5 lyp1Δ ::STE3pr-LEU2 his3Δ leu2Δ ura3Δ) strain was a kind gift from Scot Leary (University of Saskatchewan). Cultures were grown in 1% yeast extract, 2% peptone (YP) medium or in synthetic defined media with selective amino acids excluded using the appropriate carbon source. If required, further copper depletion was achieved by adding filter-sterilized extracellular copper chelator bathocuproine sulfonate (BCS).

Growth tests were performed at 30 °C with 1 in 10 serial dilutions of overnight pre-cultures grown in YP plus 1% glucose.

Aconitase activity assay

All solutions used are deoxygenated by nitrogen gas purging at rate of 1L/min for thirty minutes. To prepare active aconitase solution, porcine aconitase (Sigma-Aldrich, 9024-25-3) is suspended in 10mM Tris-HCl pH 7.4 at 10 mg/mL, then activated by adding ammonium ferrous sulfate to a final concentration of 50 µM and L-cysteine of 5 mM, followed by incubating on ice for one hour and filtering through 0.4 µm syringe filter. Citrate or homocitrate were dissolved in 10mM Tris-HCl pH 7.4 to be used as substrates. Enzyme activities are assayed by measuring the rate of change in 240 nm absorbance over thirty minutes, which indicates the changes of aconitate or homoaconitate concentration within the reaction mixture.

RNA extraction

1mL yeast culture was collected by 10,000 x *g* 5 min. After washing the cell pellet twice with water, the supernatant was removed, and the pellet was resuspended with 100 µL water. Then, 800 µL TRIzol (ThermoFisher 15596026) was added to the resuspended cells directly, and the cells were lysed by pipetting the mixture up and down for several times. After incubating at room temperature for 5 minutes, 1/5 volume of chloroform (160 µL for 800 µL total volume) was added to the tube and thoroughly mix the sample by vortex. The mixture was incubated for

2–3 minutes at room temperature then centrifuged at 12,000 x *g* for 15 minutes at 4°C. The sample will separate into a lower red phenol-chloroform organic layer, an interphase, and a colorless upper aqueous phase. The top aqueous phase containing the RNA was transferred to a new tube containing 1 volume of isopropanol. The sample was then incubated for 10 minutes at room temperature followed by centrifugation at 12,000 x *g* for 10 minutes at 4°C. The supernatant was discarded, and the total RNA pellet was washed in 1 mL 70% ice cold ethanol. The washed RNA sample were collected by centrifugation at 7500 x *g* for 5 minutes at 4°C. after removing the supernatant, the RNA pellet was air dried for 5 minutes to evaporate any residual ethanol. The pellet was the dissolved in 30 – 60 µL RNase-free water and the RNA concentration was determined by nanodrop. TURBO DNase (ThermoFisher AM2238) was added to the sample to digest DNA contaminations.

Reverse Transcription

For each reverse transcription reaction, 1 µL of 100 µM random hexamer, 1 µL of 10 mM dNTPs, 1 µL of isolated RNA, and 9 µL of RNase free water were added, the mixture was then incubated at 65°C for 5 minutes and immediately put on ice. Then, 4 µL of 5x buffer, 2 µL of 100 µM DTT, 1 µL of RNase inhibitor, and 1 µL of SuperScript II RT (ThermoFisher 18064022) were added to the tube and each sample was run on a thermal cycler at 25°C for 10 minutes followed by 42°C incubation for 50 minutes, and finally a 70°C incubation for 15 minutes. Once the reverse transcription is completed, 80 µL RNase-free water was added to the tube and cDNA template is ready to be further analyzed.

qPCR

1 µL of cDNA, 10 µL of 2xDYBR green master mix, 8 µL of RNase free water, 0.5 µL of 10 µM forward primer, and 0.5 µL of 10 µM reverse primer was loaded to the each well of a qPCR

plate. The plate was then sealed with the qPCR tape and briefly centrifuged at 1,000 RPM. The plate was then loaded to the qTower and designated program was executed.

Library Construction

The genomic library was prepared as previously described. The yeast expression plasmid pRS413 was digested with EcoRV and treated with alkaline phosphatase (New England Biolabs, NEB #M0290). The *S. cerevisiae* BY4741 genomic DNA was partially digested with EcoRV for the maximum yield of DNA fragments in the 3-10 kb size range. The digested DNA samples were then run on 1% agarose gel, the smear range from 3-10 kb were cut out of the gel and DNA were recovered with a gel extraction kit (Zymo research D4007). The cleaned DNA fragments and the digested pRS413 vector were ligated with T4 DNA ligase (New England Biolabs M0202S) at 14 ℃ overnight. The ligation mixture was used to transform NEB 10-beta Competent *Escherichia coli* cells (New England Biolabs C3019H) with electroporation method. The transformants were selected on LB plates containing 100 µg/L ampicillin. Then the transformants were scraped off the plates with liquid LB medium and used to extract the genomic library plasmid with a Qiaprep Spin Miniprep Kit.

As for the number of colonies required for entire genome coverage, we used the genomic library construction formula:

$$N = \frac{\ln (1 - p)}{\ln (1 - \frac{i}{g})}$$

Where N is the number of clones in the library, g is the genome size, i is the average insert size, and p is the probability that any point in the genome will occur at least once in the library.

For the calculation:

The genome size (g) of *S. cerevisiae* is 13.5 Mb with average open reading frames size of 1.4 kb,

and the average insert size (i) is 6 kb (partially digested genomic DNA of 3 kb-10 kb). The probability that any point in the genome will occur at least once in the library (p) is set to be 99.9%.

$$N = \frac{\ln(1-p)}{\ln(1-\frac{i}{g})} = \frac{\ln(1-0.99)}{\ln(1-\frac{6\times10^3}{1.35\times10^7})} = 10{,}359$$

This indicates a minimum number of 10,359 of *E. coli* colonies is required to cover the genome of *S. cerevisiae*.

Genomic Library Screen

After preparation, yeast genomic library was transformed into the recipient strain *pic2*Δ*aco2*Δ in complementation experiments with electroporation method. The transformants were selected on synthetic media with glucose and without histidine. To ensure the complete coverage of the yeast genome, three times of the minimum number of colonies required for complete coverage is obtained before further analysis.

Results

Copper supplementation rescues *aco2*Δ*pic2*Δ*lyp1*Δ lethality

In the screening for genetic interactions of *Saccharomyces cerevisiae* mitochondrial Cu transporters, we found Δ*aco2* is synthetically lethal with deletion of PIC2 as the haploid double mutant failed to germinate and this lethality is reversible by adding 100 µM $CuSO_4$. To validify the result, we manually dissected the sporulated progenies of *pic2*Δ*aco2*Δ diploids. The separated spores showed a severe growth defect in 1:3 ratio (Figure 4.1 A). Further analyses showed the growth defect is exaggerated under copper limiting condition with the addition of copper chelator, bathocuproinedisulfonic acid (BCS), while supplementing the media with $CuSO_4$ reverses the phenotype.

The genotypic analysis showed the slow growing spore carries *lyp1*Δ. *LYP1* encodes lysine specific cationic amino acid permease that imports lysine from the environment [29, 30]. It is deleted in Y8205 for the thialysine selection [31]. *ACO1* and *ACO2* are two paralogs in *S. cerevisiae.* Aco1 participates in the TCA cycle to convert citrate to isocitrate [32], while Aco2 is required in the lysine biogenesis α-aminoadipate pathway to remove the hydroxyl group from homocitrate and produce homoaconitate [33, 34]. The fact that the mutant misses *aco2* and *lyp1* suggests the growth defect of this triple mutant is related to lysine auxotroph.

To examine whether the rescue of the phenotype is copper specific, we added 100 µM ferrous chloride to the media with limited copper availability which did not reverse the phenotype (Figure 4.1 B). In addition to cupric ion, we added apo copper ionophores and ionophore-copper complexes to the media and they rescued the poor growth of the double mutant (Figure 4.1 C). To access the metal levels of the Δ*aco2*Δ*lyp*1double mutant, we digested the cells

grown in the rich media with metal-free nitric acid and measured the copper and iron content. Interestingly, the copper and iron content of the double mutant are not significantly different from that of the wild type and the single mutant (Figure 4.1 D).

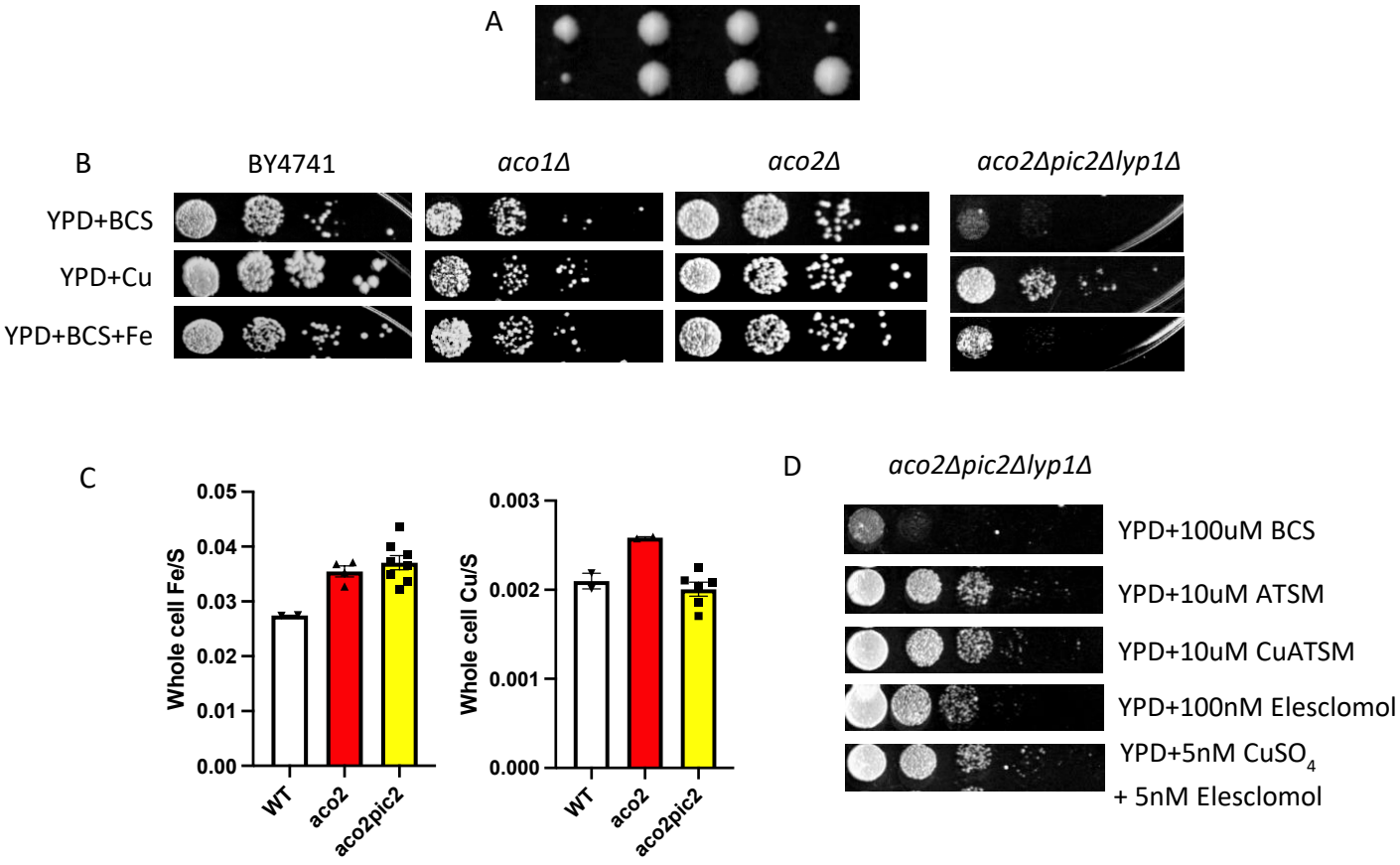

Figure 4.1: Copper rescues lysine auxotroph in *aco2Δpic2Δlyp1Δ*.

A) Tetrad dissection of the sporulated *aco2Δpic2Δ* diploid mutant showed a growth defect phenotype that segregated at ratio of 1:3. B) The serial dilution growth assay showed *aco2Δpic2Δlyp1Δ* growth defect on fermentable rich media is exaggerated under copper limiting condition. Adding 100 µM $CuSO_4$ rescued the phenotype but adding 100 µM of $FeCl_2$ did not reverse the phenotype. *aco1Δ* or *aco2Δ* single mutants did not show the grow defect. C) ICP-OES analyses showed the copper and iron content are not significantly different from that in the wild type and *aco2Δ* single mutant. D) adding apo/loaded copper ionophores to the media rescued the growth phenotype.

Amino acid auxotroph on rich media is rare because all the required nutrients are present in the media supplied by yeast extract and peptone, the amino acids essential for cell to grow exist as peptides with various lengths. Dipeptides are primarily imported into the yeast cells through Ptr2 and Dal5 [35, 36]. We investigated whether Dal5 or Ptr2 is the predominate dipeptide transporter in BY4741 yeast strain by rescuing the leucine auxotrophy with leucine-alanine dipeptide in *dal5*Δ and *ptr2*Δ. The results showed *ptr2*Δ had a worse growth defect than *dal5*Δ when supplementing the media with leucine-alanine dipeptide, suggesting Ptr2 is the predominant dipeptide transport in BY4741 strain. The expression of *PTR2* is repressed by *CUP9,* the growth of *cup9*Δ is comparable to that of the BY4741 wildtype (Figure 4.2 A) [36]. Next, we tested if Cu modulates the expression level of *PTR2*. RT-qPCR results indicated that the expression of *PTR2* is upregulated in the *aco2*Δ*pic2*Δ*lyp1*Δ triple mutant compared to the wildtype strain, however, adding Cu did not affect the expression of *PTR2* in the triple mutant significantly (Figure 4.2 B). Subsequently, we used di-lysine peptide to rescue the lysine auxotroph in the *aco2*Δ*pic2*Δ*lyp1*Δ triple mutant under low Cu and high Cu conditions, the results showed di-lysine peptide rescued the growth defect when glutamic acid is used as the nitrogen source, and the rescue is independent of Cu concentration within the media (Figure 4.2 C). Together, these results indicated the rescue of the lysine auxotroph by Cu is not related to dipeptide transporters.

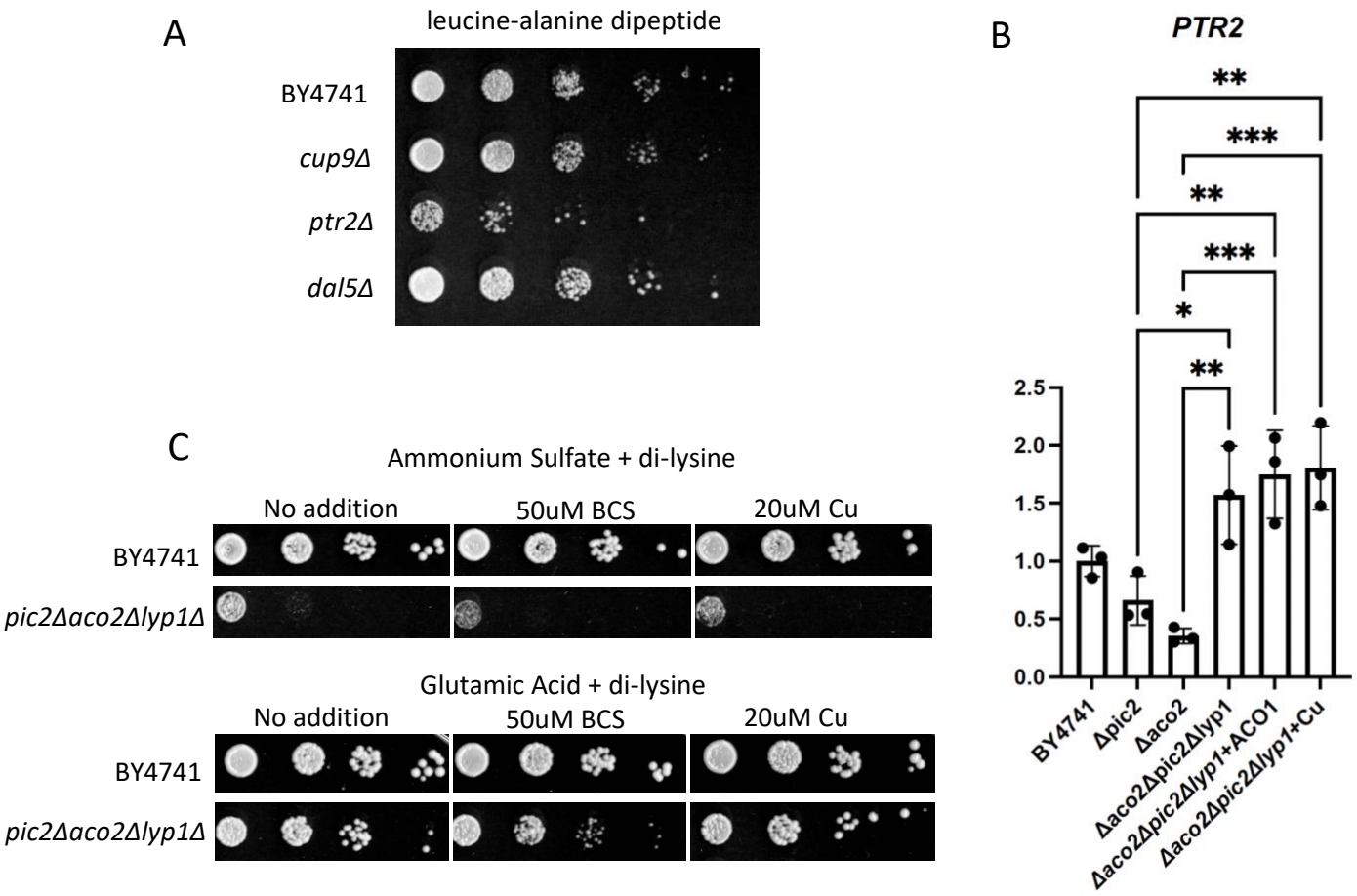

Figure 4.2: Dipeptide transport in *pic2*Δ*aco2*Δ*lyp1*Δ triple mutant

A) Using leucine-alanine dipeptide to rescue the leucine auxotroph in strains with BY4741 background. The growth defect of *ptr2*Δ is not rescued by the dipeptide, suggesting it is the predominant dipeptide transporter in this yeast strain B) The RT-qPCR results indicate the expression of PTR2 is upregulated in the *pic2*Δ*aco2*Δ*lyp1*Δ triple mutant, and adding Cu in the media did not further induce the overexpression of PTR2 in the triple mutant. C) di-lysine peptide can rescue the lysine auxotroph when glutamic acid is used as the nitrogen source. The rescue by di-lysine is independent of the Cu concentration within the media.

Identification of multi-copy suppressors by genomic DNA library transformation

To identify multi-copy suppressors of the growth defect, a *S. cerevisiae* genomic library was constructed and transformed into the mutant. The recipients of the suppressor genes showed increased colony sizes when compared to other transformants on the selection plate (Figure 4.2 A). the recipients of the suppressor genes were further confirmed by a serial dilution growth assay under copper limiting conditions. The growth defects were eliminated in the suppressor candidates under copper limiting conditions (Fugure 4.2 B). Six out of twelve suppressors were successfully recovered and identified as *ACO2* and *LYP1*. The identification of *LYP1* as one of the suppressors confirmed the growth defect of *pic2*Δ*aco2*Δ is caused by lysine auxotroph.

Lys4 is the homoaconitase in the yeast lysine biosynthesis pathway that converts homocitrate to homoisocitrate [37–39]. The enzyme contains a 4Fe-4S cluster, and thus it is susceptible to the buildup of reactive oxygen species [40]. Therefore, uncompromised cellular superoxide dismutase (SOD) activity is required for its proper function. Subsequently, we assayed the SOD activity of the mutant to examine if there is a SOD deficiency. In this assay, *ccs1*Δ was used as negative control because Ccs1 is the copper chaperone for Sod1 and deletion of *CCS1* renders Sod1 inactive as it cannot receive the copper cofactor [18]. The assay showed the triple mutant had no significant difference in SOD activity when compared to the wildtype, *pic2*Δ and *aco2*Δ single mutants, while the *ccs1*Δ strain exhibited ablated SOD activity as expected (Figure 4.2 C).

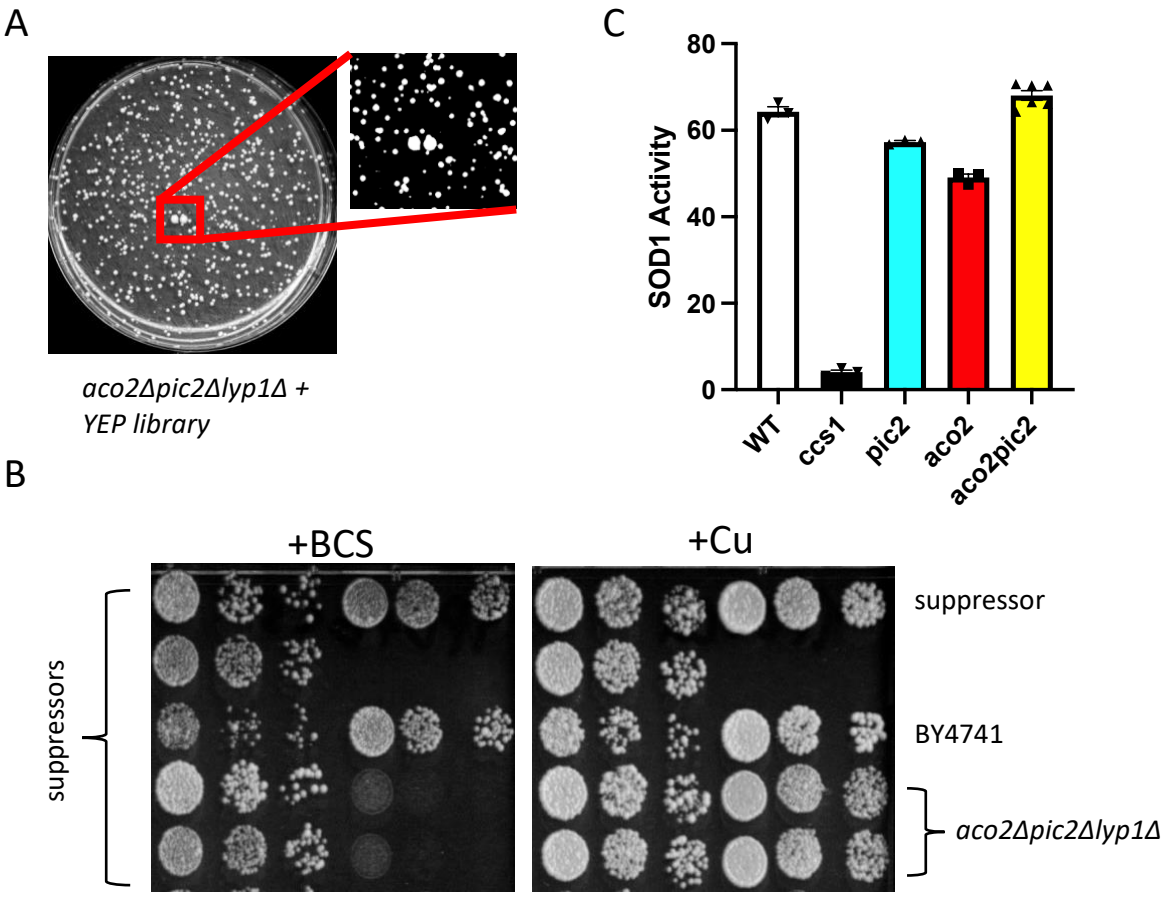

Figure 4.3: Identify multi-copy suppressors of the growth phenotype.

A) A yeast genomic library constructed with wildtype genome was transformed to the *aco2*Δ*pic2*Δ*lyp1*Δ mutant. The recipients of the suppressor genes showed enlarged colonies on the transformation selection plates comparing to the other transformants. B) The recipients of the suppressor genes were picked and cultured, serial dilution growth assay with the suppressor carriers, wildtype positive control and *aco2*Δ*pic2*Δ*lyp1*Δ mutant negative control showed the suppressor carriers no longer had growth defects under copper limiting condition. C) SOD activity in the wildtype, *pic2*Δ, *aco2*Δ and *aco2*Δ*pic2*Δ*lyp1*Δ are not significantly different, while the Δccs1 negative control showed diminished activity.

The rescue of the phenotype is dependent on *ACO1* expression

Aco1 functions as an isomerase and produce isocitrate from citrate. It protonates and removes the hydroxyl group from C3 of the citrate, while Ser-642 concurrently abstracts the proton on C2, creating a double bond between C2 and C3, and forming the intermediate cis-aconitate. The intermediate is then flipped 180^{o} within the active site of the Aco1, allowing C2 on the aconitate to be hydrated, producing isocitrate [41, 42]. In *S. cerevisiae*, *ACO2* is paralogous to *ACO1* [43, 44]. Previous studies showed that mutating a critical residue in the active site of Aco1 arginine 604 to lysine, the residue at the corresponding position in Aco2, reduces the enzymatic activity against citrate to 0.4% compared to the wildtype protein [33]. However, replacement of the lysine residue in Aco2 with arginine confers the mutant a 100-fold increase in enzymatic activity against citrate. The citrate molecule has a backbone made of three carbon atoms with three carboxyl groups attached, while homocitrate has four carbons on the backbone [45]. The proposed mechanism for this gain of function in *aco2* K604R is that the larger side chain on arginine in the active site accommodates the smaller substrate citrate.

Expression of *ACO1* is reported to be negatively correlated to the concentration of glutamic acid present in the growth media [33]. We measured the expression level of *ACO1* in the BY4741 strain grown in synthetic media with and without the presence of glutamic acid. Ammonium sulfate was used as the nitrogen source in glutamic acid-free media. RT-qPCR showed *ACO1* expression increased four fold in the yeast cells in the glutamic acid free media compared to the media with glutamic acid (Figure 4.3 A). We then tested whether the copper rescue of the growth phenotype is dependent on the expression level of *ACO1* by plating BY4741, *aco2Δpic2Δlyp1*Δ, and *aco1Δaco2Δpic2*Δ on synthetic media omitting lysine with different nitrogen sources. None of the strains showed a growth defect on synthetic complete

media (Figure 4.3 B). When grown on lysine free medium, it required less of copper to rescue the lysine auxotroph phenotype when glutamic acid is absent. This suggests the reversal of the lysine auxotroph growth defect is dependent on the *ACO1* expression level.

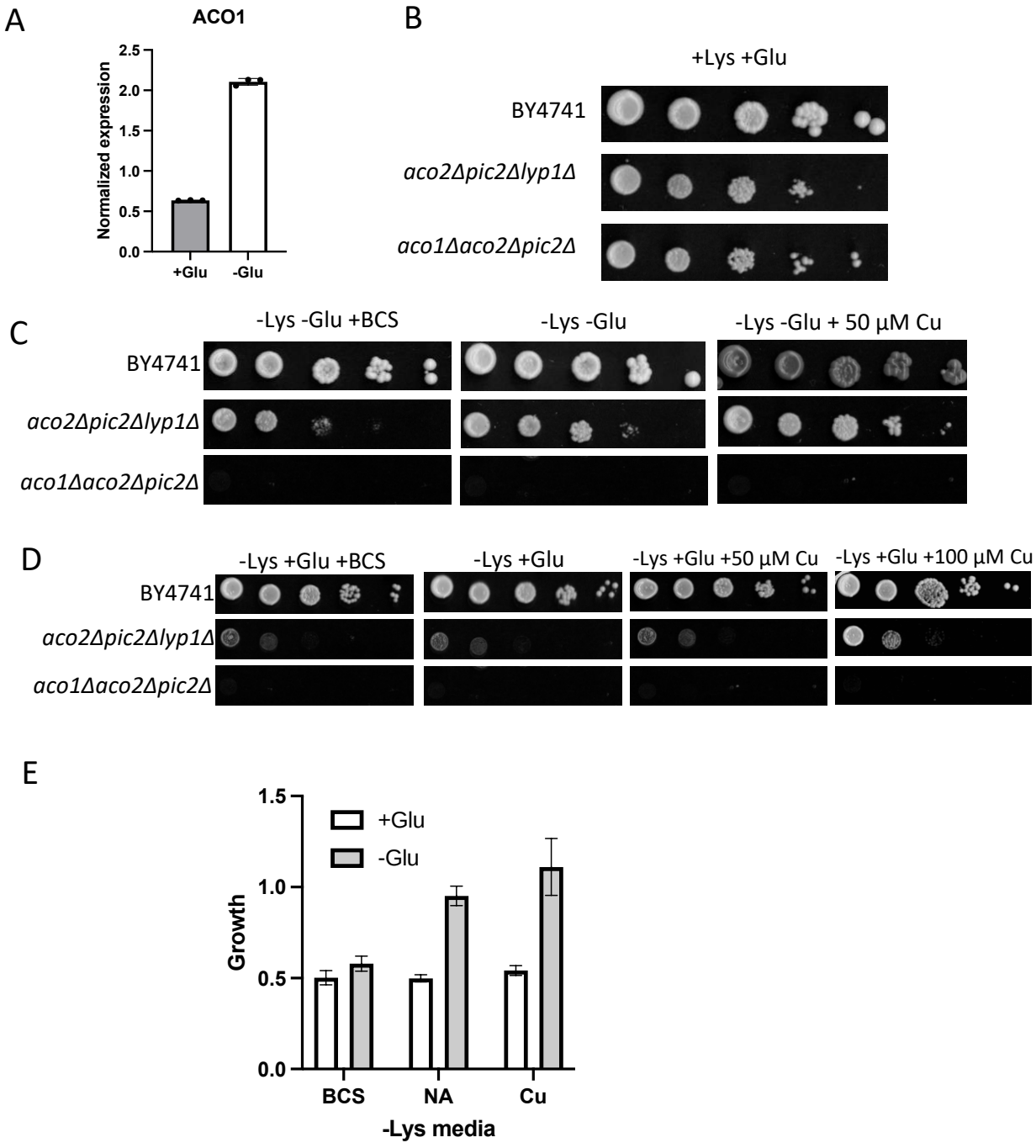

Figure 4.4: the rescue of lysine auxotroph by copper is dependent on *ACO1* expression level.

A) RT-qPCR shows the expression of ACO1 is upregulated when yeast cells are cultured in the media without glutamic acid (n=3). B) serial dilution growth assay showed *aco2*Δ*pic2*Δ*lyp1*Δ and *aco1*Δ*aco2*Δ*pic2*Δ triple mutants had no phenotype on synthetic complete media. C) on lysine-free, glutamic acid-free media, *aco2*Δ*pic2*Δ*lyp1*Δ showed a growth defect that was exaggerated under copper limiting condition and the phenotype was reversed by 50 µM $CuSO_4$ supplementation. *aco1*Δ*aco2*Δ*pic2*Δ was lethal under the tested conditions and adding copper failed to rescue it. D) on lysine-free media that contains

glutamic acid, *aco2*Δ*pic2*Δ*lyp1*Δ had a growth defect due to lysine auxotroph. 100 µM $CuSO_4$ was required to partially suppress the phenotype. *aco1*Δ*aco2*Δ*pic2*Δ was lethal under the tested conditions and adding copper failed to rescue it. E) The quantified growth demonstrated that the rescue of the lysine related growth defect is dependent on the expression of *ACO1* (n=3).

Copper metalloallersterily regulates substrate specificity of Aco1

Alignment of yeast Aco1 and Aco2 sequences showed the residue that dictates substrate specificity in Aco2 is a lysine, while the equivalent position is occupied by an arginine residue (Figure 4.4 A). Previous studies established the specificity of the Aco1 and Aco2 is related to steric inhibition of homocitrate binding and repositioning of a single residue could change specificity [33]. A site-directed mutation that replace the lysine residue to an arginine in Aco2 confered the mutant substrate specificity against citrate. However, the reciprocal Aco1 mutant did not result in gain the function. We tested the ability of copper to modulate this structural change. We hypothesize that the substrate specificity of Aco1 can be modulated by a conformational change in the active site because of Cu metalloallostery. We propose this change in substrate specificity of Aco1 partially compensates the loss of Aco2 (Figure 4.4 B). In the TCA cycle, Aco1 isomerizes citrate to isocitrate through the intermediate aconitate, the reaction occurs in both directions, while in the α-aminoadipate pathway, Aco2 converts isocitrate to homoaconitate. Both aconitate and homoaconitate have absorption peak at 240 nm [39].

In this study, we performed an in vitro biochemical assay to demonstrate the modulation of porcine mitochondrial aconitase. We set up reaction mixtures with increased concentration of Cu, monitored the change of 240 nm absorbance over 30 minutes at 37^{o}C for each reaction. The results show that the enzyme had diminished activity with increasing Cu concentration when citrate was used as the substrate; however, when the substrate was switched to homocitrate, we observed an increase in 240 nm absorbance from the reaction mixtures as Cu concentration increased, indicating enzyme activity was enhanced when homocitrate was used as the substrate. Together, the results demonstrate Cu can modulate the substrate specificity of porcine mitochondrial aconitase.

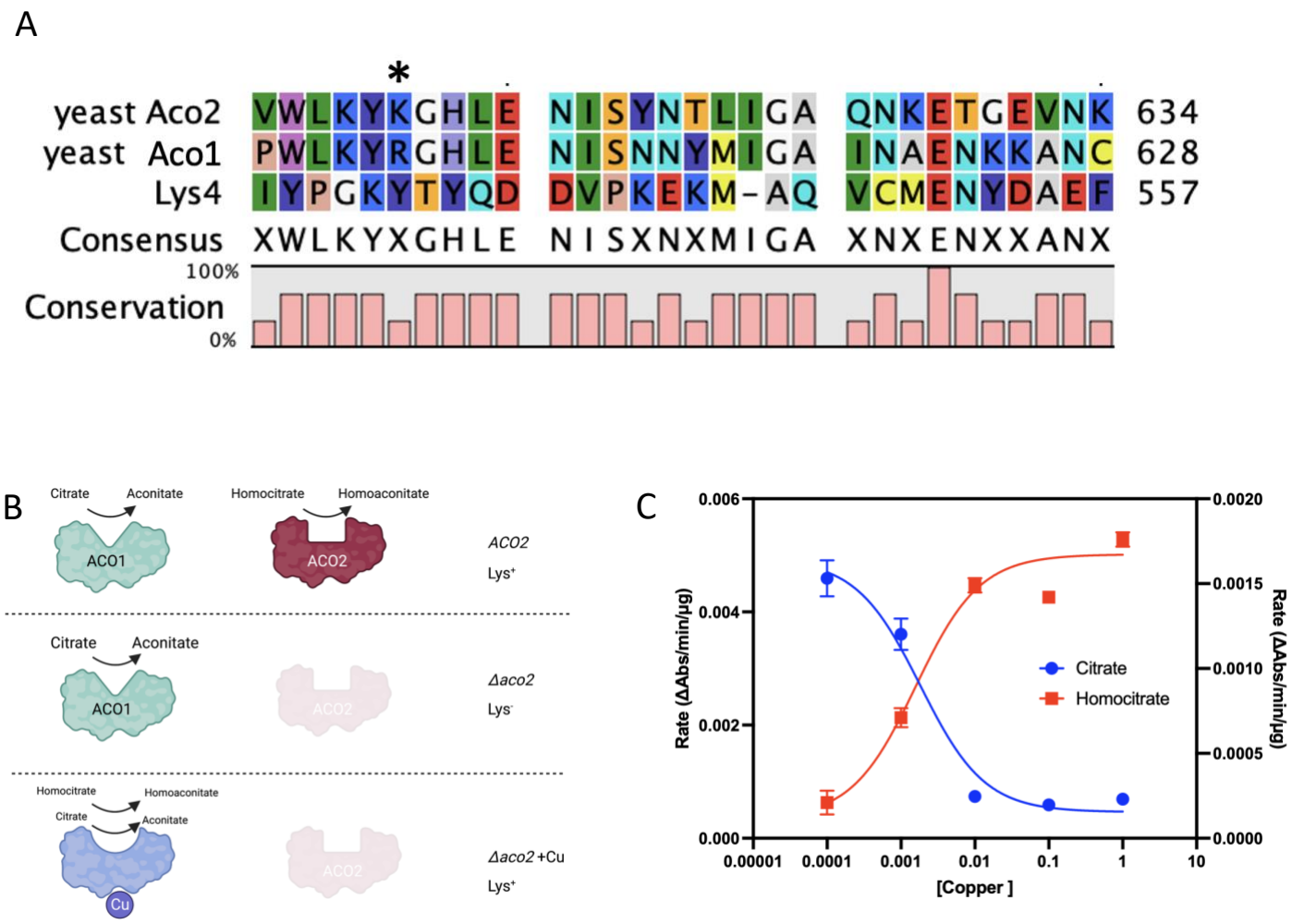

Figure 4.5: Cu modulates substrate specificity of aconitase.

A) Alignment of Aco1 and Aco2 amino acid sequence shows the critical residue within the active site of the enzymes that dictate the substrate specificity. A positively charged amino acid arginine is present in Aco1, allows tight contact between the smaller substrate citrate and Fe-Sulfur cluster catalytic center. While in Aco2, the equivalent position is occupied by a lysine residue to accommodate a slightly larger substrate, homocitrate. B) in WT cells, Aco1 catalyzes the reaction that converts citrate to isocitrate through aconitate and Aco2 produce homoaconitate from homocitrate in the lysine synthesis pathway. *aco2*Δ losses lysine biosynthesis capacity and becomes lysine auxotroph. We hypothesize that Cu transiently binds to Aco1, modulates its substrate specificity to compensate the loss of Aco2. C) in vitro biochemical assays demonstrated the production of aconitate was decreased as Cu concentration increases in the reaction mixture, indicating aconitase losing the activity when citrate was used as substrate. However, when homocitrate was used under the same conditions, the enzyme showed enhanced activity. These results indicated the substrate specificity can be modulated by the presence of Cu within the reaction mixture.

Discussion

It is well established that cells use Cu as a cofactor for numerous enzymes that catalyze crucial biochemical reactions in vivo [46, 47]. In these cupro-enzymes, Cu ions are inserted into the active site of the enzyme to structurally stabilize the protein as well as activate their enzymatic activity [14, 48, 49]. Cupro-enzymes play critical roles in cellular physiology, Fet3 is involved in high-affinity iron transport, Sod1 is required for protection against oxidative stress in the cytosol, and cytochrome c oxidase complex is the terminal electron accepting complex in the energy-producing electron transport chain located in mitochondria that is essential for respiration. In *S. cerevisiae*, Cu has been shown to be able to interact with Cu-sensing transcription factors to regulate the expression of genes involved in maintaining Cu homeostasis [50–53].

Results from recent studies have discovered new roles of Cu in cellular physiology and broadened the view of Cu as a mediator in multiple signaling pathways. They show Cu exists as a labile pool that is capable of rapidly moving and exchanging between targets in different locations through a thermodynamic gradient of Cu-binding sites to funnel into the tightly bound static Cu pool [25]. Therefore, Cu can potentially serve as allosteric regulator for different enzymes. In lipolysis pathway, Cu transiently binds to a key allosteric site of PDE3B and inhibits the enzyme activity responsible for cAMP-dependent lipolysis of triglycerides into fatty acids and glycerol [28]. Cu can also function as allosteric activator. Brady, Thiele, and Counter showed Cu transiently binds to MEK1 through CCS and enhances the kinase activity, whereas mutation in the cellular Cu importer CTR1 reduced the ability of MEK1 to phosphorylate MAP kinases extracellular signal-regulated kinase 1 and 2 (ERK1/2) [26, 54]. Another example of

kinase activated by Cu is ULK1/2, a pair of kinases that drive autophagy controlled by mTOR. Mutations that render ULK1/2 unable to bind Cu reduced autophagosome complex formation and has the potential to be targeted for cancer therapy [27]. Likewise, Cu transiently binds to tyrosine kinase receptors EGFR and MET, activates receptor tyrosine kinase (RTK)-mediated cellular signaling, increasing downstream protein kinase B and ERK signal transduction and increasing cancer cell proliferation and migration. These examples show the dynamic Cu pool plays a critical role in regulating signaling pathways through metalloallostery and given the close relationship between the involved pathways and cancer, this interaction can be potentially targeted for developing cancer treatment [55–58].

Although previous studies showed Cu can either enhancing or inhibiting enzyme activities through metalloallostery, no precedence of Cu modulation of substrate specificity has been reported. In this study, we showed Cu rescued lysine auxotroph in *aco2*Δ is dependent on the expression of *ACO1*. Although previous study showed replacement of the arginine residue in the active site of Aco1 with lysine did not confer the enzyme the activity with homocitrate being the substrate [33], we proposed Cu can transiently bind to the enzyme, modulates its conformation to accommodate homocitrate as the substrate and bypass the need of Aco1 to produce lysine. This Cu mediated rescue can be achieved by supplementation of exogenous $CuSO_4$, adding apo Cu ionophores or ionophore-Cu complexes. The fact that adding apo-ionophore can rescue the growth defect suggest the redistribution of Cu within the cell is sufficient. Under normal physiology, cells meticulously maintain the Cu homeostasis. Irving-Williams series suggest Cu is the most active transition metal that is readily form complexes with other metabolites and bind to different proteins [59]. Cells use multiple strategies to ensure Cu is delivered to the designated destinations without interacting with nonspecific off-targets,

these strategies including: keep Cu at lower abundancy comparing to other divalent metals; metalate the metal containing enzymes at specific sub-cellular compartments to avoid competitions between different transition metals; and using dedicated chaperons to deliver Cu to specific targets, although some recent studies showed that some Cu chaperons have promiscuities for their targets. For example, CCS can deliver Cu to both Sod1 and MEK1/2 [26]. A non-proteinaceous Cu ligand has also been isolated and demonstrated to be able to bind to Cu, interacting with mitochondrial Cu importer and mediating the translocation of Cu across the inner membrane of mitochondria [60]. The identification of Cu ligand remarks the potential discovery of a new realm of intracellular Cu regulations. Some possible roles of the ligand play include Cu acquisition, transportation, storage, and delivery to the potential targets. The possibility of mitochondria use this ligand to acquire Cu from cytosol in a similar fashion as bacterial or fungal cells use siderophore to acquire iron cannot be ruled out. Apo ligand might interact with plasma Cu importer or metallothionines to be metalated and bring the Cu to the mitochondria. The Cu ligand might also be capable of interacting with proteins to mediate Cu translocation and exchange. One of the open questions regarding to mitochondrial Cu homeostasis is that what is the Cu exporter [23]. Since major mitochondrial cuproenzymes such as COX and Sod1 are metalated in the inter membrane space of mitochondria, Cu are required to be exported from the matrix to be utilized [21]. However, a dedicated mitochondrial Cu exporter has yet to be identified. One possible mechanism for Cu exportation is that when Cu-ligand/apo-ligand ratio is elevated, the Cu-ligand complexes interact with the MCF responsible for importing Cu from the matrix side, change the conformation of the carrier and release the bound Cu into the channel of the carrier thus export it.

The transporters might not be the only class of proteins the ligand interact with. Within

the mitochondrial matrix, the Cu ligand functions like metallothionines in a way that it binds to Cu to prevent it from interacting with metabolites and enzymes. Our data suggest under physiological relevant concentration, Cu can bind to mitochondrial enzyme aconitase, change its substrate specificity, and regulate its activity. Combing with the observations of increased aconitase activity in cells with mitochondrial Cu deficiency, it suggests Cu has a regulatory role on TCA cycle activity through metalloallostery regulation of aconitase. Under high energy demanding conditions when hyperactive TCA activity is required, mitochondria need to withdraw Cu from binding to the aconitase, in this case, mitochondria can increase the production of apo ligand to mediate the transfer of Cu from aconitase to the ligand to a point when Cu-ligand/apo-ligand ratio start to elevate and promote the export of Cu from matrix to cytosol. On the other hand, when cells are under low energy demanding conditions, mitochondria can slow down the production of apo ligand, destruct excess ligand, and promote import of Cu into mitochondria. In both cases, the ligands act like a capacitor of Cu within the mitochondria to fine tune the availability of Cu to the target enzymes based on the cellular metabolism needs.

References

1. Cunningham CN, Rutter J (2020) 20,000 picometers under the OMM: diving into the vastness of mitochondrial metabolite transport. EMBO Rep 21:e50071. https://doi.org/10.15252/embr.202050071

2. Cobine PA, Moore SA, Leary SC (2021) Getting out what you put in: Copper in mitochondria and its impacts on human disease. Biochim Biophys Acta Mol Cell Res 1868:118867–118867. https://doi.org/10.1016/j.bbamcr.2020.118867

3. Barber RG, Grenier ZA, Burkhead JL (2021) Copper Toxicity Is Not Just Oxidative Damage: Zinc Systems and Insight from Wilson Disease. Biomedicines 9:316. https://doi.org/10.3390/biomedicines9030316

4. Yuan DS, Stearman R, Dancis A, Dunn T, Beeler T, Klausner RD (1995) The Menkes/Wilson disease gene homologue in yeast provides copper to a ceruloplasmin-like oxidase required for iron uptake. Proceedings of the National Academy of Sciences 92:2632–2636. https://doi.org/10.1073/pnas.92.7.2632

5. Zischka H, Lichtmannegger J, Schmitt S, Jägemann N, Schulz S, Wartini D, Jennen L, Rust C, Larochette N, Galluzzi L, Chajes V, Bandow N, Gilles VS, DiSpirito AA, Esposito I, Goettlicher M, Summer KH, Kroemer G (2011) Liver mitochondrial membrane crosslinking and destruction in a rat model of Wilson disease. J Clin Invest 121:1508–1518. https://doi.org/10.1172/JCI45401

6. Trist BG, Fifita JA, Freckleton SE, Hare DJ, Lewis SJG, Halliday GM, Blair IP, Double KL (2018) Accumulation of dysfunctional SOD1 protein in Parkinson's disease is not associated with mutations in the SOD1 gene. Acta Neuropathol 135:155–156. https://doi.org/10.1007/s00401-017-1779-6

7. Nikseresht S, Hilton JBW, Kysenius K, Liddell JR, Crouch PJ (2020) Copper-ATSM as a Treatment for ALS: Support from Mutant SOD1 Models and Beyond. Life (Basel) 10:271. https://doi.org/10.3390/life10110271

8. Culotta VC, Lin SJ, Schmidt P, Klomp LW, Casareno RL, Gitlin J (1999) Intracellular pathways of copper trafficking in yeast and humans. Adv Exp Med Biol 448:247–254. https://doi.org/10.1007/978-1-4615-4859-1_22

9. Aller SG, Unger VM (2006) Projection structure of the human copper transporter CTR1 at 6-Å resolution reveals a compact trimer with a novel channel-like architecture. Proceedings of the National Academy of Sciences 103:3627–3632. https://doi.org/10.1073/pnas.0509929103

10. Okada M, Miura T, Nakabayashi T (2017) Comparison of extracellular Cys/Trp motif between Schizosaccharomyces pombe Ctr4 and Ctr5. Journal of Inorganic Biochemistry 169:97–105. https://doi.org/10.1016/j.jinorgbio.2017.01.009

11. Beaudoin J, Thiele DJ, Labbé S, Puig S (2011) Dissection of the relative contribution of the Schizosaccharomyces pombe Ctr4 and Ctr5 proteins to the copper transport and cell surface delivery functions. Microbiology (Reading) 157:1021–1031. https://doi.org/10.1099/mic.0.046854-0

12. De Feo CJ, Aller SG, Siluvai GS, Blackburn NJ, Unger VM (2009) Three-dimensional structure of the human copper transporter hCTR1. Proceedings of the National Academy of Sciences 106:4237–4242. https://doi.org/10.1073/pnas.0810286106

13. Peña MMO, Puig S, Thiele DJ (2000) Characterization of the *Saccharomyces cerevisiae* High Affinity Copper Transporter Ctr3*. Journal of Biological Chemistry 275:33244–33251. https://doi.org/10.1074/jbc.M005392200

14. Arnesano F, Banci L, Bertini I, Huffman DL, O'Halloran TV (2001) Solution Structure of the Cu(I) and Apo Forms of the Yeast Metallochaperone, Atx1,. Biochemistry 40:1528–1539. https://doi.org/10.1021/bi0014711

15. Robinson NJ, Winge DR (2010) Copper metallochaperones. Annu Rev Biochem 79:537–562. https://doi.org/10.1146/annurev-biochem-030409-143539

16. Askwith C, Eide D, Van Ho A, Bernard PS, Li L, Davis-Kaplan S, Sipe DM, Kaplan J (1994) The *FET3* gene of S. cerevisiae encodes a multicopper oxidase required for ferrous iron uptake. Cell 76:403–410. https://doi.org/10.1016/0092-8674(94)90346-8

17. Davis-Kaplan SR, Askwith CC, Bengtzen AC, Radisky D, Kaplan J (1998) Chloride is an allosteric effector of copper assembly for the yeast multicopper oxidase Fet3p: An unexpected role for intracellular chloride channels. Proceedings of the National Academy of Sciences of the United States of America 95:13641–13645. https://doi.org/10.1073/pnas.95.23.13641

18. Carroll MC, Girouard JB, Ulloa JL, Subramaniam JR, Wong PC, Valentine JS, Culotta VC (2004) Mechanisms for activating Cu- and Zn-containing superoxide dismutase in the absence of the CCS Cu chaperone. Proceedings of the National Academy of Sciences of the United States of America 101:5964–5969. https://doi.org/10.1073/pnas.0308298101

19. Tainer JA, Getzoff ED, Richardson JS, Richardson DC (1983) Structure and mechanism of copper, zinc superoxide dismutase. Nature 306:284–287. https://doi.org/10.1038/306284a0

20. Vest KE, Zhu X, Cobine PA (2019) Copper Disposition in Yeast. Clinical and Translational Perspectives on WILSON DISEASE 115–126. https://doi.org/10.1016/b978-0-12-810532-0.00012-4

21. Cobine PA, Pierrel F, Winge DR (2006) Copper trafficking to the mitochondrion and assembly of copper metalloenzymes. Biochimica et Biophysica Acta (BBA) - Molecular Cell Research 1763:759–772. https://doi.org/10.1016/j.bbamcr.2006.03.002

22. Tsukihara T, Aoyama H, Yamashita E, Tomizaki T, Yamaguchi H, Shinzawa-Itoh K, Nakashima R, Yaono R, Yoshikawa S (1996) The Whole Structure of the 13-Subunit Oxidized Cytochrome c Oxidase at 2.8 Å. Science 272:1136–1144. https://doi.org/10.1126/science.272.5265.1136

23. Vest KE, Leary SC, Winge DR, Cobine PA (2013) Copper Import into the Mitochondrial Matrix in *Saccharomyces cerevisiae* Is Mediated by Pic2, a Mitochondrial Carrier Family Protein*. Journal of Biological Chemistry 288:23884–23892. https://doi.org/10.1074/jbc.M113.470674

24. Ruprecht JJ, Kunji ERS (2020) The SLC25 Mitochondrial Carrier Family: Structure and Mechanism. Trends in Biochemical Sciences 45:244–258. https://doi.org/10.1016/j.tibs.2019.11.001

25. Pham VN, Chang CJ (2023) Metalloallostery and Transition Metal Signaling: Bioinorganic Copper Chemistry Beyond Active Sites. Angewandte Chemie International Edition 62:e202213644. https://doi.org/10.1002/anie.202213644

26. Turski ML, Brady DC, Kim HJ, Kim B-E, Nose Y, Counter CM, Winge DR, Thiele DJ (2012) A novel role for copper in Ras/mitogen-activated protein kinase signaling. Mol Cell Biol 32:1284–1295. https://doi.org/10.1128/MCB.05722-11

27. Tsang T, Posimo JM, Gudiel AA, Cicchini M, Feldser DM, Brady DC (2020) Copper is an essential regulator of the autophagic kinases ULK1/2 to drive lung adenocarcinoma. Nat Cell Biol 22:412–424. https://doi.org/10.1038/s41556-020-0481-4

28. Krishnamoorthy L, Cotruvo JA, Chan J, Kaluarachchi H, Muchenditsi A, Pendyala VS, Jia S, Aron AT, Ackerman CM, Vander Wal MN, Guan T, Smaga LP, Farhi SL, New EJ, Lutsenko S, Chang CJ (2016) Copper Regulates Cyclic AMP-Dependent Lipolysis. Nat Chem Biol 12:586–592. https://doi.org/10.1038/nchembio.2098

29. Sychrova H, Chevallier MR (1993) Cloning and sequencing of the Saccharomyces cerevisiae gene LYP1 coding for a lysine-specific permease. Yeast 9:771–782. https://doi.org/10.1002/yea.320090711

30. Regenberg B, Düring-Olsen L, Kielland-Brandt MC, Holmberg S (1999) Substrate specificity and gene expression of the amino-acid permeases in Saccharomyces cerevisiae. Curr Genet 36:317–328. https://doi.org/10.1007/s002940050506

31. Tong AHY, Boone C (2006) Synthetic genetic array analysis in Saccharomyces cerevisiae. Methods Mol Biol 313:171–192. https://doi.org/10.1385/1-59259-958-3:171

32. Sumegi B, Sherry AD, Malloy CR, Srere PA (1993) Evidence for orientation-conserved transfer in the TCA cycle in Saccharomyces cerevisiae: carbon-13 NMR studies. Biochemistry 32:12725–12729. https://doi.org/10.1021/bi00210a022

33. Fazius F, Shelest E, Gebhardt P, Brock M (2012) The fungal α-aminoadipate pathway for lysine biosynthesis requires two enzymes of the aconitase family for the isomerization of homocitrate to homoisocitrate. Molecular Microbiology 86:1508–1530. https://doi.org/10.1111/mmi.12076

34. Jia Y, Tomita T, Yamauchi K, Nishiyama M, Palmer DRJ (2006) Kinetics and product analysis of the reaction catalysed by recombinant homoaconitase from Thermus thermophilus. Biochem J 396:479–485. https://doi.org/10.1042/BJ20051711

35. Becerra-Rodríguez C, Marsit S, Galeote V (2020) Diversity of Oligopeptide Transport in Yeast and Its Impact on Adaptation to Winemaking Conditions. Front Genet 11:. https://doi.org/10.3389/fgene.2020.00602

36. Cai H, Hauser M, Naider F, Becker JM (2007) Differential Regulation and Substrate Preferences in Two Peptide Transporters of Saccharomyces cerevisiae. Eukaryotic Cell 6:1805–1813. https://doi.org/10.1128/ec.00257-06

37. Weidner G, Steffan B, Brakhage AA (1997) The Aspergillus nidulans lysF gene encodes homoaconitase, an enzyme involved in the fungus-specific lysine biosynthesis pathway. Mol Gen Genet 255:237–247. https://doi.org/10.1007/s004380050494

38. Maragoudakis ME (1967) Homoaconitic Acid Accumulation by a Lysine-Requiring Yeast Mutant1. J Bacteriol 94:1060–1065

39. Strassman M, Ceci LN (1966) Enzymatic formation of cis-homoaconitic acid, an intermediate in lysine biosynthesis in yeast. J Biol Chem 241:5401–5407

40. Liu XF, Elashvili I, Gralla EB, Valentine JS, Lapinskas P, Culotta VC (1992) Yeast lacking superoxide dismutase. Isolation of genetic suppressors. Journal of Biological Chemistry 267:18298–18302. https://doi.org/10.1016/s0021-9258(19)36959-5

41. Han D, Canali R, Garcia J, Aguilera R, Gallaher TK, Cadenas E (2005) Sites and Mechanisms of Aconitase Inactivation by Peroxynitrite: Modulation by Citrate and Glutathione. Biochemistry 44:11986–11996. https://doi.org/10.1021/bi0509393

42. Lloyd SJ, Lauble H, Prasad GS, Stout CD (1999) The mechanism of aconitase: 1.8 A resolution crystal structure of the S642a:citrate complex. Protein Sci 8:2655–2662

43. Kwong JQ, Davis J, Baines CP, Sargent MA, Karch J, Wang X, Huang T, Molkentin JD (2014) Genetic deletion of the mitochondrial phosphate carrier desensitizes the mitochondrial permeability transition pore and causes cardiomyopathy. Cell Death Differ 21:1209–1217. https://doi.org/10.1038/cdd.2014.36

44. Przybyla-Zawislak B, Gadde DM, Ducharme K, McCammon MT (1999) Genetic and Biochemical Interactions Involving Tricarboxylic Acid Cycle (TCA) Function Using a Collection of Mutants Defective in All TCA Cycle Genes. Genetics 152:153–166. https://doi.org/10.1093/genetics/152.1.153

45. Rees DC (2002) Great Metalloclusters in Enzymology. Annual Review of Biochemistry 71:221–246. https://doi.org/10.1146/annurev.biochem.71.110601.135406

46. Rae TD, Schmidt PJ, Pufahl RA, Culotta VC, O'Halloran TV (1999) Undetectable intracellular free copper: The requirement of a copper chaperone for superoxide dismutase. Science 284:805–808. https://doi.org/10.1126/science.284.5415.805

47. Boal AK, Rosenzweig AC (2009) Structural biology of copper trafficking. Chem Rev 109:4760–4779. https://doi.org/10.1021/cr900104z

48. Banci L, Bertini I, Cantini F, Felli IC, Gonnelli L, Hadjiliadis N, Pierattelli R, Rosato A, Voulgaris P (2006) The Atx1-Ccc2 complex is a metal-mediated protein-protein interaction. Nat Chem Biol 2:367–368. https://doi.org/10.1038/nchembio797

49. Huffman DL, O'Halloran TV (2000) Energetics of Copper Trafficking between the Atx1 Metallochaperone and the Intracellular Copper Transporter, Ccc2*. Journal of Biological Chemistry 275:18611–18614. https://doi.org/10.1074/jbc.C000172200

50. Dameron CT, Winge DR, George GN, Sansone M, Hu S, Hamer D (1991) A copper-thiolate polynuclear cluster in the ACE1 transcription factor. Proc Natl Acad Sci U S A 88:6127–6131. https://doi.org/10.1073/pnas.88.14.6127

51. Gralla EB, Thiele DJ, Silar P, Valentine JS (1991) ACE1, a copper-dependent transcription factor, activates expression of the yeast copper, zinc superoxide dismutase gene. Proc Natl Acad Sci U S A

88:8558–8562. https://doi.org/10.1073/pnas.88.19.8558

52. Yamaguchi-Iwai Y, Serpe M, Haile D, Yang W, Kosman DJ, Klausner RD, Dancis A (1997) Homeostatic Regulation of Copper Uptake in Yeast via Direct Binding of MAC1 Protein to Upstream Regulatory Sequences of*FRE1* and *CTR1* *. Journal of Biological Chemistry 272:17711–17718. https://doi.org/10.1074/jbc.272.28.17711

53. Brown KR, Keller GL, Pickering IJ, Harris HH, George GN, Winge DR (2002) Structures of the cuprous-thiolate clusters of the Mac1 and Ace1 transcriptional activators. Biochemistry 41:6469–6476. https://doi.org/10.1021/bi0160664

54. Brady DC, Crowe MS, Turski ML, Hobbs GA, Yao X, Chaikuad A, Knapp S, Xiao K, Campbell SL, Thiele DJ, Counter CM (2014) Copper is required for oncogenic BRAF signalling and tumorigenesis. Nature 509:492–496. https://doi.org/10.1038/nature13180

55. Chojnowski JE, Li R, Tsang T, Alfaran FH, Dick A, Cocklin S, Brady DC, Strochlic TI (2022) Copper Modulates the Catalytic Activity of Protein Kinase CK2. Front Mol Biosci 9:878652. https://doi.org/10.3389/fmolb.2022.878652

56. Guo J, Cheng J, Zheng N, Zhang X, Dai X, Zhang L, Hu C, Wu X, Jiang Q, Wu D, Okada H, Pandolfi PP, Wei W (2021) Copper Promotes Tumorigenesis by Activating the PDK1-AKT Oncogenic Pathway in a Copper Transporter 1 Dependent Manner. Adv Sci (Weinh) 8:2004303. https://doi.org/10.1002/advs.202004303

57. Salvi M, Sarno S, Cesaro L, Nakamura H, Pinna LA (2009) Extraordinary pleiotropy of protein kinase CK2 revealed by weblogo phosphoproteome analysis. Biochim Biophys Acta 1793:847–859. https://doi.org/10.1016/j.bbamcr.2009.01.013

58. Opazo CM, Lotan A, Xiao Z, Zhang B, Greenough MA, Lim CM, Trytell H, Ramírez A, Ukuwela AA, Mawal CH, McKenna J, Saunders DN, Burke R, Gooley PR, Bush AI (2021) Nutrient copper signaling promotes protein turnover by allosteric activation of ubiquitin E2D conjugases

59. Foster AW, Osman D, Robinson NJ (2014) Metal Preferences and Metallation*. Journal of Biological Chemistry 289:28095–28103. https://doi.org/10.1074/jbc.R114.588145

60. Cobine PA, Ojeda LD, Rigby KM, Winge DR (2004) Yeast Contain a Non-proteinaceous Pool of Copper in the Mitochondrial Matrix*. Journal of Biological Chemistry 279:14447–14455. https://doi.org/10.1074/jbc.M312693200